

Perivascular adipose tissue-dependent chemerin release: The role of statins and thromboxane.

Tariq Ghazi Alsahli, MSc. Pharmacology

School of Life Sciences

Faculty of Medicine and Health Sciences

University of Nottingham

Thesis submitted to the University of Nottingham

for the degree of Doctor of Philosophy

March 2021

Abstract

Perivascular adipose tissue (PVAT) is the fat tissue that surrounds most systemic blood vessels. Owing to its' unique anatomical location, PVAT can directly regulate vascular tone and other aspects of vascular function via its secretome. Chemerin is an adipokine secreted from liver and adipose tissue, including PVAT, and is implicated in blood pressure regulation, with well-established roles in inflammation and obesity. Despite the fact that PVAT and chemerin have emerged as promising drug targets for many diseases, including obesity and obesity-associated cardiovascular diseases, less is known about their interaction with current cardiovascular drugs. Considering the well-documented pleiotropic effects of statins, which are not related to statin's ability to inhibit cholesterol biosynthesis, the principal aim of this study was to determine the possible effects of statins on PVAT's regulation of porcine coronary arteries (PCAs).

PVAT from porcine coronary caused a time-dependent contraction of PCAs at baseline tone and potentiated contraction in the presence of the thromboxane mimetic U46619 through Ca^{2+}-dependent pathways. The lipophilic simvastatin, but not the hydrophilic pravastatin, caused a concentration-dependent inhibition of PVAT-induced contraction at baseline tone and in the presence of U46619. Simvastatin caused inhibition of PVAT-induced contraction through a direct effect on PCAs and on the release of vasocontractile chemerin from PVAT.

Simvastatin consistently inhibited the basal release of total chemerin in a concentration-dependent manner from both porcine coronary PVAT and 3T3-L1 adipocytes through a mevalonate-independent pathway. Simvastatin also prevented

enhanced chemerin release from 3T3-L1 adipocytes following incubation with lipopolysaccharide (LPS) or the K_{ATP} channels opener, pinacidil. Furthermore, 48 h, but not 24 h, treatment with the PPARγ agonist rosiglitazone stimulated the release of chemerin levels and reversed simvastatin-mediated inhibition of chemerin release from cultured 3T3-L1 adipocytes.

Pre-contraction with U46619 enhanced chemerin-9-induced contraction of isolated PCA, and chemerin-9-induced contraction involved ERK, Rho kinase, and calcium influx, with a role for calcium influx, in particular, in the enhancement of the contraction by U46619.

Clinically, there is evidence that statins produce beneficial effects, including anti-inflammatory effects and reduction in blood pressure unrelated to cholesterol lowering, and the present study suggests that reducing chemerin release may be, at least partially, behind this effect. This thesis demonstrated that the co-release of thromboxane and chemerin from PVAT may produce a synergistic effect on coronary arteries that enhances contractile responses. These findings may be important for the control of adipose tissue-induced vascular alterations in obesity and associated diseases.

Publications

Submitted Paper

1. **Tariq G. Alsahli**, Abdulla Ahmad, Andrew J. Bennett, Michael D. Randall & Richard E. Roberts. 2021. Enhancement of chemerin-induced contractions in the presence of raised tone in porcine isolated coronary artery: role of calcium channels.

Abstracts for conferences

1. **Alsahli, T.G.,** Roberts, R.E. and Randall, M.D. (2017). Pre-contraction with U46619 enhances the contraction to perivascular adipose tissue in porcine coronary artery: effect of statins. *Pharmacology 2017*. Queen Elizabeth II conference centre, London, UK.
2. **Alsahli, T.G.,** Roberts, R.E. and Randall, M.D. (2018). Pre-contraction with the thromboxane mimetic U46619 enhances the chemerin-induced contraction in porcine isolated coronary artery: Role of L-type calcium channels. *Pharmacology 2018*. Queen Elizabeth II conference centre, London, UK.
3. **Alsahli, T.G.,** Roberts, R.E. and Randall, M.D. (2019). Statin and hypoxia decrease coronary perivascular adipose tissue-induce chemerin release in porcine. *Pharmacology 2019*. Edinburgh International Conference Centre, Edinburgh, UK.

Dedication

To my beloved late father,

Ghazi Sonaid Alsahli,

who believed in science, supported me, and was always by my side.

yet left shortly before he could see his dream comes true

May his soul rest in peace.

Acknowledgements

First and foremost, I would like to thank Prof. Michael Randall and Dr. Richard Roberts, my supervisors, for the continuous support throughout my PhD study. Your guidance, patience, and encouragement since day one has been invaluable. Your advices helped me grown as a person and as a scientist.

I would like to thank all my friends in and outside the university for their company and help on all levels. My thanks also go to the laboratory staff and faculty members in the University of Nottingham, School of Life Sciences who have given any technical, administrative or educational help during the course of my research. Additionally, thanks go to Qulayl Aldossari for helping me with my cell culture experiments.

I want to express my sincere gratitude to the government of the Kingdom of Saudi Arabia and Al-Jouf University for their support and funding of my PhD study.

I am heartily thankful to my beloved mother, sisters, brothers, and all my family members who have encouraged and supported me during my study in the UK throughout the years. My sincere love and thanks go to my wife and my little princess. Thank you for being in my life, without your love and support this work would have been impossible.

Table of Contents

Abstract i

Publications iii

Acknowledgements v

Abbreviations xi

Chapter 1 General Introduction 1

1.1 Cardiovascular diseases 2

1.2 Adipose tissue 4

1.3 Perivascular adipose tissue (PVAT) 6

1.3.1 PVAT in vascular functions 9

1.3.2 PVAT in vascular pathologies 13

1.4 Chemerin 19

1.4.1 Chemerin receptors 19

1.4.2 Chemerin synthesis 21

1.4.3 Chemerin functions 23

1.5 Statins 26

1.5.1 Pharmacokinetics of statins 28

1.5.2 Mechanism of action 28

1.5.3 The pleiotropic effects of statins 29

1.6 Statins and adipose tissue 33

1.7 Aims 38

Chapter 2 Effects of statins on perivascular adipose tissue-induced vasoconstriction of porcine coronary arteries 39

2.1 Introduction 40

2.2 Materials and Methods 43

2.2.1 Tissue preparation 43

2.2.2 Experimental protocol 45

2.2.3 Determination of TXB_2, $PGF_{2\alpha}$, and chemerin levels by ELISA in the presence of simvastatin 48

2.2.4 Statistical analysis 49

2.2.5 Drugs and chemicals 49

2.3 Results 50

2.3.1 Effects of PVAT re-addition on vascular tone at baseline and after U46619 precontraction 50

2.3.2 Effects of simvastatin on PVAT-induced contraction in PCAs at baseline tone and after U46619 precontraction 51

2.3.3 Effects of pravastatin on PVAT-induced contraction in PCAs at baseline tone and after U46619 precontraction 54

2.3.4 Effects of lovastatin on PVAT-induced contraction in PCAs at baseline tone and after U46619 precontraction 55

2.3.5 Effects of indomethacin on PVAT-induced contraction in PCAs at baseline tone and after U46619 precontraction 58

2.3.6 Effects of simvastatin on transferring bath solution from PVAT to PCA rings 60

2.3.7 Effects of Ca^{2+} reintroduction in KCl-depolarised PCAs in the presence of simvastatin 61

2.3.8 Effects of Ca^{2+} removal on simvastatin-mediated inhibition of PVAT-induced contraction in PCAs 62

2.3.9 Effects of simvastatin on release of thromboxane, prostaglandin, and chemerin from PVAT. 63

2.4 Discussion 66

Chapter 3 Effects of statins on chemerin release from 3T3-L1 adipocytes and PVAT 73

3.1 Introduction 74

3.2 Materials and Methods 77

3.2.1 Determination of PVAT-induced chemerin release in the presence of simvastatin, pravastatin, hypoxia, and EFS 77

3.2.2 Differentiation of 3T3-L1 cells 77

3.2.3 3T3-L1 cells stained with oil red O stain 79

3.2.4 Treatment of cultured 3T3-L1 adipocytes 80

3.2.5 MTT assay 82

3.2.6 Statistical analysis 83

3.2.7 Drugs and chemicals 84

3.3 Results 85

3.3.1 Effects of simvastatin on chemerin production by cultured 3T3-L1 adipocytes 85

3.3.2 Effects of simvastatin on chemerin production by PVAT 88

3.3.3 Effects of pravastatin on chemerin production by cultured 3T3-L1 adipocytes 89

3.3.4 Effects of pravastatin on chemerin production by PVAT 91

3.3.5 Role of Ca^{2+} in the simvastatin-mediated inhibition of chemerin release by cultured 3T3-L1 adipocytes 92

3.3.6 Role of LPS in the simvastatin-mediated inhibition of chemerin release by cultured 3T3-L1 adipocytes 94

3.3.7 Role of TNF-α on chemerin production by cultured 3T3-L1 adipocytes 95

3.3.8 Role of K_{ATP} in the simvastatin-mediated inhibition of chemerin release by cultured 3T3-L1 adipocytes 97

3.3.9 Role of PPARγ in the simvastatin-mediated inhibition of chemerin release by cultured 3T3-L1 adipocytes 98

3.3.10 Effects of hypoxia and EFS on chemerin release by PVAT 101

3.3.11 MTT assay of simvastatin 102

3.4 Discussion 103

Chapter 4 Effects of precontraction with the thromboxane mimetic U46619 on chemerin-induced contraction in porcine coronary arteries 113

4.1 Introduction 114

4.2 Materials and Methods 118

4.2.1 Tissue preparation 118

4.2.2 Experimental protocol 118

4.2.3 Determination of PVAT-induced chemerin release in the presence of U46619 by ELISA 120

4.2.4 Estimation of total and phosphorylated ERK and MYPT-1 expression in PCA by immunoblotting 121

4.2.5 Statistical analysis 122

4.2.6 Drugs and chemicals 123

4.3 Results 124

4.3.1 The level of PVAT-derived chemerin in the presence of U46619 124

4.3.2 Effects of U46619 precontraction on the response to chemerin in PCA 125

4.3.3 Effects of Ca^{2+}-free buffer and L-type calcium channels on chemerin-induced contraction in PCA 128

4.3.4 Role of ERK in chemerin-induced contraction in PCA 129

4.3.5 Role of Rho kinase in chemerin-induced contraction in PCAs 132

4.3.6 Role of PI3 kinase and Nox1 in chemerin-induced contraction in PCA..... 135

4.3.7 Effects of KCl and BAY K8644 precontraction on the response of PCA to chemerin 137

4.3.8 Effects of hypoxia on direct and enhanced chemerin-induced contraction in PCA..... 138

4.4 Discussion 142

Chapter 5 General Discussion 152

5.1 Conclusions 163

Appendices 165

A. Immunoblots 166

References 170

Abbreviations

ADCF	Adipose-derived constricting factor
ADRF	Adipose-derived relaxing factor
AT	Adipose tissue
AT_1 receptor	Type-1 angiotensin II receptor
BAT	Brown adipose tissue
BMI	Body mass index
BP	Blood pressure
CHD	Coronary heart disease
$Chemerin_1$	Chemerin receptor 1
CVD	Cardiovascular disease
DMSO	Dimethyl sulfoxide
EFS	Electrical field stimulation
ERK	Extracellular signal-regulated kinases
h	Hours
H_2O_2	Hydrogen peroxide
H_2S	Hydrogen sulphide
HMG-CoA reductase	3-Hydroxy-3-Methyl-Glutaryl-Coenzyme A reductase
IL	Interleukin
K_{ATP}	ATP-sensitive potassium channel
L-NAME	NG-nitro-L-arginine methyl ester
LPS	Lipopolysaccharides
Min	Minutes
MLC	Myosin light chain
NA	Noradrenaline
NO	Nitric oxide
Nox	NADPH oxidase enzyme
PCA	Porcine coronary artery
$PGF_{2\alpha}$	Prostaglandin $F_{2\alpha}$
PI3K	Phosphatidylinositol-3-kinase

PPARγ	Peroxisome proliferator-activated receptors
PVAT	Perivascular adipose tissue
SAT	Subcutaneous adipose tissue
TNF-α	Tumour necrosis factor-alpha
TP	TXA_2 receptor
TXA_2	Thromboxane A_2
TXB_2	Thromboxane B_2
U46619	9,11-dideoxy-11α,9α-epoxymethanoprostaglandin $F_{2α}$
VAT	Visceral adipose tissue
VSM	Vascular smooth muscle
VSMC	Vascular smooth muscle cell
WAT	White adipose tissue

Chapter 1
General Introduction

1.1 Cardiovascular diseases

Cardiovascular diseases (CVDs) are the leading cause of mortality globally and are responsible for almost a third of all deaths worldwide [1]. According to the latest statistics from the British Heart Foundation, CVDs cause more than a quarter (27 %) of all deaths in the UK, which accounts for more than 160,000 deaths each year and costs the UK economy around £19 billion annually [2]. Major CVDs include coronary heart disease (CHD), cerebrovascular disease, heart failure, and rheumatic heart disease [1]. In 2019, the main cause of CVD death was CHD, with approximately one in eight men and one in 13 women dying as a result of CHD in the UK. Also, CHD is the leading cause of premature death, with around 22,000 people under the age of 75 in the UK dying from CHD each year. Stroke causes over 34,000 deaths a year in the UK and is the second most common cause of death across the world in 2019 [2].

The risk factors for CVD may be broadly divided into two types: factors that are modifiable through lifestyle changes, for example, exercise, diet, alcohol consumption, and smoking; and those that are not modifiable, such as biological sex, ethnicity, age, and genetic factors [3]. Intensive research in the last decades has outlined a cluster of several risk factors associated with CVDs, including but not limited to obesity, hypertension, hyperlipidaemia, and glucose intolerance, which are referred to as "metabolic syndrome" (MetS) [4, 5]. Although each component of MetS is considered an independent risk factor, obesity, in particular, is considered a major risk factor for cardiovascular complications [6-8].

The most widely used index to define obesity is body mass index (BMI), the World Health Organisation has estimated that more

than 1.9 billion adults in the world are overweight (BMI > 25.0 kg/m²), of which at least 650 million are obese (BMI >30.0 kg/m²) [9]. Consistent clinical and epidemiological evidence has linked obesity and increased BMI to a broad spectrum of CVDs, including CHD, heart failure, hypertension, stroke, atrial fibrillation, and sudden cardiac death [10, 11]. For example, according to the Framingham Heart Study, about 11 % of heart failure cases in men and 14 % in women are attributable to obesity; each BMI increment by one unit is associated with a 5 % increased heart failure risk in men and 7 % in women, indicating a positive correlation between BMI and risk of heart failure [12, 13]. In a recent meta-analysis study that compared new-onset heart failure in over 500,000 participants, being overweight was associated with a 33 % higher risk of developing heart failure compared with having a normal body weight [14].

The relationship between obesity and hypertension is well established in children, adults, and the elderly [15-19]. BMI was significantly correlated with systolic and diastolic blood pressures, and obesity has been independently associated with an increased prevalence of hypertension [18, 20]. In a prospective study, strong evidence suggests that obesity and weight gain alone are associated with an increased future risk of CHD even before clear clinical symptoms appear [21]. Further, a clinical study found that bariatric surgery is associated with a reduction of CVD incidence by about 60 % [22]. These findings show that obesity is independently associated with a significantly higher incidence of CVDs and demonstrate the importance of understanding the complex relationship between obesity and CVDs.

Although obesity-related CVDs have risen alongside the growing global obesity pandemic, the precise mechanisms that make an obese individual more likely to suffer CVDs are not fully understood. Recently, there has been a focus on adipose tissue, the active paracrine and endocrine organ that induces several bioactive mediators that might contribute to cardiovascular outcomes and provide a molecular link between obesity and cardiovascular diseases.

1.2 Adipose tissue

Adipose tissue (AT) is a complex and highly active metabolic and endocrine tissue that comprises a set of cell types, including adipocytes, adipocyte precursor cells (pre-adipocytes), immune cells such as macrophages and T cells, fibroblasts, nerves, and capillaries [23]. The non-adipose cells form the stromal vascular fraction of adipose tissue, the cell composition and phenotype of which are usually different depending on the location and type of adipose tissue [24]. Historically, adipose tissue was thought simply as a passive reservoir for energy storage, but since the identification of leptin in 1994, this traditional view of adipose tissue is no longer valid [25]. Adipose tissue is now known to express and secrete a variety of bioactive peptides, collectively known as adipokines (or adipocytokines), which act at both the local (autocrine/paracrine) and systemic (endocrine) levels [26]. Besides the different adipokines secreted by AT, there is also the expression of numerous receptors that influence their ability to respond to intracellular signals. These receptors include cytokine receptors, adrenoceptors, and receptors for endocrine hormones [27].

Adipose tissue is divided into white adipose tissue (WAT) and brown adipose tissue (BAT), according to the size of the lipid droplets and the number of mitochondria in the adipocytes.

Morphologically, adipocytes in WAT consist of a single lipid droplet (comprising triglycerides), which accounts for more than 90 % of the cell volume and has a thin and low number of mitochondria. By contrast, BAT contains triglycerides as multiple small vacuoles with large and numerous numbers of mitochondria, which explains its brown colour and high vascularization (reviewed in [28]). WAT is distributed throughout the whole body and comprises up to 20 % to 25 % of total adult body weight. It is generally used to store energy in the form of triglycerides, which are then mobilized to other tissues during times of restrictive caloric intake. BAT, however, is located in dedicated local depots, for instance, the interscapular region in human infants and rodents, and specializes in the dissipation of energy through the production of heat [29, 30]. Additionally, WAT and BAT are thought to express different proteins, such as leptin, which is more highly expressed in WAT than in BAT, and uncoupling protein 1 (UCP1), which is considered a protein marker of BAT [28]. For years, it was thought that in humans, BAT was present mainly in the neonatal period for thermoregulation but was very scarce in adults [31]. However, recent data have indicated that a significant amount of what appears to be active BAT is also present in adult humans [32, 33].

Apart from the classic white and brown adipocytes, a "browning process" has been identified, which consists of the appearance of brown-like adipocytes in WAT depots in response to specific stimuli, such as chronic cold exposure, β-adrenoceptor stimulation, and other pharmacological and nutritional agents (for more see [34, 35]). The brown-like adipocytes that appear in classical WAT depots have been called "brite" (brown-in-white) or "beige" adipocytes [36].

Sites of adipose tissue deposition in humans fall into two categories: visceral adipose tissue (VAT) and subcutaneous adipose tissue (SAT). VAT is largely located in the abdominal cavity surrounding internal organs, whereas SAT, as the name implies, predominates in subcutaneous areas. In healthy individuals, about 80 % of all body fat is in the subcutaneous area compared to 10–20 % visceral fat [37]. However, these two major adipose tissue depots are widely thought to be metabolically and clinically distinct, as visceral adipose tissue generally has more metabolic activity and greater impact on cardiovascular diseases than subcutaneous adipose tissue (reviewed in [38]). Visceral obesity is associated with coronary heart disease and peripheral arterial disease; for instance, only obese individuals characterized by elevated VAT show the predictive complications of type 2 diabetes and cardiovascular disease [39].

1.3 Perivascular adipose tissue (PVAT)

Perivascular adipose tissue (PVAT) is the fat tissue that surrounds most systemic blood vessels and lies on the outside of the adventitia with no clear anatomical barrier that separates the two (Figure 1.1) [29]. Other names for PVAT include the fourth layer of the blood vessel, or the "*tunica adiposa*" [40]. Except in the cerebral circulation, PVAT is widely distributed around large arteries and veins, small and resistance vessels, and skeletal muscle microvessels. PVAT has also been found within organs, like in the renal sinus of the kidney, surrounding the renal artery and vein [41].

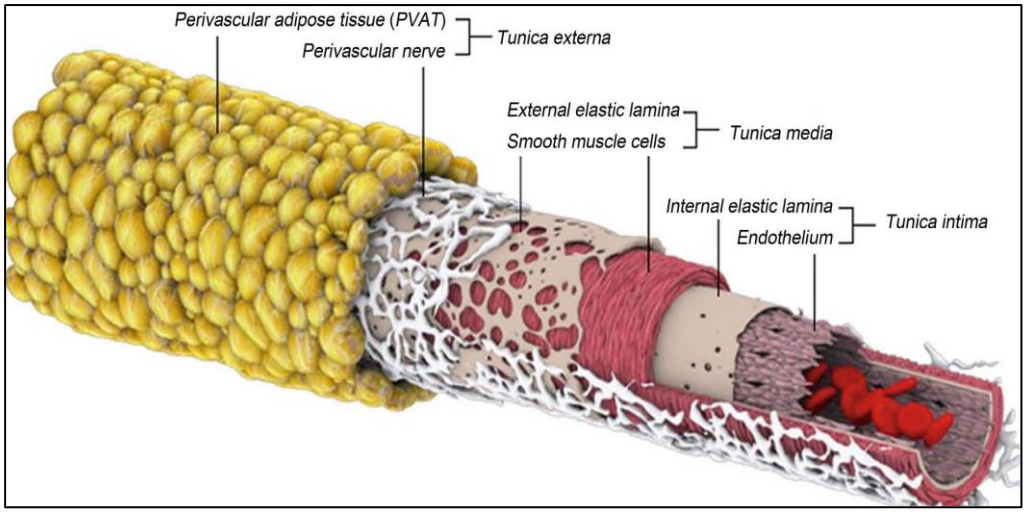


Figure 1.1: The structure of an artery wall. Perivascular adipose tissue (PVAT) is located directly around blood vessels where it acts as a paracrine modulator of different vascular functions. Figure adapted from [42].

Similar to other adipose tissue depots, PVAT is a highly vascularized network comprised of several cell types, including adipocytes (white or brown) as well as a stromal vascular fraction that includes pre-adipocytes, macrophages, lymphocytes, fibroblasts, *vasa vasorum* endothelial cells, mesenchymal stem cells, and nerve endings [43]. However, the composition of PVAT often varies depending on vascular beds and physiological status, possibly to accommodate its distinct, tissue-specific roles. For instance, PVAT around atherosclerotic aortae recruits immune cells, such as macrophages and T cells, responsible for the production of proinflammatory cytokines during atherogenesis [41, 44].

Although the literature has yet to fully describe the classification of PVAT as either white (WAT), brown (BAT), or beige adipose tissue, the accepted view nowadays is that PVAT shares characteristics with all three types of adipose tissues, depending on the anatomical location and species. In rodents, the mesenteric artery is surrounded by WAT, whereas the

thoracic aorta is surrounded by BAT-like tissue, and the abdominal aorta is surrounded by adipose tissue with a mixture of white and brown adipocytes [29]. Findings from animal studies are consistent with data from human PVAT studies, in which PVAT surrounding the aorta and its main branches reportedly contains BAT [45]. However, studies on human coronary perivascular adipocytes indicate conflicting results regarding the phenotype of PVAT. For example, Chatterjee *et al.* (2013) demonstrated that human coronary PVAT exhibits a histological appearance and gene expression pattern similar to white rather than brown adipocytes. This was shown by the equal expression of brown adipocyte-related genes between subcutaneous adipocytes and PVAT, as well as by the significant overexpression of the selective WAT marker (TCF21) in coronary adipocytes [46, 47]. By contrast, Sacks *et al*. (2009) showed that human epicardial PVAT has a greater expression of some brown adipocyte markers, such as UPC-1, compared to other fat depots [48].

Furthermore, given the structural differences in PVAT variations, there are also differences relating to its secretory-profile and gene-expression, similar to those identified in WAT and BAT. For example, a comparison of white mesenteric PVAT and brown aortic PVAT in a rat model revealed morphological differences in the expression of renin-angiotensin system components [43]. Additionally, mesenteric PVAT was found to express a higher angiotensin AT_{1a}- and AT_2-receptors and an increased activity of angiotensin II [49]. Taken together, these findings suggest that PVAT exhibits considerable phenotypic heterogeneity depending on its anatomical location.

1.3.1 PVAT in vascular functions

For a long time PVAT did not attract attention, until 1991 when Soltis and Cassis reported its influence on the isolated rat thoracic aorta, demonstrating that removal of the PVAT around the aorta shifted the contraction to NE to the left [50]. The unique anatomical location and the absence of a separating fascia layer between PVAT and the vasculature promote paracrine communications within the vessel wall, allowing PVAT to directly regulate vascular tone as well as other aspects of vascular function. The ability of PVAT to release bioactive proteins—collectively termed adipokines (or adipocytokines)—such as adiponectin, leptin, omentin, thromboxane, and chemerin, as well as vital cytokines including interleukins and tumour necrosis factor α (TNFα) and gaseous molecules like H_2S and H_2O_2, allows PVAT to participate in the regulation of vascular function and pathophysiology in both paracrine and autocrine manner [51, 52]. PVAT contributions in vascular physiology include regulation of thermogenesis, smooth muscle cell proliferation and migration, involvement in vascular inflammation, and, more importantly, the ability to manipulate vascular tone [29]. Furthermore, PVAT is known to actively respond to different signals from the vascular bed, allowing it to dynamically detect alterations in vascular biology and modify its secretome appropriately [53, 54].

PVAT has a potential role in vascular remodelling and in the proliferation and migration of VSMCs, functions it generally stimulates. PVAT secretes adipokines, such as chemerin, visfatin, resistin, and leptin, which are known to be potent stimulators of VSMC proliferation and migration [54, 55]. Barandier *et al*. (2005) showed that cultured media from the PVAT of rat aorta stimulated VSMC growth, which is enhanced

in aged rats and in high-fat diet-induced obesity but not in leptin receptor-deficient obese rats [56]. In another study, leptin stimulated VSMC proliferation through ERK1/2 [57]. PVAT-derived visfatin was found to be a VSMC growth factor, which was proven by visfatin-specific antibody/inhibitor and direct observation of recombinant visfatin [58]. In the same study, exogenous visfatin stimulated nicotinamide mononucleotide production, which in turn triggered VSMC proliferation in a dose- and time-dependent manner via ERK1/2 and p38 signalling pathways [58]. Resistin also contributes to both the proliferation and migration of VSMCs, and its expression is increased after injury in the carotid artery [59]. However, by regulating the proliferation of VSMCs, PVAT is potentially able to regulate vascular angiogenic responses to a variety of stimuli, an effect with physiological and pathophysiological implications [60].

Some PVAT depots have phenotypes similar to those of BAT, including the expression of thermogenic genes (like UCP-1), which is necessary for non-shivering thermogenesis. PVAT is reported to have significant physiological and pathophysiological thermogenesis properties [29]. In a study that used a murine model lacking PVAT, the authors demonstrated that PVAT can generate heat, which helped in maintaining intravascular temperature and was associated with increased activity of metabolic enzymes when mice were housed at a reduced temperature (16°C). In this study, the development of atherosclerotic plaques in mice was attenuated, and serum triglyceride concentrations decreased markedly [61].

1.3.1.1 Role in regulation of vascular tone

It has long been accepted that PVAT offers mechanical protection of the vessels against neighbouring tissue during contraction [52]. Indeed, methods for preparing blood vessels for experimental manipulation *ex vivo* routinely begin by cleaning the vessel, essentially removing the PVAT [29]. However, with an increased understanding of the function of adipose tissue in general, PVAT research is undergoing its own renaissance. The ability of PVAT to regulate vascular tone was the first recognised functional role of PVAT in a study conducted by Soltis and Cassis (1991) [50]. The authors demonstrated an anti-contractile effect of PVAT, in which the presence of PVAT significantly attenuated noradrenaline-induced contraction of the rat aorta in comparison with PVAT-free vessels. This effect was explained by the uptake of noradrenaline into adrenergic nerves in the fat tissue [50]. A decade later, Löhn *et al*. (2002) demonstrated that the anticontractile effect of PVAT was not due to the uptake of noradrenaline, as it was also observed with other vasoconstrictors, including angiotensin II, serotonin, endothelin-1, and phenylephrine, given that these agonists could not be taken up by PVAT [62]. In the same study, the authors suggested that PVAT releases transferable relaxing factors that act by tyrosine kinase-dependent activation of K^+ channels in vascular smooth muscle cells, and they first proposed the idea of "adventitium-derived relaxing factors" (ADRF), which are now known as PVAT-derived relaxing factors [62].

Extensive studies on the anticontractile effects of PVAT in rodents have been extended to human studies as well. Gao *et al.* (2005) was the first to report that PVAT in human internal thoracic arteries releases transferable relaxation factors that act

through the activation of calcium-dependent potassium channels [63]. In another study that used segments of the human internal thoracic artery, the authors demonstrated that adipokines released by PVAT are able to induce vascular relaxation even if the fat tissue has been loosely added to the tissue bath and is not in direct contact with the artery [64]. However, the mechanism and endothelial-dependence by which PVAT induced vascular relaxation are not fully understood. Potential PVAT-derived vasorelaxant substances include leptin [65], adiponectin [66], prostacyclin (PGI_2) [67], angiotensin (1-7) [68], nitric oxide (NO) [69], H_2S [70] and H_2O_2 [71] (Table 1).

Alongside the studies that indicated a role of PVAT in vasorelaxation effect, many studies have reported the production of vasoconstrictor factors by PVAT. In the initial study by Soltis and Cassis (1991), PVAT greatly enhanced contractions in response to electrical field stimulation and indirect sympathomimetic tyramine in rat aorta [50]. Also, Gao *et al.* (2006) demonstrated that electrical field stimulation of rat mesenteric artery rings produced greater contractile responses in the presence of PVAT through the production of superoxide mediated by NAD(P)H oxidase, and that this enhancement involved activation of tyrosine kinase and MAPK/ERK pathway in mesenteric arteries [72]. Gao and co-workers were the first to propose the term PVAT-derived contracting factors (PVCF) in 2007 [73]. As listed in Table 1, PVCF includes many factors, such as chemerin, thromboxane, angiotensin II, noradrenaline, and leptin [74]. The role of chemerin in vasocontraction will be discussed in detail in section 1.4.3.

Except for renin, all the components of the renin–angiotensin–aldosterone system (RAAS), including angiotensinogen,

angiotensin converting enzyme (ACE), and angiotensin receptor 1a and 1b, have been detected in PVAT [75]. PVAT-derived Ang II enhanced electrical field stimulation-induced contraction through the activation of AT_1 receptors in rat mesenteric arteries [76]. However, other factors that may contribute to the contractile effects of PVAT are prostanoids, such as thromboxane and prostaglandins. Meyer *et al.* (2013) identified ADCF formed through COX-dependent pathways in PVAT and detected formation of thromboxane A_2 from PVAT in lean and, to a greater extent, obese mice [77]. Additionally, the presence of the "adrenergic system" has been demonstrated in PVAT and includes release, take up, and metabolism of noradrenaline (NA) [78]. In rat thoracic aorta and superior mesenteric arteries, noradrenaline, and the enzymes involved in its synthesis have been detected in PVAT adipocytes, in which PVAT enhances vasocontraction via α_1-adrenoceptors [79]. Also, α-adrenoceptor antagonists inhibit PVAT-induced constriction of rat vessel rings [29].

Taken together, it is apparent that PVAT exerts both contractile and vasorelaxant actions through the release of different adipokines and cytokines, which act in both autocrine and paracrine ways. Under physiological conditions, the balance between the pro-contractile and anti-contractile effects of PVAT seems to be tissue- and species-specific with a greater tendency towards vasorelaxation effects in humans [74]. In pathophysiological conditions, a dysfunctional PVAT produces a panel of pro-inflammatory and vasoconstrictor factors, which will be discussed below.

1.3.2 PVAT in vascular pathologies

Many reports have identified the ability of PVAT to regulate vascular tone as well as other aspects of vascular function via

its secretome. These abilities are altered in disease states, such as obesity, metabolic syndromes (MetS), and cardiovascular disease, where the quantity and functional phenotype of PVAT differ [60]. In the Framingham Heart Study, measurement of adipose tissue surrounding the thoracic aorta revealed a significant correlation of this depot with body mass index, visceral obesity, hypertension and diabetes [80]. In an *in vitro* study on small arteries with and without PVAT obtained by gluteal biopsies from individuals with and without MetS, PVAT was shown to exert an anticontractile effect on adjacent vessels in healthy humans by increasing NO bioavailability. However, in patients with obesity and MetS, there was an increase in adipocyte area and the anticontractile effect of PVAT was absent [81]. In the same study, application of TNF-α and IL-6 and induction of hypoxia to PVAT around healthy arteries reduced their vasodilator activity and resulted in an obese PVAT phenotype [81]. Similarly, bariatric surgery also reverses the lost anticontractile activity of PVAT by reducing adipocyte hypertrophy, PVAT inflammation and increasing both PVAT-derived NO and adiponectin availability [82]. These results are supported by animal studies that showed a reduction in the vasorelaxant properties of PVAT in obese rats, combined with an increase in local TNF-α and a reduction in NO bioavailability within PVAT [83].

The PVAT depot expands in obesity and vascular diseases with changes in quantity and functional phenotype. For example, epicardial adipose tissues, which are visceral thoracic fat depots located along the large coronary arteries (i.e., perivascular) and on the surface of the ventricles, are found in high volumes in patients with obesity and atherosclerotic lesions compared to healthy individuals [84, 85]. Also, Eiras *et al.* (2008) found that

epicardial PVAT expresses lower levels of adiponectin in patients with coronary artery disease (CAD) and higher levels of inflammatory adipokines, such as IL-6 and leptin, than in non-CAD patients [86]. To sum up, as PVAT is an essential part of the blood vessel environment and shows significant change in pathological conditions, PVAT should be regarded as a strong predictor of cardiovascular pathology.

Table 1. Role of known PVAT-derived factors in vasomotor regulation

PVAT-derived factor	Role in vasomotor	Vascular bed	Mechanism	Ref.
Adiponectin	Vasodilator	Human small arteries	↑ NO bioavailability	[81]
	Vasodilator	Porcine coronary artery	Unknown	[87]
	Vasodilator	Murine Small mesenteric arteries	Activation of BK_{Ca}	[66]
Leptin	Vasodilator	Canine small mesenteric arteries and veins	↑ Endothelial release of NO	[88]
	Vasodilator	Forearm blood flow in human	Unknown	[89]
	Vasoconstrictor	Porcine coronary artery	↑ Rho kinase pathway	[90]

Prostanoids: PGE_2 and PGI_2	Anti-contractile	Human saphenous vein	Activation of EP_4 and IP receptors	[91]
Thromboxane	Vasoconstrictor	Porcine coronary artery	Activation of TP receptors	[92]
Chemerin	Vasoconstrictor	Human saphenous vein and resistance arteries	↓ cAMP accumulation	[93]
	Vasoconstrictor	Rat thoracic aorta and mesenteric artery	↑ Intracellular Ca^{2+}	[94]
Angiotensin II	Vasoconstrictor	Rat mesenteric arteries	Activation of AT_1 receptors	[76]
Nitric oxide	Vasodilator	Rat aorta	Activation of smooth muscle K^+ channels	[73]
TNF-α	Vasodilator	Rat cerebral arterioles	↑ NO synthase	[95]
	Endothelium-independent Vasodilator	Rat thoracic aorta	↑ PLA_2	[96]
	Vasoconstrictor	Sheep bronchial artery	↑ Release of ET-1	[97]
Angiotensin [1-7]	Vasodilator	Rat aorta	Open BK_{Ca} channels	[68]

Interleukin-6	Vasodilator	Rat aorta	↑ Prostacyclin in VSMCs	[98]
H_2S	Vasodilator	Rat aorta	Open Kv channels	[99]

Abbreviations: NO, nitric oxide; BK_{ca}, large conductance calcium-activated potassium channel; cAMP, cyclic adenosine monophosphate; PGE_2, Prostaglandin E_2; PGI_2, prostacyclin; EP_4 receptor, Prostaglandin E_2 receptor 4; IP receptor, prostacyclin receptor; TP, thromboxane receptor; AT_1 receptors, angiotensin 1 receptor; PLA_2, Phospholipases A_2; ET-1, endothelin-1; Kv channels, voltage-dependent K^+ channels; VSMCs, vascular smooth muscle cells; H_2S, hydrogen sulphide.

1.4 Chemerin

The chemerin gene was initially identified in 1997 as a retinoid-responsive gene present in psoriatic skin lesions [100]. Chemerin was formerly known as tazarotene-induced gene 2 (TIG2) because the treatment of skin raft cultures with tazarotone (a synthetic retinoid) resulted in apparent increased expression of this gene [100]. Another initial name for chemerin was retinoic acid receptor responder 2 (RARRES2), due to its increased expression in response to retinoids in general [101]. Studies in humans indicated that chemerin is involved in inflammation and that chemerin gene expression and circulating levels are positively correlated with increased BMI, obesity-related biomarkers, and hypertension [101].

1.4.1 Chemerin receptors

Three G protein-coupled receptors (GPCRs) are currently known to bind chemerin: chemerin receptor 1 (ChemR23 or CMKLR1), chemerin receptor 2 (GPR1), and C-C chemokine receptor-like 2 (CCRL2) [102]. Chemerin receptor 2 ($Chemerin_2$) was first identified in 1994 in the human hippocampus [103] and linked to chemerin in 2007 [104]. $Chemerin_2$ is expressed in the central nervous system, adipose tissue, skeletal muscle, and the skin [105]. CCRL2 was discovered in humans in 1998 [106] and linked to chemerin 10 years later in experiments based on binding assays [107]. The CCRL2 gene was found in high concentrations in the spleen, liver, lymph nodes, bone marrow, leukocytes, and, to a lesser extent, mast cells [108]. However, there are little to no data on the signal transduction pathways of $Chemerin_2$ and CCRL2 [102, 109].

Chemerin is thought to primarily mediate its functions via chemerin receptor 1 ($Chemerin_1$) [108]. Even though the gene for $Chemerin_1$ was described in 1996 [110], it was not linked to

chemerin (or TIG2 at that time) until 2003, when Wittamer *et al.* (2003) purified human inflammatory fluids and identified TIG2 as a natural ligand stimulator for $Chemerin_1$ [111]. The activation of the receptor displayed chemotactic properties for leukocytes that expressed $Chemerin_1$, and thus the peptide was named "chemerin" [111]. Therefore, chemerin activation of $Chemerin_1$ is best known for promoting chemotaxis of dendritic cells and leukocytes.

$Chemerin_1$ is expressed in human endothelial cells [112], PVAT, VSMCs [94], pre-adipocytes, adipocytes [113], stomal vascular cells of adipose tissue [114], haematopoietic tissues such as thymus, bone marrow, spleen, fetal liver, and lymphoid organs [110], as well as in immune cells, including immature plasmacytoid dendritic cells, myeloid dendritic cells, macrophages, and natural killer cells [115]. $Chemerin_1$ reportedly acts through many post-receptor signalling pathways. For example, in transfected Chinese hamster ovary cells, chemerin has been demonstrated to lead to Ca^{2+}-mobilization, inhibition of cAMP accumulation, and phosphorylation of p42 and p44 MAPK [111]. Chemerin dose-dependently activated ERK1/2, PI3K/Akt and MAPKs pathways in various cells, including endothelial cells, adipocytes, and skeletal muscle cells, through $Chemerin_1$ [112, 116, 117]. Also, activation of the protein kinase C by chemerin-9 stimulated the internalization of $Chemerin_1$ [118]. Most of these pathways, however, are blocked by pertussis toxin, indicating that $Chemerin_1$ is coupled to the Gi family of G proteins [111, 119].

Agonists for $Chemerin_1$ include the full-length recombinant chemerin peptide, which consists of 136 amino acids, and other short peptides derived from the full chemerin C-terminus, with chemerin-9 being the most used agonist in pharmacological

experiments [120]. Chemerin-9 constitutes the last nine amino acid residues of the C-terminal of the full-size chemerin and shows a similar EC_{50} (5 nM) in the recruitment of intracellular Ca^{2+} using Chinese hamster ovary cells expressing the human $Chemerin_1$, retaining most of the functional activity of the full-size protein [121]. In addition, the lipid Resolvin E1 (RvE1) was also reported as an activator of $Chemerin_1$ [122]. RvE1 is an anti-inflammatory lipid mediator and one study indicated a concentration-dependent inhibition of TNF-α by RvE1 in $Chemerin_1$-transfected HEK293 cells [122]. However, the activation of $Chemerin_1$ by RvE1 is still a matter of debate, as later studies have failed to confirm these findings [102]. On the other hand, CCX832 was developed as a selective antagonist for $Chemerin_1$ and shows low affinity over the other two chemerin receptors ($Chemerin_2$ and CCRL2) [93, 94].

1.4.2 Chemerin synthesis

In humans, chemerin is mainly secreted by the liver and adipose tissue, and the estimated concentration of active chemerin in plasma and serum is 3.0 and 4.4 nM, respectively [116, 123-125]. Chemerin is synthesised initially in mammalian cells as pre-prochemerin (1-163), a protein made up of 163 amino acids, before 20 amino acids from its N-terminal undergo proteolytic cleavage to form Prochemerin (21-163) (Figure 1.2). Prochemerin (18-kDa) has a low biological activity and shows poor $Chemerin_1$ binding and activation [111]. Most of the circulating chemerin is in the form of inactive prochemerin and is converted to the active chemerin by a proteolytic process when needed [105]. However, the C-terminal arm of prochemerin undergoes further cleavage at various sites by a number of serine and cysteine proteases to generate different isoforms of chemerin. To date, eight proteases have been

shown to C-terminally process prochemerin or chemerin in vitro, including carboxypeptidases, cathepsins, elastase, Factor XIIIa, Factor XIa, chymase, plasmin, and tryptase [120, 126]. The generated chemerin isoforms indicated different affinities for Chemerin$_1$; for example, the serine proteases elastase and cathepsin G remove six and seven amino acids from the C-terminal end of prochemerin, resulting in the most active form of chemerin (21-157 and 21-156, respectively) [127]. Also, neutrophil-derived enzymes can convert prochemerin and chemerin into shorter and inactive chemerin fragments, such as chemerin 21–155 [128]. Therefore, the C terminus is very important for chemerin function at Chemerin$_1$, which has also been proven by the synthetic C-terminal fragments of human chemerin, Chemerin-9, which contains the last nine amino acids from the full-size protein with similar functional activity.

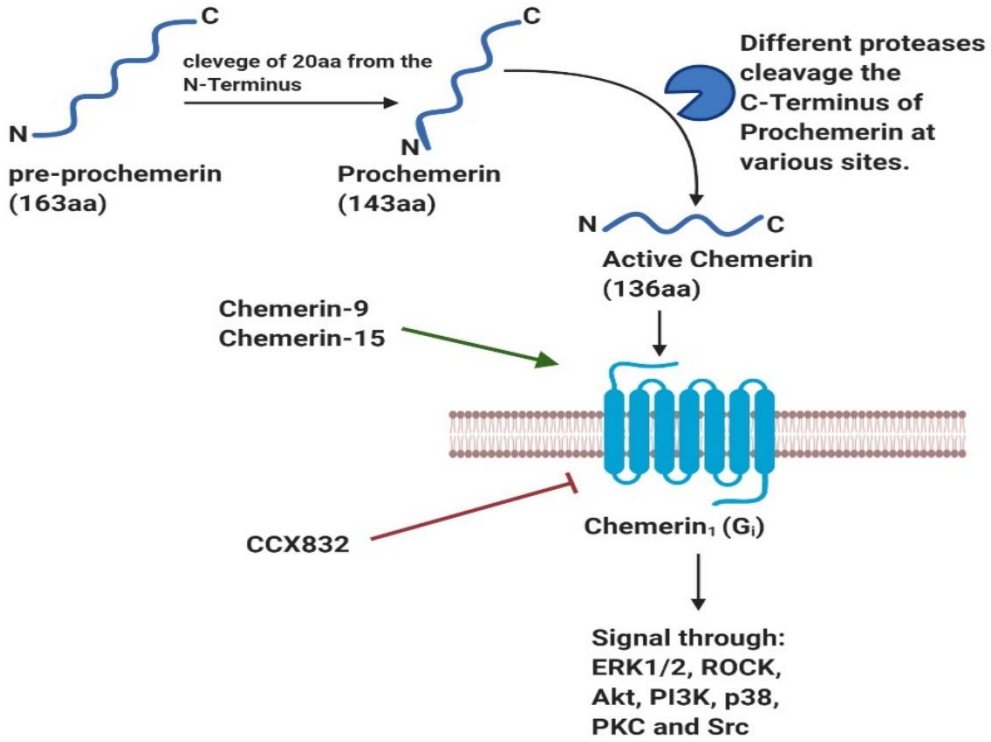


Figure 1.2: Chemerin synthesis and function at Chemerin$_1$. Prochemerin undergoes cleavage by different proteases like carboxypeptidases, cathepsins, elastase, Factor XIIIa, Factor

XIa, chymase, plasmin, and tryptase to form different isoforms of chemerin.

1.4.3 Chemerin functions

Initially, chemerin was described as a chemoattractant agent in the study by Wittamer *et al.* (2003), where chemerin promoted chemotaxis of leukocyte populations that expressed $Chemerin_1$ [111]. However, subsequent studies revealed that chemerin is also involved in adipogenesis, angiogenesis, cardiovascular diseases, and metabolic disorders. Chemerin was shown to exert both pro-inflammatory and anti-inflammatory effects via $Chemerin_1$. The pro-inflammatory chemotactic effect of chemerin is well characterized by the transmigration of leukocytes and macrophages in humans and mice [129-133]. Positive correlations of systemic chemerin with inflammatory cytokines have been described in chronic inflammatory diseases, such as rheumatoid arthritis, inflammatory bowel disease, psoriasis, and chronic renal disease [134-136]. Furthermore, $Chemerin_1$ is upregulated by proinflammatory cytokines, including TNF-a, IL-1b, and IL-6, in human endothelial cells [112]. By contrast, the anti-inflammatory effects of chemerin were shown by Cash and colleagues (2008), in which the chemerin peptide chemerin15 (which consisted of 15 amino acids from the C-terminal end of the full peptide), but not the full-size protein, enhanced macrophage phagocytosis, leading to improved microbial particle clearance and apoptotic neutrophil ingestion [137]. However, this anti-inflammatory effect of chemerin may be attributed to the different roles played by chemerin via its various isoforms in different phases of inflammation.

Chemerin was first described as an adipokine in a study by Goralski *et al.* (2007), which showed high level expression of

chemerin and Chemerin$_1$ in mouse and human adipocytes as well as the ability of cultured 3T3-L1 adipocytes to secrete chemerin protein [116]. Chemerin and Chemerin$_1$ gene knockdown with small hairpin RNA (shRNA) impaired differentiation of 3T3-L1 preadipocytes, indicating an important role of chemerin in obesity and adipogenesis [116]. This was shortly followed by another study confirming chemerin and Chemerin$_1$ in rat adipocytes and pre-adipocytes, with their mRNA expression dramatically increased during the differentiation of 3T3-L1 cells and human preadipocytes into full adipocytes [113]. In this latter study, the author demonstrated that recombinant chemerin induced the activation of ERK1/2 and lipolysis in fully differentiated 3T3-L1 adipocytes [113]. Consistent with these findings, data from human studies indicated a positive correlation between total chemerin plasma level and BMI, waist-to-hip ratio, visceral adipose tissue mass, glucose levels, and circulating triglycerides [123, 138-141]. Additionally, exercise and bariatric surgery-induced weight loss resulted in decreased chemerin levels in obese individuals [138, 141, 142]. Also, disruption of Chemerin$_1$ gene in vivo reduces body mass and fat deposition of mice [143]. Taken together, these results support chemerin as a risk factor and an effective biomarker for obesity and obesity-associated metabolic and cardiovascular diseases.

In the vasculature, chemerin is released from PVAT, and the expression of Chemerin$_1$ has been confirmed in endothelial cells, VSMCs, and PVAT [94, 144, 145]. Chemerin is involved in angiogenesis, and there is a positive correlation between chemerin serum/plasma concentration and various vascular pathologies, including hypertension, atherosclerosis, and atrial fibrillation [112, 120, 146, 147]. In human aortic and coronary

arteries with atherosclerotic lesions, chemerin and Chemerin$_1$ were expressed in PVAT and foam cells, and both were positively correlated with the severity of atherosclerosis [144]. Also, the proinflammatory nature of chemerin that induces chemotaxis of dendritic cells, macrophages, and natural killer cells that express Chemerin$_1$ may contribute to the progression of atherosclerosis [102].

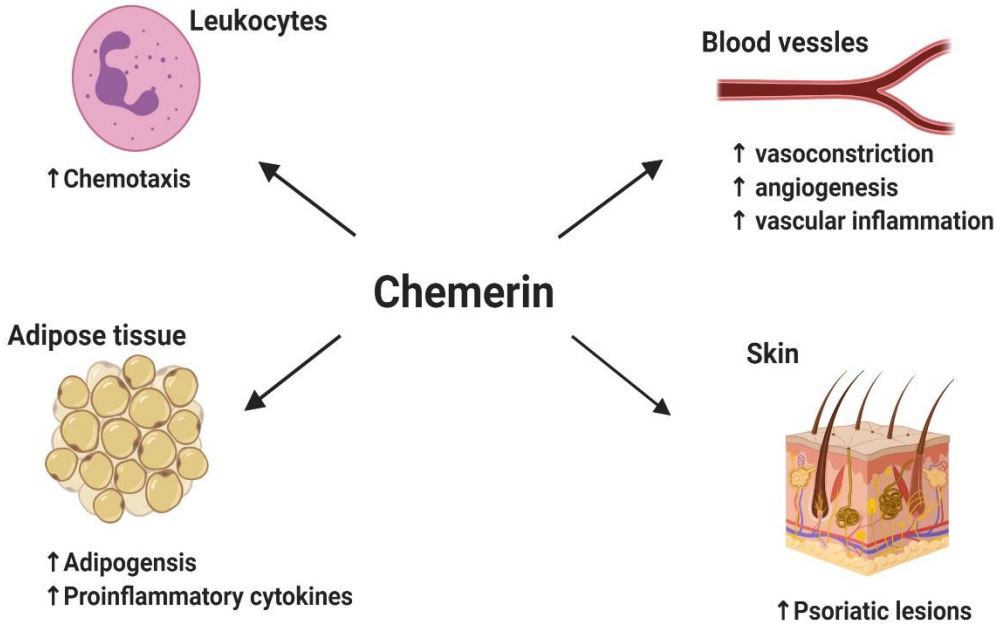


Figure 1.3: Summary of some chemerin functions on leukocytes, blood vessels, adipose tissue and skin. Chemerin is involved in adipogenesis, angiogenesis, cardiovascular diseases, and metabolic disorders.

Chemerin, either as chemerin-9 or full-length recombinant peptide, caused concentration-dependent contractions in the isolated rat thoracic aorta, superior mesenteric artery, and mesenteric resistance artery through increased intracellular calcium [94]. In chemerin knockout rats, blood pressures at baseline were not different between the knockout and wild type but with the hypertensive challenge of deoxycorticosterone acetate and salt, the male knockout rats developed a significant

higher blood pressure than the wild type [148]. Also, two recent studies demonstrated that destruction of chemerin pre-mRNA using antisense oligonucleotide resulted in reductions of whole body chemerin and caused small, yet statistically significant blood pressure reductions in normal chow-fed male rats and large reduction of blood pressure in high-fat diet-fed rats [149, 150]. In the same vain, Kennedy *et al.* (2014) reported that chemerin-9 induced direct vasocontraction in human saphenous vein and resistance arteries, as well as increased blood pressure in rats; however, all these effects were absent with the use of the $Chemerin_1$ antagonist CCX832 [93]. Also, the selective $Chemerin_1$ antagonist CCX832 inhibited PVAT-induced contraction in rat thoracic aorta and mesenteric resistance artery, identifying PVAT as an important source of chemerin and indicating a new mechanism of PVAT-mediated regulation of blood pressure [94]. Additionally, chemerin reportedly potentiated vascular responses to established vasoconstrictors, such as endothelin-1, serotonin, and electrical field-stimulation, in isolated rat arteries [151-153]. Taken together, these data from human and animal studies indicate that endogenous chemerin significantly contributes to vasocontraction, and the upregulation of chemerin serum levels could independently lead to hypertension.

In summary, chemerin, is an adipokine that is upregulated in obese and hypertensive patients and able to promote chemotaxis of most leukocyte populations as well as induce direct vasoconstriction, might therefore constitute a link between obesity, inflammation, and hypertension.

1.5 Statins

Statins or 3-hydroxy-3-methylglutaryl coenzyme A (HMG-CoA) reductase inhibitors are a group of lipid-lowering agents that

inhibit cholesterol biosynthesis and are considered principal drugs in the primary and secondary prevention of CVDs and in the treatment of hypercholesterolaemia. Statins are extremely effective in reducing both the morbidity and mortality associated with adverse cardiovascular and cerebrovascular events, particularly CVDs and stroke, in high-risk populations [154]. In the UK, there are five types of statin available on prescription, including atorvastatin, fluvastatin, pravastatin, rosuvastatin, and simvastatin [155]. These statins are well tolerated, very safe and effectively lower serum LDL-cholesterol levels and maintain this effect over periods of many years [156]. Side effects of statins are rare, including statin myopathy (any muscle pain related to statins), rhabdomyolysis (the breakdown of skeletal muscle fibres), and increased liver enzymes [157, 158]. The mechanism by which statin-induced skeletal muscle manifestations is not fully understood; it might be due to the inhibitory effect of statins on the regulatory proteins (such as Ras, Rho, and Rac), although other researchers have attributed that to accumulation of statins in myocytes [159, 160]. Also, it has been suggested that statins may interfere with mitochondrial function, which could in turn impair muscle function and damage muscle morphology [161].

Even though statins have the same mode of action and relative effects on cholesterol levels, it is possible to categorise them into large groups based on the methods of their derivation. These are the natural statins of fungal origin and synthetically derived statins. Naturally derived statins, such as lovastatin, pravastatin, and simvastatin, have closely related homological structures. Examples of synthetic statins include atorvastatin and fluvastatin [162].

1.5.1 Pharmacokinetics of statins

Statins have varied pharmacokinetic properties and show major differences in terms of bioavailability, lipophilicity, metabolism and half-lives [163]. Regarding lipophilicity, lipophilic statins, such as simvastatin and lovastatin, have the ability to enter different cells by passive diffusion, whereas hydrophilic statins, such as pravastatin and rosuvastatin, are assumed to primarily target the liver, where the organic anion transporter (OATP-C) is expressed for their uptake [164]. The differences in lipophilicity of statins are widely thought to account for some of the observed differences in their peripheral side effects [165]. All statins are administered orally in their active form, except simvastatin and lovastatin, which are taken as a lactone prodrug and are hydrolysed by liver enzymes to the active drug [166]. Moreover, statins are extensively metabolised in the liver by cytochrome P450, and most statins have a plasma half-life of 1 to 3 hours, except rosuvastatin and atorvastatin, with half-lives that can reach up to 20 and 14 hours, respectively [167].

1.5.2 Mechanism of action

The primary mode of action of statins is a competitive and reversible inhibition of HMG-CoA reductase; this is a rate-limiting process in cholesterol biosynthesis responsible for the conversion of HMG-CoA to L-mevalonic acid (mevalonate) (Figure 1.4). Inhibition of HMG-CoA reductase leads to a reduction of cholesterol levels in the hepatocytes, which in turn leads to upregulation of low-density lipoprotein (LDL) receptors and promotes the uptake of cholesterol-rich LDL and LDL precursors from the circulation [168]. The endogenous HMG-CoA moiety of all statins binds competitively with the HMG-CoA reductase catalytic domain, which prevents HMG-CoA access to the active sites [169]. Further, statins have been shown to

cause a reduction in triglyceride levels and an increase in high-density lipoprotein (HDL) content in patients with coronary heart disease [170, 171]. In humans, treatment with statins reduced levels of total cholesterol (20-35 %), LDL-C (25–55 %), and triglycerides (10–20 %), as well as increased levels of HDL-C (5-10 %) [172].

1.5.3 The pleiotropic effects of statins

Several landmark clinical trials indicated that statins exert significant effects beyond their impact on lowering cholesterol synthesis; such cholesterol-independent effects are called pleiotropic effects. Examples of these clinical trials include the West of Scotland Coronary Prevention (WOSCOP) and Cholesterol and Recurrent Events (CARE) studies, where the sub-analysis of both studies indicated that in age-matched individuals with equal serum cholesterol levels, the statins-treated group showed a significantly lower risk of coronary heart disease compared to the placebo group [173-175]. However, as statins are used in the prevention of CVDs, most of the observed statins' pleiotropic effects were also related to the cardiovascular system. These cardiovascular-related pleiotropic effects of statins include improving and restored endothelial function [176, 177], decreasing vascular inflammation [178], attenuated vascular and myocardial remodelling, increasing the bioavailability of nitric oxide with subsequent vasodilatation [179], decreasing blood pressure [180], enhancing the stability of atherosclerotic plaques, inhibiting the thrombogenic response, lowering oxidative stress, and decreasing VSMC proliferation and migration [181].

Mevalonate is a precursor for many biologically active molecules; thus, the inhibition of mevalonate by statins also results in the inhibition of these molecules (Figure 1.4). The

best known of them are the lipophilic isoprenyl groups farnesyl-pyrophosphate (FPP) and geranylgeranyl-pyrophosphate (GGPP). FPP and GGPP are important in facilitating cell membrane attachments for many intracellular signalling molecules, including GTP-binding proteins such as Ras, Rac, and Rho [182]. Ras, for example, depends on farnesylation for its translocation from the cytoplasm to the cell membrane, whereas Rho translocation is dependent on geranylgeranylation [183]. However, these small GTP-binding proteins are thought to be important in the regulation of different vascular activity, such as increased expression of endothelial -1 (ET-1), upregulation of endothelial NO synthase (eNOS) expression, elevation of VSMC proliferation and migration, and increasing oxidative stress [181, 184]. Therefore, the end result of statins in the inhibition of Rho, Ras, and their downstream targets is a likely mechanism mediating some of the pleiotropic effects of statins on vascular cells.

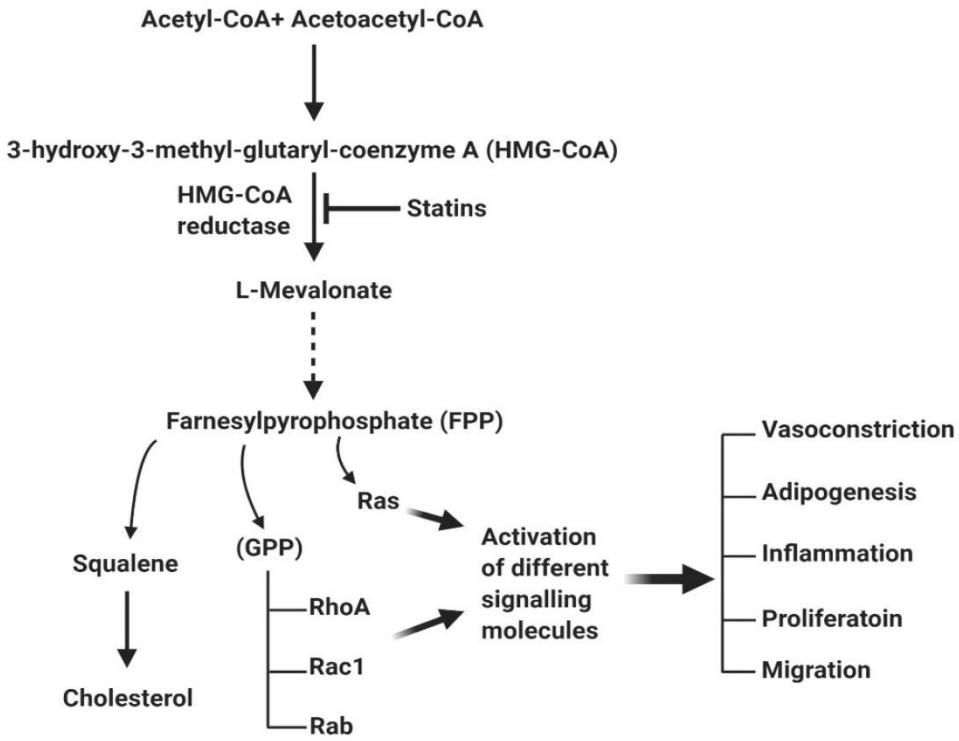


Figure 1.4: Cholesterol biosynthesis pathway and site of statins action. Inhibition of HMG-CoA reductase by statins decrease isoprenoid intermediates such as farnesyl-pyrophosphate (FPP) and geranylgeranyl-pyrophosphate (GPP), with subsequent inhibition in isoprenylation of signalling molecules, such as Ras, Rho, and Rac, leads to modulation of various functions.

1.5.3.1 Pleiotropic effects on vascular tone

One important pleiotropic effect of statins is the regulation of vasomotor, as different statins showed the ability to induce vascular relaxation in endothelium-dependent and independent manners mediated through multiple pathways. Several studies have revealed that statins could modulate the activities of different ion channels of the blood vessels such as inhibition of calcium influx through L-type calcium channels and opening of Ca^{2+}-activated K^{+} channels [185, 186]. In isolated porcine coronary arteries, simvastatin, but not pravastatin, produced

endothelium-independent relaxation by reducing calcium influx through effects on the mitochondria [187]. Lipophilic statins showed similar vasorelaxation effects in other vascular beds from different species, including bovine coronary arteries [188], rat aorta and small mesenteric arteries [189], rats' internal anal sphincter [190] and isolated rabbits' jejunal preparations [191]. To a lesser extent, hydrophilic pravastatin can induce endothelium-dependent relaxation of vascular tone in vitro and in vivo [192, 193]. The observed lipophilicity dependency of the statin-induced vasoactive effect is most likely attributed to the organic anion transporters required for the cellular uptake of hydrophilic statins [194]. Lastly, further evidence in support of the statin-induced vasorelaxation effect comes from clinical studies, where simvastatin lowered blood pressure in patients with hypertension and in patients with type II diabetes [195, 196].

1.5.3.2 Pleiotropic effects on nitric oxide bioavailability

Endothelium derived nitric oxide (NO) produced by endothelial NO synthase (eNOS) is a major regulator of vascular function. The low bioavailability of NO is considered a biomarker for endothelial dysfunction due to the contribution of endothelial NO in vasodilatation, platelet aggregation, and vascular smooth muscle proliferation [197]. However, Rho/Rho kinase pathway negatively regulates eNOS phosphorylation, most likely through inhibition of protein kinase B (Akt) [198, 199]. As previously mentioned, statins can lead to the inhibition of Rho isoprenylation and thus regulate NO bioavailability. Shiga *et al.* (2005) showed that treatment with simvastatin attenuated vascular contractility by enhancing endothelial NO production in rabbit mesenteric arteries [199]. Furthermore, atorvastatin promotes NO production in endothelial cells by decreasing

caveolin-1 (inhibitor of eNOS activation) expression, regardless of the level of extracellular LDL-cholesterol, indicating another mechanism of statins-induced enhancement of NO bioavailability [200]. Therefore, one of the main contributors to statins' protective pleiotropic effect is the increase in NO bioavailability, resulting in increased vasodilatation and may enhance myocardial blood flow under hypoxic conditions [181].

1.5.3.3 Anti-inflammatory pleiotropic effects

An early step in atherogenesis involves leukocyte adhesion to the endothelium, an effect that is enhanced by adhesion molecules, such as intercellular adhesion molecule-1 [179]. The mechanism of statins' anti-inflammatory effect is thought to occur through reducing the number of inflammatory cells in atherosclerotic plaques as well as inhibition of adhesion molecules, such as intercellular adhesion molecule-1 and cytokines like IL-6, which are involved in the recruitment of inflammatory cells [201, 202]. Moreover, two clinical trials have demonstrated a significant reduction in the levels of C-reactive protein (CRP) in response to statin therapy at the end of one year and over a five-year period, indicating a role of statins in reducing systemic and vascular inflammatory response [203, 204]. However, more studies are needed to draw a conclusion about the exact mechanism of the anti-inflammatory effect of statins.

1.6 Statins and adipose tissue

Adipose tissue is an active endocrine and paracrine organ that modulates vascular function, with implications for the pathophysiology of CVDs (see Section 1.2). The possible interaction between statins and adipose tissue is poorly characterized. In 3T3-L1 cells, two independent studies reported that treatment with atorvastatin inhibited the

differentiation of 3T3-L1 pre-adipocytes into full adipocytes and decreased cell viability in a Rho kinase-dependent mechanism [205, 206]. Also, lovastatin inhibited adipocyte differentiation, apparently by downregulating the expression of fat cell specific gene peroxisome proliferator-activated receptors gamma (PPARγ) [207]. However, adipose tissue surrounding blood vessels, namely PVAT, secretes several molecules (cytokines, adipokines, nitric oxide, and hydrogen sulphide) and is able to influence different functions on the underlying vasculature (see Section 1.3). In a very interesting study, Zeng *et al.* (2009) examined the vasorelaxant effect of PVAT in spontaneously hypertensive rats and reported that contraction of the thoracic aorta induced by phenylephrine was significantly attenuated in the presence of PVAT from normotensive rats or spontaneously hypertensive rats treated with atorvastatin (50mg/kg/day) [208]. This effect was not seen in thoracic rings from the control spontaneously hypertensive rats, indicating that atorvastatin is able to restore the beneficial anti-contractile properties of PVAT, which are lost in the hypertensive model [208]. Furthermore, another group observed that a high concentration of lipophilic atorvastatin, but not hydrophilic pravastatin, increased net H_2S production in PVAT by inhibiting its mitochondrial oxidation, which resulted in the augmentation of PVAT anticontractile effect [209]. Lastly, epicardial adipose tissue thickness and pro-inflammatory status were significantly lowered in patients with aortic stenosis taking statins [210].

Adipose tissue-induced release of adipokines, such as chemerin, leptin, and adiponectin, are important in their ability to influence vascular and non-vascular biology [211]. There are contradictory results in the literature regarding the effect of statins on the adipokine profile. Pravastatin treatment

increased adiponectin production and expression in 3T3-L1 adipocytes, and plasma adiponectin levels were significantly increased in pravastatin-treated mice [212]. In patients with CVD and hypercholesterolaemia, serum adiponectin concentrations increased in response to atorvastatin, pitavastatin, and pravastatin [213-216]. By contrast, other studies in healthy humans and patients with hypercholesterolemia indicated no change or even reduced serum concentration of adiponectin following treatment with statins like simvastatin, pravastatin, fluvastatin, and atorvastatin [217-220]. However, even in studies that indicated the inhibitory effect of statins on adiponectin levels, this effect is more likely related to the lipid-lowering action of statins (and not a pleiotropic effect), given that other lipid-lowering agents, such as fibrates and niacin, are widely reported to increase adiponectin in studies on humans and *in vitro* studies [221-225] (for more see [226, 227]).

Similar to adiponectin, the effect of statins and other lipid-lowering drugs on leptin serum concentrations indicated controversial findings. Atorvastatin treatment (40 mg/day) in obese subjects with type 2 diabetes and in rabbits with hypercholesterolaemia significantly reduced plasma leptin concentrations [228, 229]. However, in healthy individuals and in patients with hypercholesterolaemia, treatment with atorvastatin (10 mg/day) and pravastatin (10 mg/day) showed no effect on serum leptin concentration [213, 217]. A possible explanation for this discrepancy may be attributed to the difference in doses used. Also, niacin and fibrate therapy showed opposite and no effect on leptin serum concentrations in humans and in hypercholesterolemic rabbits [225, 230-233]. However, more studies are needed to make a definitive

conclusion on the effects of statins on serum leptin levels, especially in healthy humans, as the existing studies are scarce and inconclusive.

The effects of statins and other lipid-lowering agents on chemerin synthesis and release is poorly documented. In fact, only two recent studies in the literature compared the effects of statins on the levels of chemerin; the first was an observational clinical study in 63 patients with acute myocardial infarction (AMI) [234]. AMI patients were randomized to receive treatment with high-dose atorvastatin (80 mg/day) or rosuvastatin (40 mg/day) for 4 weeks. The results indicated 50 % and 40 % decreases in serum chemerin levels in patients treated with atorvastatin and rosuvastatin, respectively [234]. The second study was done by Guo *et al.* (2020), in which they examined the effect of simvastatin on the differentiation of bone-marrow derived mesenchymal stem cells (BMSCs) into full adipocytes [235]. Incubation of the BMSCs with 100 nM simvastatin during the differentiation process downregulated the gene expression of chemerin and upregulated the expression of $Chemerin_1$, which resulted in the inhibition of adipogenesis. The authors attributed this effect to the ability of simvastatin to inhibit the upregulation of PPARγ and PPARγ-mediated enhanced chemerin expression in BMSCs [235]. However, the study makes no attempt to verify the change in chemerin release or if the decrease in chemerin gene expression might be reflected on the protein level following the simvastatin treatment. Regarding other lipid-lowering agents, one study reported that 24 h treatment of differentiated bovine adipocytes with 10 μM nicotinic acid indicated a 3-fold increase in the mRNA abundance of chemerin [236].

In summary, on the basis of the evidence currently available, it seems fair to suggest that statins exert many pleiotropic effects in addition to the lowering of serum cholesterol levels. These additional properties are evident not only in patients with hypercholesterolemia but also in those with normal cholesterol levels [237]. Most of the pleiotropic effects of statins in the literature nowadays are related to the role of statins in the inhibition of isoprenoid synthesis. Despite the fact that adipose tissue and PVAT, in particular, have emerged as potential modulators of vascular activity in normal and disease states, studies on possible interactions with statins are scarce. Thus, it remains to be determined whether statins' pleiotropic regulation of vascular biology is dependent on their effect on the functional responses of vascular modulators such as PVAT. Understanding the beneficial pleiotropic effects of statins is not only important to optimize and expand statin use in the treatment and prevention of cardiovascular disease but also to find potential drug targets in the future.

1.7 Aims

The majority of blood vessels are surrounded by adipose tissue, which is referred to as perivascular adipose tissue (PVAT). The recent acknowledgement of the role of PVAT in vascular modulation has been supported by many studies indicating PVAT as a promising drug target in many diseases, including obesity and obesity-related CVDs. However, less is known about the ability of current cardiovascular drugs to alter PVAT functional responses. Statins seem to be potential candidates due to their well-known pleiotropic effects. Therefore, the principal aim of this study was to determine the possible effects of statins on PVAT vascular regulation of the porcine coronary artery (PCA). Porcine coronary artery was chosen as a model in the current thesis because cardiovascular system of pigs is in similar fashion to human in terms of heart size, anatomy and coronary distribution, hemodynamic parameters as well as in pathology like hypertension and obesity [238, 239]. Also, using PCA to study PVAT effects on vascular tone has been validated by many studies in the literature (see [87, 240, 241]).

The specific aims of the present study are as follows:

- To assess the effect of statins on PVAT-induced contraction in porcine coronary arteries.
- To examine the effect of statins on chemerin release by porcine coronary PVAT and chemerin release by 3T3-L1 adipocytes.
- To determine the effect of thromboxane receptor activation on chemerin-induced contraction of the porcine coronary artery and to investigate the possible signalling pathway that underlies this process.

Chapter 2

Effects of statins on perivascular adipose tissue-induced vasoconstriction of porcine coronary arteries

2.1 Introduction

Statins or 3-hydroxy-3-methylglutaryl coenzyme A (HMG-CoA) reductase inhibitors are a group of therapeutic agents that inhibit cholesterol biosynthesis and are 'drugs of choice' for the prevention of hypercholesterolaemia. The primary mode of action of statins is a competitive and reversible inhibition of HMG-CoA reductase—a rate-limiting process in cholesterol biosynthesis that is responsible for the conversion of HMG-CoA to L-mevalonic acid (mevalonate) [242].

Statins have been shown to have major clinical effects on improving cardiovascular outcomes; however, these cardiovascular benefits cannot be totally attributed to changes in lipid profile alone, suggesting that the beneficial effects of statins may extend beyond their effects on the reduction of cholesterol levels [181, 182]. Several studies have demonstrated the role of statins in the regulation of vascular smooth muscle tone through different mechanisms. Treatment with simvastatin has been shown to produce vasorelaxation of both rat aorta and superior mesenteric arteries, with and without functional endothelial cells [243]. Also, pravastatin, atorvastatin, and cerivastatin were reported to induce concentration-dependent relaxation of isolated rat aortic rings and small mesenteric arteries via endothelium-dependent and mevalonate-related pathways [244, 245]. In a previous study, our group found that simvastatin produced an endothelium-independent relaxation of porcine coronary arteries through alteration of mitochondrial membrane potential, which could lead to inhibition of calcium influx [187].

Multiple mechanisms have been suggested to underpin the vasorelaxation effects of statins. Most studies have only focused on their effects on vascular smooth muscle and/or the

endothelium. However, recent evidence indicates that perivascular adipose tissue (PVAT), which surrounds most of the systemic blood vessels throughout the body, can affect vascular functions by producing vasoactive mediators. PVAT-induced release of adipokines (such as adiponectin, prostaglandin, and chemerin), cytokines (such as IL-6 and TNF-α), and gasotransmitters (especially H_2S and NO) can influence different functions of the underlying vasculature [43]. It is therefore reasonable to hypothesise that at least some beneficial effects of statins on vascular tone may occur through their direct action on PVAT.

In a study that examined the effects of atorvastatin (50 mg/kg/day) on PVAT-dependent modulation of vascular relaxation, the influence of hypertension was assessed in spontaneously hypertensive rats (SHRs). The study indicated that the contraction of PVAT-intact thoracic aorta induced by phenylephrine was attenuated in both the normotensive control rats and in the SHR arteries treated with atorvastatin; this effect was not observed in the SHR group that are not treated with atorvastatin. Notably, there was no difference between the SHRs treated with atorvastatin and the control SHRs in the contraction induced by phenylephrine in the PVAT-free thoracic aorta. This suggests that atorvastatin acts via PVAT (but not on VSMC) and is able to restore the beneficial anti-contractile properties of PVAT, which are lost in the hypertensive model [208]. In another study by Wójcicka *et al.* (2011), treatment with lipophilic atorvastatin, but not hydrophilic pravastatin, increased net H_2S production in PVAT by inhibiting its mitochondrial oxidation via a mevalonate-dependent pathway. This effect of atorvastatin resulted in the augmentation of the anticontractile effects of PVAT on the adjacent vessels [209].

Based on recent literature, only a few studies have investigated the direct effects of statins on PVAT, and none of them tested the ability of statins to affect adipokine release via PVAT. Therefore, the aim of the present study was to determine the effects of statins on PVAT regulation of vascular tone of porcine coronary arteries (PCAs).

2.2 Materials and Methods

2.2.1 Tissue preparation

Hearts from pigs of both sex (large white hybrid pigs, 4–6 months old) were brought to the laboratory from a local abattoir in ice-cold modified Krebs–Henseleit solution (composed of 118 mM NaCl, 4.8 mM KCl, 1.1 mM $MgSO_4$, 25 mM $NaHCO_3$, 1.2 mM KH_2PO_4, 11.6 mM D-glucose, and 1.25 mM $CaCl_2$) previously gassed with 95 % O_2 and 5 % CO_2. Upon arrival from the abattoir, the left PCAs were dissected and then refrigerated overnight at 4 °C in Krebs–Henseleit solution. The following day, PCAs were finely dissected and cleaned of adherent connective tissue and fat. The distal parts of the PCAs were then carefully cut into rings of about 2 mm in length and 0.5 to 1 mm in diameter and mounted between two wires in a four-channel wire myograph (Model 610M, DMT, Aarhus N, Denmark; Figures 2.1–2.3) filled with 5 ml Krebs–Henseleit solution maintained at 37 °C and aerated with a 95 % O_2 and 5 % CO_2 gas mixture, or with air and 5 % CO_2 gas, in different experiments. The wire myograph was connected to a PowerLab recording system (ADInstruments, Oxfordshire, UK) to measure and record tension in the PCAs.

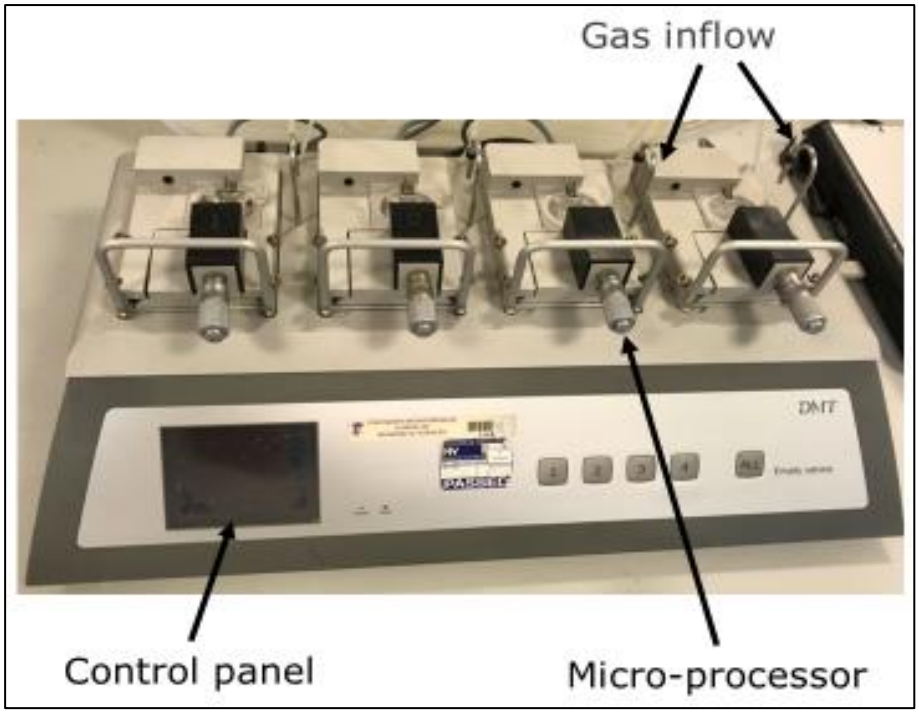


Figure 2.1. Multichannel wire myograph.

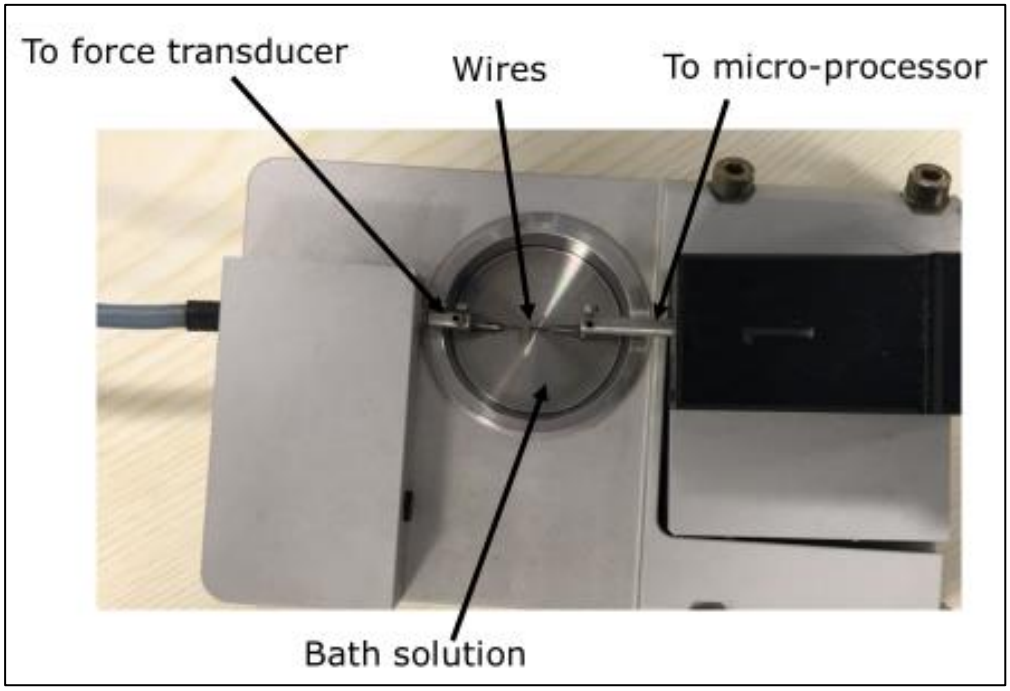


Figure 2.2. Single channel of a wire myograph.

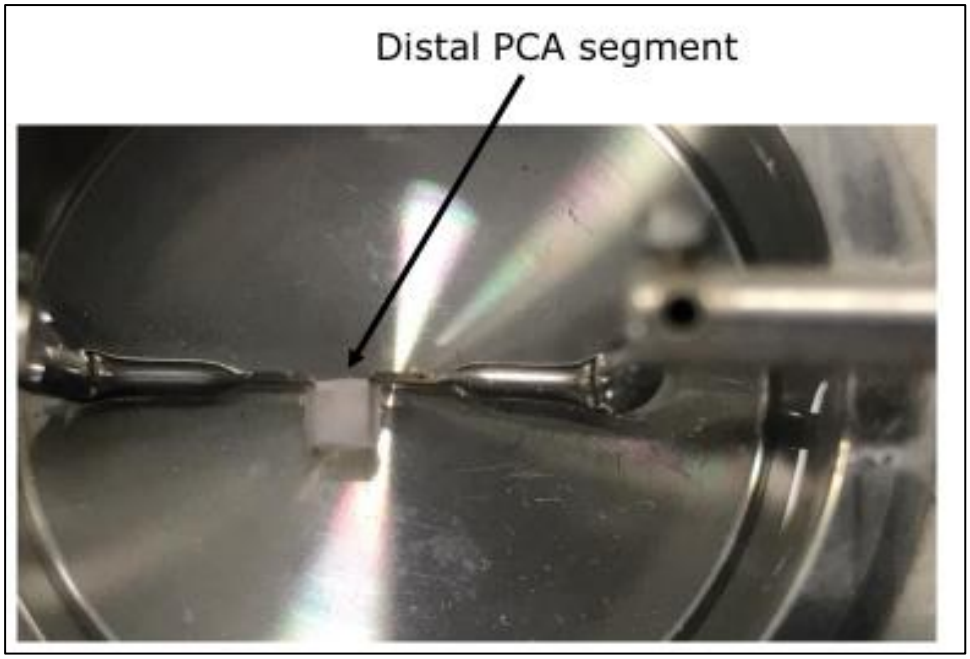


Figure 2.3. Distal PCA ring mounted in a wire myograph channel.

2.2.2 Experimental protocol

Vessels were mounted in a wire myograph and equilibrated for about 45 min under 3 g tension, determined from preliminary studies in the laboratory as the base optimal tension [246]. After equilibration, KCl (60 mM) was added to the bath to confirm tissue viability. After 20 min, the KCl was washed with fresh Krebs–Henseleit solution, and following the return to a stable baseline (15–20 min), exposure to 60 mM KCl was repeated to determine the contractile capacity of each vessel. Again, the tissue was washed with Krebs–Henseleit solution to allow the segment tone to re-stabilise to the baseline. To avoid seasonal and individual variations, adjacent coronary arterial segments from the same animal were always used as controls, and the data were calculated and expressed as percentages of the contraction in response to the second KCl addition. After reaching the baseline level, 0.3 g of PVAT taken from the distal parts of fresh PCAs was added to the side of the bath either at

the baseline or following the precontraction of the vessels with the thromboxane A_2 mimetic, 9,11- dideoxy-9a,11a-epoxymethanoprostaglandin $F_{2\alpha}$ (U46619), to a level between 40 and 60 % of the maximum second KCl response. In tissues precontracted with U46619, the change in tension was recorded from the point where 0.3 g of PVAT was added to the bath. The PVAT was re-added to the bath rather than left attached to the tissue in order to examine the effect of statins on the fat itself and dismiss any direct effect of statins on the blood vessel. The amount of PVAT used (0.3 g) was determined from preliminary studies in the lab [92], and other published work [240] as the amount that produces a measurable, reproducible response in PCA. The concentration of U46619 required to produce this level of contraction in the control PCA rings ranging from 1 nM to 10 nM but this concentration was different depending on the conditions (for example, the presence of inhibitors). Therefore, the concentration was adjusted accordingly, as indicated in the results section.

Effects of simvastatin, pravastatin, lovastatin, and indomethacin on PVAT-induced contraction in PCAs

To study the effects of statins and indomethacin on PVAT, the PCAs were separately incubated with either simvastatin (1 or 10 μM), lovastatin (10 μM), or pravastatin (10 μM) for 2 h, or with indomethacin (10 μM) for 30 min, to inhibit cyclooxygenase (COX) [64]. The concentrations and incubation time of simvastatin were determined from previous study in the lab that showed 10 μM was the optimal concentration for simvastatin which reached maximum relaxation in PCA following 2 h incubation [187]. Control segments contained vehicle only (0.1 % v/v DMSO for simvastatin, lovastatin, and indomethacin). Following the incubation time, 0.3 g of fresh

distal PVAT was added to the side of the bath either at baseline tone or after precontraction with U46619 to a level between 40–60 % of the second KCl, and tension was then recorded for up to 60 min. In a different set of experiments, to determine whether extracellular calcium was involved in the simvastatin-mediated inhibition of PVAT-induced contraction in PCAs, the Krebs–Henseleit buffer was replaced with calcium-free Krebs–Henseleit buffer in which the calcium chloride had been replaced with 2 mM ethylene glycol bis (β amino ethyl ether)-N,N,N,N-tetra acetic acid (EGTA), with or without 10 μM simvastatin. In control segments, vessels were incubated in normal Krebs–Henseleit buffer in the presence or absence of 10 μM simvastatin. A higher concentration of U46619 was required to induce contraction in the absence of extracellular calcium as well as in tissues exposed to the previously mentioned drugs; thus, U46619 concentrations were adjusted accordingly as indicated in the results section.

Effects of simvastatin on transferring bath solution from PVAT to PCA rings

To determine whether simvastatin could affect PVAT-derived transferable molecules, the bath solutions (7.5 ml) in one wire myograph were incubated in the absence of PCA with either PVAT + 10 μM simvastatin, PVAT + vehicle control (0.1 % v/v DMSO), 10 μM simvastatin only, or 0.1 % v/v DMSO only. After 2 h of incubation, the entire bath solution was then manually transferred to another wire myograph containing four PCA segments from the same animal (as a bioassay), and the change in tone was recorded for 60 min.

Effects of Ca^{2+} reintroduction in KCl-depolarised PCA in the presence of 10 μM simvastatin

To assess the effects of simvastatin on the influx of calcium through voltage-gated calcium channels, the effects of simvastatin on $CaCl_2$-induced contraction in calcium-free Krebs–Henseleit solution were investigated. PCA vessels were incubated with simvastatin (10 μM) or vehicle control (0.1 % v/v DMSO) for 120 min in calcium-free Krebs–Henseleit buffer, followed by the addition of 60 mM KCl. Once stable tone was achieved, cumulative concentration curves for responses to calcium chloride re-introduction (10 μM– 30 mM) were constructed.

2.2.3 Determination of TXB_2, $PGF_{2\alpha}$, and chemerin levels by ELISA in the presence of simvastatin

ELISA was used to determine the levels of $PGF_{2\alpha}$, chemerin, and TXB_2 (a stable metabolite of thromboxane (TXA_2)) released by PVAT into the Krebs–Henseleit solution. 0.3 g of PVAT was taken from fresh PCAs and added to a four-channel wire myograph filled with 7.5 ml Krebs–Henseleit solution maintained at 37 °C and aerated with a 95 % O_2 and 5 % CO_2 gas mixture. The PVAT was incubated in the Krebs–Henseleit buffer with simvastatin (1 μM or 10 μM) or vehicle control (0.1 % v/v DMSO) for 120 min to maintain consistency with the functional studies. After treatment, the Krebs–Henseleit solution was collected and stored in -80 °C for ELISA study. $PGF_{2\alpha}$, chemerin, and TXB_2 levels in the Krebs–Henseleit solution were then determined using a pig $PGF_{2\alpha}$ ELISA Kit (ab133041, Abcam, Cambridge, UK), a pig chemerin ELISA Kit (abx257462, Abbexa, Cambridge, UK), or a pig TXB_2 ELISA Kit (ab133022, Abcam, Cambridge, UK). Samples were added directly to the provided 96 well plate without dilution and the protocol was followed according to the manufacturer's instructions. The results were expressed as

picograms (pg) of $PGF_{2\alpha}$, chemerin, or TXB_2 released per ml of Krebs–Henseleit solution.

2.2.4 Statistical analysis

All values are expressed as means ± SEM (standard error of the mean) from at least six independent experiments, with n representing the number of different animals. Time-response curves were obtained graphically using Graphpad Prism (version 7, GraphPad Software, La Jolla, California, USA). The contractile responses were expressed as percentages (%) of the contraction induced by 60 mM KCl. Statistical tests were performed using a two-tailed, paired Student's *t*-test to compare differences between the two groups. Differences between three or more groups were assessed using one-way ANOVA or two-way ANOVA in conjunction with a Sidak's *post-hoc* test. *p* values less than 0.05 ($p < 0.05$) were considered to be statistically significant. Asterisks (*) indicate differences between the groups of data whereas hash tags (#) indicate differences at individual time points. **** indicates $p < 0.001$, *** indicates $p < 0.001$, ** indicates $p < 0.01$, and * indicates $p < 0.05$.

2.2.5 Drugs and chemicals

All drugs were purchased from Tocris–Cookson (Bristol, UK), except indomethacin, which was obtained from Sigma-Aldrich (Poole, UK). Stock solutions of pravastatin and KCl were dissolved in distilled water. Stock solutions of indomethacin, U46619, simvastatin, and lovastatin were dissolved in dimethyl sulfoxide (0.1 % v/v DMSO). All further dilutions of the stock solutions were made using distilled water, except for simvastatin, which was further diluted with 0.1 % v/v DMSO. All stocks were kept frozen at -20 °C, except for KCl, which was kept at room temperature.

2.3 Results

2.3.1 Effects of PVAT re-addition on vascular tone at baseline and after U46619 precontraction

Addition of PVAT to segments of PCA at baseline tone caused a slow, time-dependent contraction that peaked at 60 min (12.1 ± 1.1 % of KCl contraction, n = 15). However, the addition of PVAT to vessels precontracted with U46619 produced an initial rapid contraction and significant overall enhancement in PCA vasocontraction response, peaking at 13 min (26.9 ± 3.5 % of KCl contraction, n = 15; Figure 2.4). Contractile responses then declined, before reaching a steady contraction at around 30 min. The concentration of U46619 needed to induce 40– 60 % contraction of the maximum KCl response was 1-10 nM.

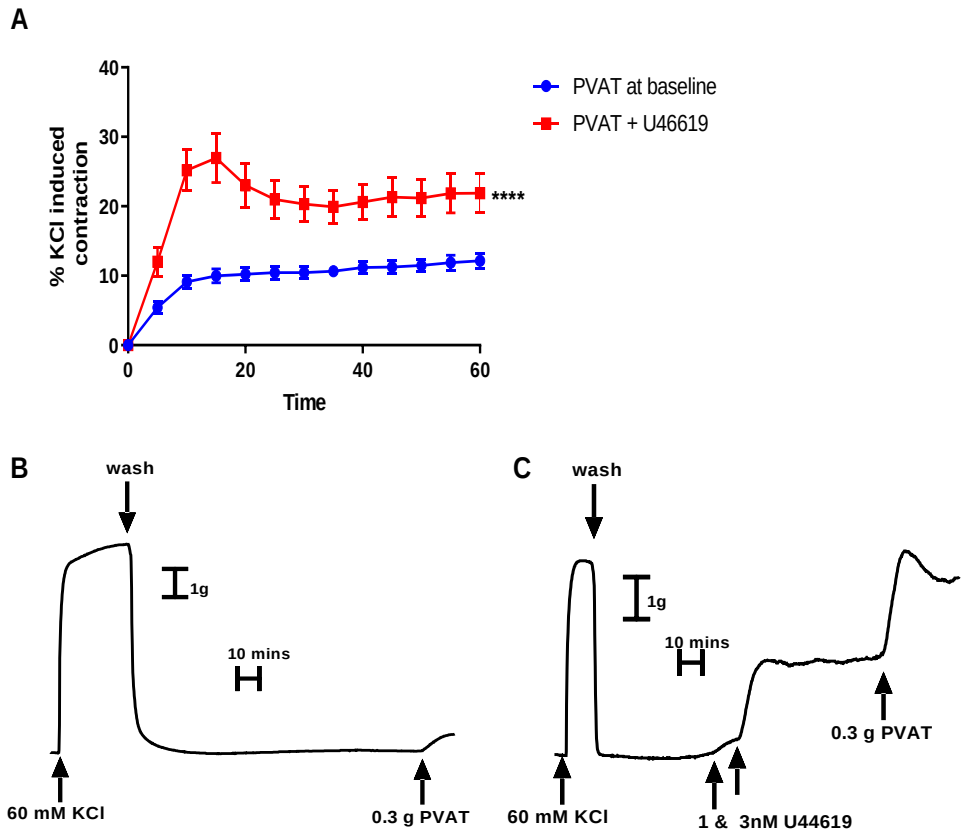


Figure 2.4. (A) Contractions in response to the addition of fresh PVAT (0.3 g) in the absence (PVAT at baseline tone) or presence of U46619. Example trace recordings showing the response of PCA to the addition of PVAT at baseline tone **(B)** and after precontraction with U46619 (1–10 nM) **(C)**. Data are expressed as percentages of the contraction induced by 60 mM KCl and are means ± SEM (n = 15). Asterisks compare the significant differences with values obtained from the control: ****$p < 0.0001$ two-way ANOVA followed by a Sidak's *post-hoc* test.

2.3.2 Effects of simvastatin on PVAT-induced contraction in PCAs at baseline tone and after U46619 precontraction

To study the effects of simvastatin on PVAT functional responses, time-response curves to PVAT re-addition were determined in distal PCAs in the presence of 1 or 10 μM simvastatin either at baseline tone (Figure 2.5A) or in U46619

precontracted segments (Figure 2.5B). At baseline tone, simvastatin caused a concentration-dependent inhibition of the PVAT-induced contraction as the incubation of PCAs with 1 μM simvastatin reduced R_{max} from 14.4 ± 2.2 % to 8.8 ± 1.9 %, while in the presence of 10 μM simvastatin, R_{max} decreased to 2.9 ± 1.3 %. In vessels precontracted with U46619, only 10 μM simvastatin was able to inhibit the contractile effect of PVAT, with R_{max} reduced from 18.9 ± 3.3 % in control vessels to 5.8 ± 0.6 % when the vessel was incubated with 10 μM simvastatin. Additionally, the concentration of U46619 needed to induce 40–60 % contraction of the maximum KCl response was 10–30 nM in the presence of 1 μM simvastatin and 40–70 nM in PCA rings incubated with 10 μM simvastatin, whereas in the control segments the concentration of U46619 needed was 1–10 nM.

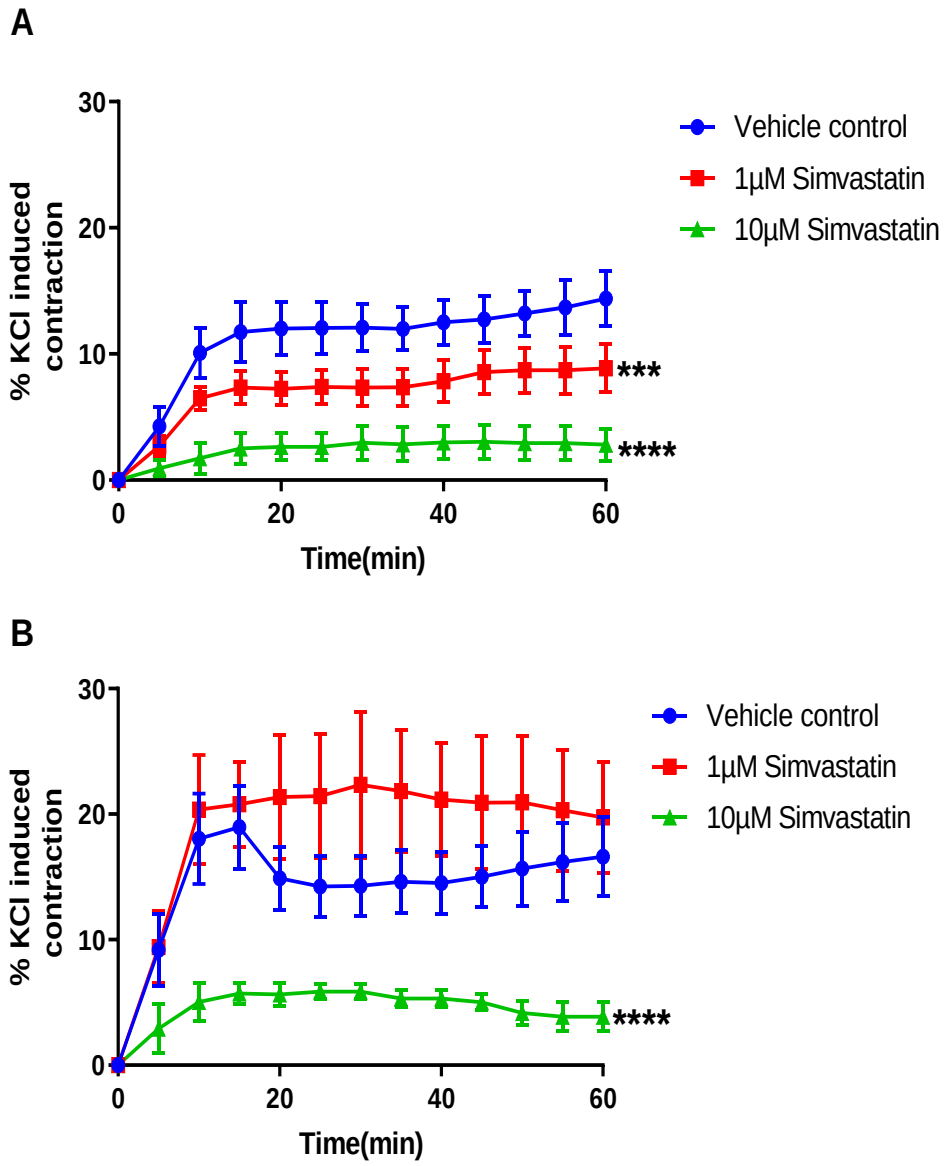


Figure 2.5. The inhibitory effects of 1 and 10 µM simvastatin on PVAT-induced contraction in PCAs at baseline tone **(A)** and in the presence of U46619 (1-10 nM in vehicle control, 10-30 nM in the presence of 1 µM simvastatin and 40-70 nM in the presence of 10 µM simvastatin) **(B)**. Data are expressed as percentages of the contraction elicited by 60 mM KCl. Data represent the means ± SEM (n = 6), and asterisks compare the significant differences with values obtained from the vehicle control (0.1 % v/v DMSO): ***$p < 0.001$, ****$p < 0.0001$ using two-way ANOVA followed by a Sidak's *post-hoc* test.

2.3.3 Effects of pravastatin on PVAT-induced contraction in PCAs at baseline tone and after U46619 precontraction

To examine the effects of hydrophilic statins on PVAT-induced vasocontraction, 10 μM pravastatin was used. It was found that the pre-treatment of distal PCA segments with 10 μM pravastatin had no significant effects on PVAT-induced contraction at baseline tone (Figure 2.6A) or in vessels precontracted with U46619 (Figure 2.6B). Also, U46619 concentrations used in the presence of 10 μM pravastatin were equal to those used for control segments (1–10 nM).

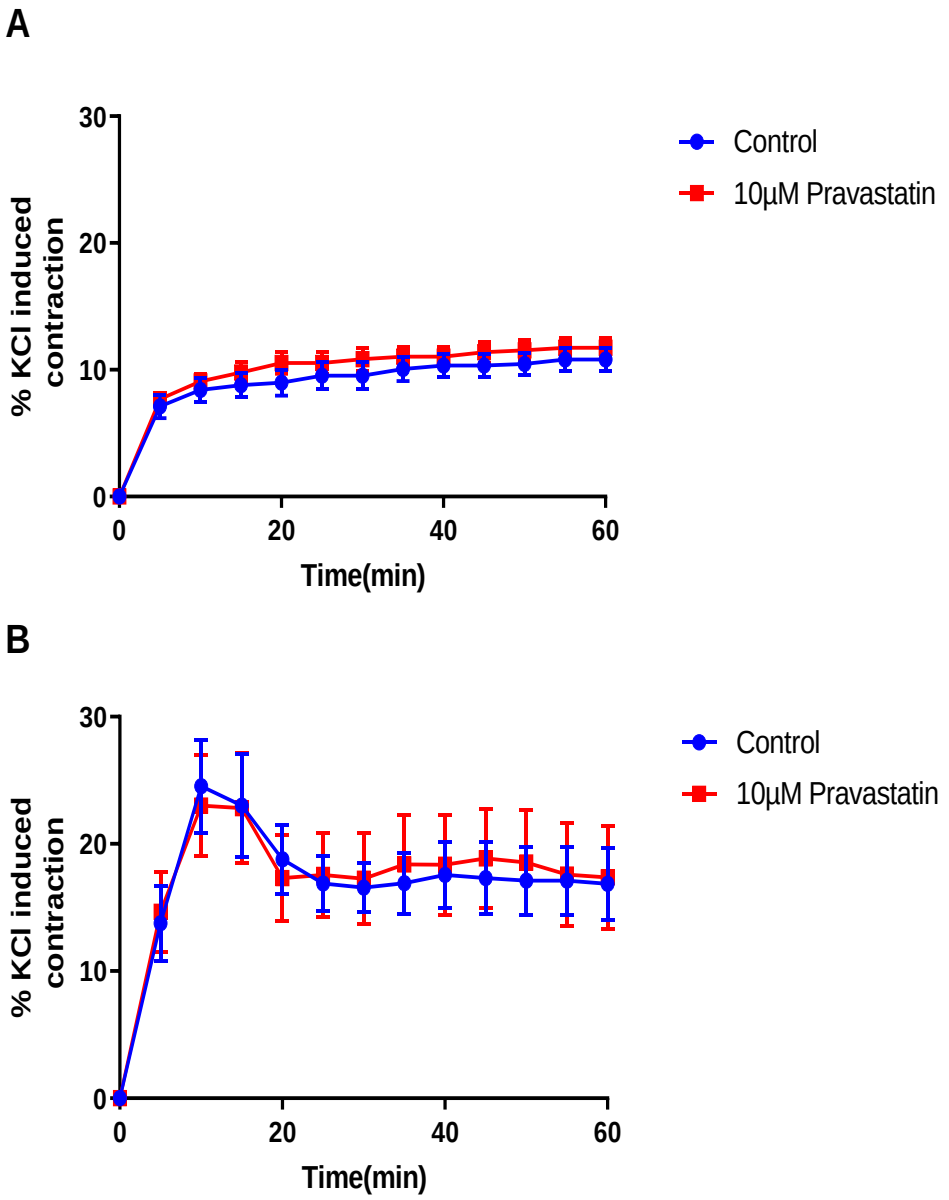


Figure 2.6. Time-dependent contractions of 0.3 g PVAT in PCAs at baseline tone **(A)** and after precontraction with U46619 (1–10 nM) **(B)**. Data are expressed as percentages of the contraction induced by 60 mM KCl. Data represent the means ± SEM (n = 6).

2.3.4 Effects of lovastatin on PVAT-induced contraction in PCAs at baseline tone and after U46619 precontraction

Pre-treatment of the distal PCA segments with 10 μM lovastatin (another lipophilic statin) produced a partial reduction in PVAT-

induced contraction at baseline tone (Figure 2.7A), while in the presence of U46619 precontraction, 10 μM lovastatin caused significant inhibition of the PVAT vasoconstriction effect, and the maximum response (R_{max}) to PVAT addition decreased from 26.5 ± 2 % in the control segments to 8.3 ± 1.9 % in the presence of 10 μM lovastatin (Figure 2.7B). Additionally, the concentrations of U46619 needed to induce 40–60 % contraction versus the maximum KCl response was 5–15 nM in the presence of 10 μM lovastatin compared to 2–10 nM in the vehicle control segments.

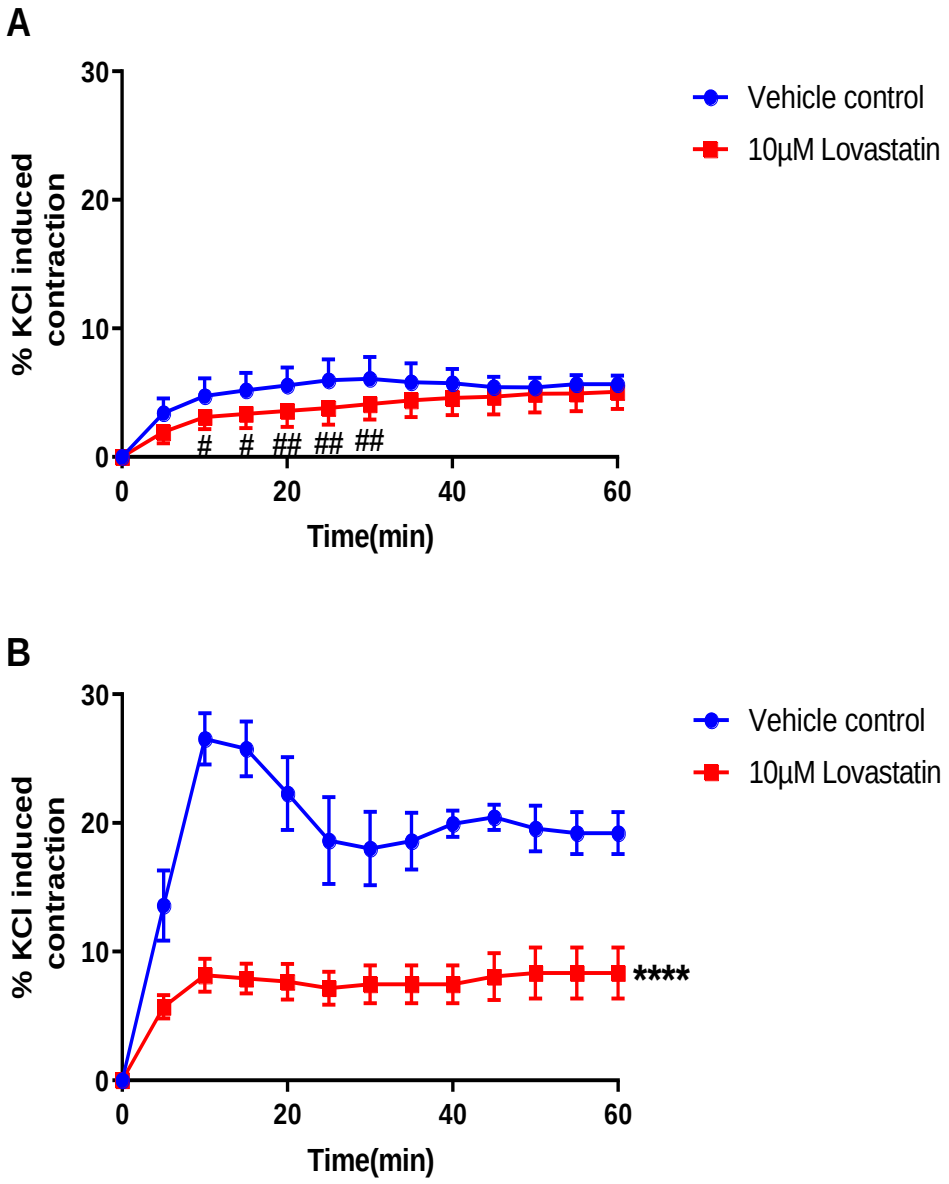


Figure 2.7. The inhibitory effects of 10 µM lovastatin on PVAT-induced contraction in PCAs at baseline tone **(A)** and in the presence of U46619 (2-10 nM in vehicle control and 5–15 nM in the presence of 10 µM lovastatin) **(B)**. Data are expressed as percentages of the contraction induced by 60 mM KCl and represent the means ± SEM (n = 6). Asterisks compare the significant differences with values obtained from the vehicle control (0.1 % v/v DMSO) while hash tags indicate the significant differences between individual time points: *#p* <

*0.05, ##p < 0.01, *p < 0.05, **p < 0.01, ****p < 0.0001* using two-way ANOVA followed by a Sidak's *post-hoc* test.

2.3.5 Effects of indomethacin on PVAT-induced contraction in PCAs at baseline tone and after U46619 precontraction

To examine the involvement of the cyclooxygenase (COX) pathway in contractile responses to PVAT in distal PCAs, the vessels were incubated with 10 μM indomethacin before the addition of PVAT either at baseline tone (Figure 2.8A) or in the presence of U46619 (Figure 2.8B). At baseline tone, indomethacin caused significant inhibition of the PVAT-induced contraction, with R_{max} decreased from 9.2 ± 2.1 % to 4.8 ± 1.3 % of 60 mM KCl contraction. However, this inhibitory effect of indomethacin was attenuated in the presence of U46619 precontraction. Also, the concentration of U46619 needed to induce 40-60 % of the maximum KCl response was 10–25 nM in the presence of 10 μM indomethacin compared to 1–10 nM in the control.

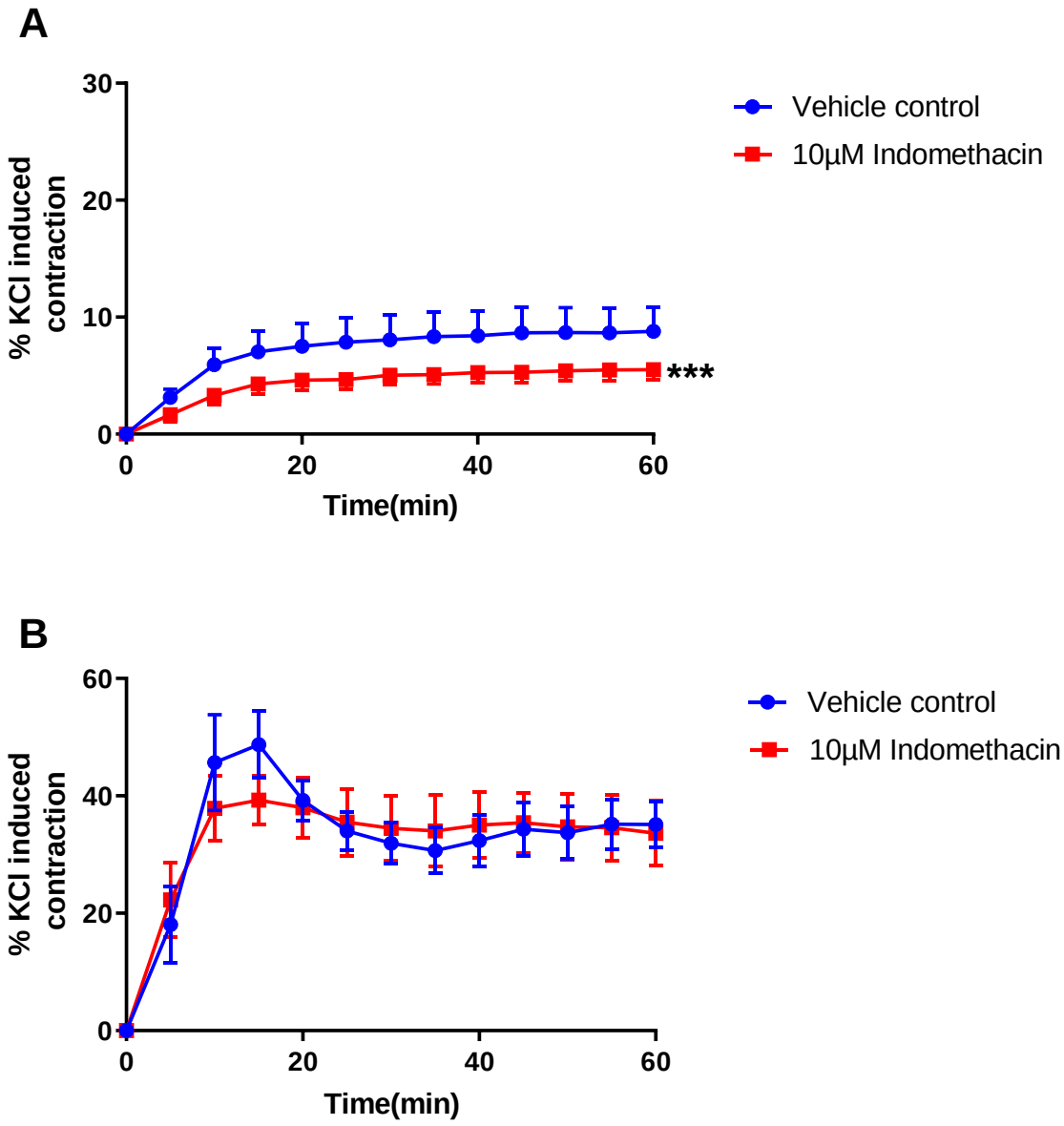


Figure 2.8. The effects of pre-incubation with 10 μM indomethacin on PVAT-induced contraction in PCAs at baseline tone **(A)** and in the presence of U46619 (1-10 nM in vehicle control and 10–25 nM in the presence of 10 μM indomethacin) **(B)**. Data are expressed as percentages of the contraction elicited by 60 mM KCl. Data represent the means ± SEM (n = 6) and asterisks indicate the significant differences with values obtained from the vehicle control (0.1 % v/v DMSO): ***$p < 0.001$ using two-way ANOVA followed by a Sidak's *post-hoc* test.

2.3.6 Effects of simvastatin on transferring bath solution from PVAT to PCA rings

To determine whether simvastatin had a direct effect on PVAT-dependent transferable factors, bioassay experiments were performed, for which the bath solution from PVAT incubated for two h with or without simvastatin was transferred to segments of another PCA. Transfer of the bath solution in which PVAT had been incubated without simvastatin (i.e. PVAT + 0.1 % v/v DMSO) resulted in a time-dependent contraction that peaked at 60 min (6 ± 1.4 % of KCl contraction). Transfer of buffer from the PVAT combined with simvastatin incubation (10 μM), however, had no effect on the initial 20 min of the contraction before inducing a slow relaxation to the level of 2.2 ± 0.6 % of KCl contraction at 60 min (Figure 2.9). Moreover, to compare the effects of simvastatin on the PCA vessels with the similar previous conditions, bath solution with 10 μM simvastatin alone (no PVAT present) was also tested. Transfer of the buffer incubated with simvastatin only induced relaxation of the PCA rings below baseline tone to the level of -3.4 ± 1 % of KCl contraction after 60 min, while 0.1 % v/v DMSO only had no effect on the PCA tone (-0.5 ± 0.5 % of KCl-induced contraction).

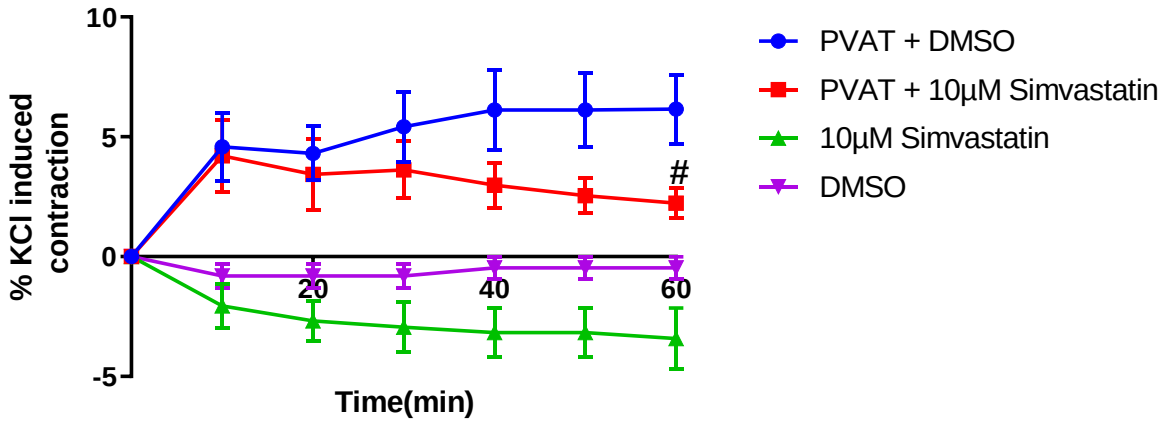


Figure 2.9. Vasomotor effects of transfer of the bath solution incubated with isolated PVAT in the presence or absence of 10 μM simvastatin (blue and red), 10 μM simvastatin only (green), or 0.1 % v/v DMSO only (purple) on segments of PCA. Data are expressed as percentages of the contraction induced by 60 mM KCl and represent the means ± SEM (n = 6). Hash tag indicates the significant difference with values obtained from PVAT + 0.1 % v/v DMSO at the 60 min time point: *#p < 0.05* using two-way ANOVA followed by a Sidak's *post-hoc* test.

2.3.7 Effects of Ca^{2+} reintroduction in KCl-depolarised PCAs in the presence of simvastatin

Previous studies indicated that statins have the ability to inhibit calcium influx [185, 247]; therefore, the effects of simvastatin on Ca^{2+}-induced contraction in the distal PCAs were investigated. Re-addition of calcium in KCl-depolarised PCAs produced a concentration-dependent contraction with a maximum response of 22.6 ± 3 % of KCl contraction. Pre-incubation with simvastatin (10 μM) for 120 min caused a significant inhibition of calcium-induced contraction in PCAs (4.9 ± 0.6 % of KCl contraction; Figure 2.10).

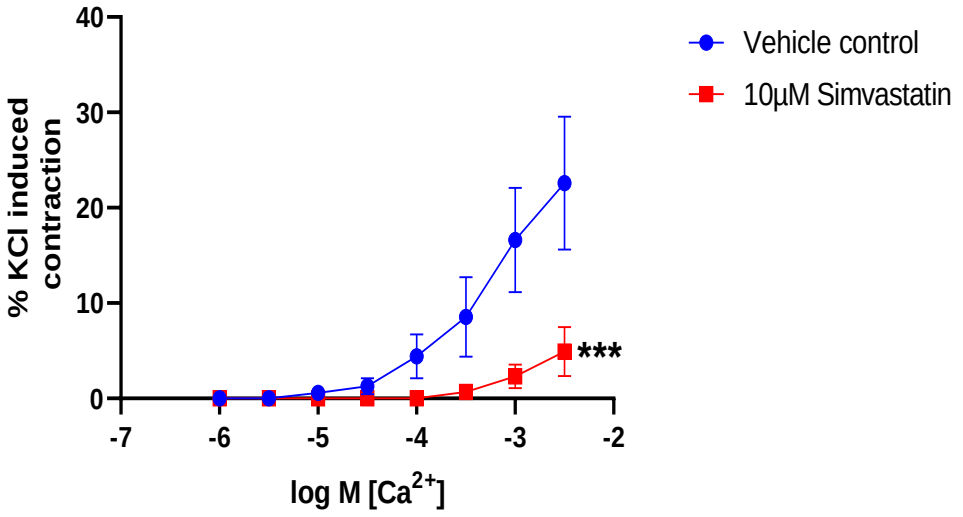


Figure 2.10: Log concentration–response curve for the contractile effects of reintroducing Ca^{2+} in KCl-depolarised PCAs in the presence or absence of 10 μM simvastatin. Data are expressed as percentages of the contraction elicited by 60 mM KCl. Data represent the means ± SEM (n = 8), and asterisks indicate the significant differences with values obtained from the vehicle control (0.1 % v/v DMSO): ***$p < 0.001$ using two-way ANOVA followed by a Sidak's *post-hoc* test.

2.3.8 Effects of Ca^{2+} removal on simvastatin-mediated inhibition of PVAT-induced contraction in PCAs

In the absence of extracellular Ca^{2+}, the maximum response (R_{max}) to PVAT addition was 1.8 ± 0.6 % of KCl-induced contraction compared to 8.4 ± 1.1 % in normal Krebs–Henseleit buffer (Figure 2.11). In the presence of simvastatin (10 μM), the R_{max} was 1 ± 0.5 % of KCl response in normal Krebs–Henseleit solution, but no response was observed when PVAT was added to vessels incubated with 10 μM simvastatin in the absence of extracellular calcium (Figure 2.11).

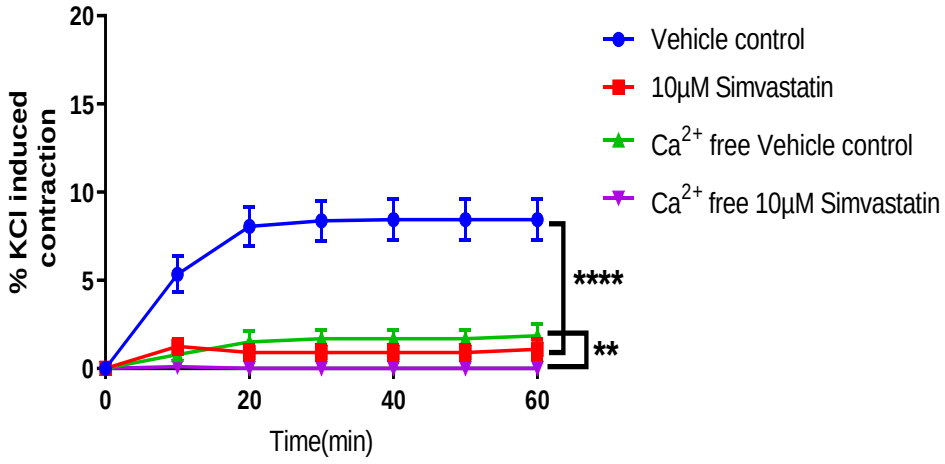


Figure 2.11. Time-dependent contractions induced by PVAT on distal PCAs in the presence or absence of extracellular Ca^{2+} with or without 10 μM simvastatin. The vehicle control received an equal amount of DMSO (0.1 % v/v) and data are expressed as percentages of the contraction elicited by 60 mM KCl and represent the means ± SEM (n = 6). Asterisks indicate the significant differences with values obtained from normal buffer in the presence or absence of 10 μM simvastatin or with values obtained from Ca^{2+}-free buffer in the presence or absence of 10 μM simvastatin: $**p < 0.01$, $****p < 0.0001$, using two-way ANOVA followed by a Sidak's *post-hoc* test.

2.3.9 Effects of simvastatin on release of thromboxane, prostaglandin, and chemerin from PVAT.

Since simvastatin inhibited PVAT-induced contraction, the ability of simvastatin to inhibit vasocontractile molecules released from PVAT was assessed. Previous studies in the laboratory demonstrated the release of three contractile factors from PVAT: thromboxane, prostaglandins, and chemerin [92]. Therefore, the effect of simvastatin on the release of these compounds was determined using ELISA. The stable thromboxane A_2 metabolite (TXB_2), prostaglandin ($PGF_{2\alpha}$), and chemerin were all detected in the buffer incubated with PVAT.

However, only PVAT-induced chemerin significantly decreased in the presence of simvastatin, with chemerin levels reduced from 931 ± 195 pg/ml to 255 ± 1.5 pg/ml in the presence of 10 μM simvastatin (Figure 2.12C). As a control, the levels of TXB_2 and $PGF_{2\alpha}$ were found to be significantly reduced in the presence of the cyclooxygenase inhibitor, indomethacin (10 μM; Figure 2.12A and B).

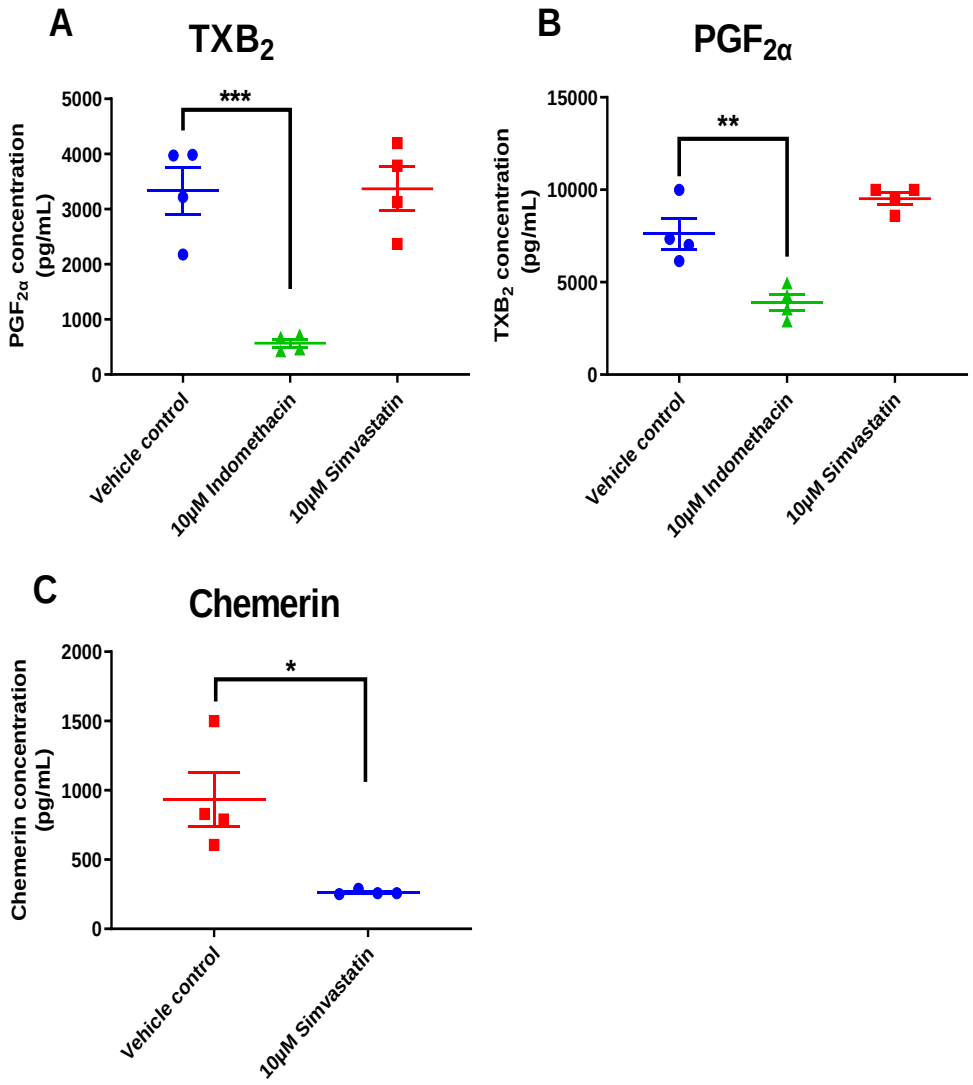


Figure 2.12. (A) The levels of TXB_2 released from 0.3 g PVAT into the Krebs–Henseleit buffer in the presence or absence of 10 μM indomethacin, 10 μM simvastatin, or vehicle control (0.1 % v/v DMSO). **(B)** The levels of $PGF_{2\alpha}$ released from 0.3 g PVAT

into the Krebs–Henseleit buffer in the presence or absence of 10 μM indomethacin, 10 μM simvastatin, or vehicle control (0.1 % v/v DMSO). **(C)** The levels of chemerin released from 0.3 g PVAT into the Krebs–Henseleit buffer in the presence or absence of 10 μM simvastatin. Data are expressed as a pg of TXB_2, $PGF_{2\alpha}$ or chemerin released per ml of Krebs–Henseleit buffer and are means ± SEM (n = 4). Asterisks indicate significant differences with values obtained from 10 μM indomethacin for TXB_2 and $PGF_{2\alpha}$ and with values from vehicle control (0.1 % v/v DMSO) for chemerin: $*p < 0.05$, $**p < 0.01$, $***p < 0.001$, using one-way ANOVA followed by a Sidak's *post-hoc* test for TXB_2 and $PGF_{2\alpha}$, and a Student's two-tailed, paired *t*-test for chemerin.

2.4 Discussion

PVAT is recognised as a promising therapeutic target due to its unique position and ability to secrete a wide range of vasoactive molecules, which may influence vascular tone. The main finding from this chapter is that simvastatin-induced inhibition of PVAT vasoconstriction was via a dual mechanism, involving direct vascular smooth muscle effects and an effect on release of chemerin from PVAT (see Figure 2.13). These findings may reinforce the already identified anti-contractile effect of simvastatin on vascular tone as well as introducing a new mechanism by which simvastatin affects cardiovascular control through the inhibition of chemerin release by PVAT. To the best of my knowledge, the present study is the first to provide evidence that simvastatin may inhibit chemerin release from PVAT.

As with previous studies, the addition of PVAT at baseline tone caused a slow and time-dependent contraction of the PCAs [92, 240]. After PCA vessels were precontracted with U46619, the presence of PVAT induced a more rapid and amplified contraction compared to baseline tension. A similar study demonstrated that porcine coronary and mesenteric PVAT induced constriction of isolated PCAs from lean swine, and the addition of coronary PVAT to $PGF_{2\alpha}$ pre-constricted arteries significantly amplified this contraction [240]. However, in the present study, the PVAT contractile response at baseline tone was inhibited by cyclooxygenase inhibitors, indicating a role for contractile prostanoids in this contraction response. Like previous findings from the laboratory [92], the ELISA results from the present study further supported the presence of PVAT-induced contractile prostanoids, with thromboxane and $PGF_{2\alpha}$ detected in the buffer incubated with PVAT and the release of

both inhibited by indomethacin. Interestingly, in the presence of U46619, the PVAT-induced contraction was not only enhanced but also responded differently in response to indomethacin, whereby PVAT contraction in vessels precontracted with U46619 was not inhibited by pre-incubation with indomethacin (in contrast to baseline tone), suggesting that the presence of U46619 could initiate a series of events in PVAT that could either amplify the release of contractile factors from PVAT, or enhance the vasocontraction response through effects on the vascular smooth muscles. The mechanism underlying this enhanced contraction in response to PVAT in the presence of U46619 will be investigated further in Chapter 4.

The present study demonstrated that simvastatin and lovastatin, but not pravastatin, caused significant inhibitions of PVAT-induced contraction in PCAs at baseline and in U46619 pre-constricted vessels. The different effects obtained by different statins are most likely associated with their lipid/water solubility. Simvastatin and lovastatin are both lipophilic and easily permeate the plasma membranes of peripheral tissues [248]. In particular, lipophilic statins would be expected to accumulate in PVAT as well as in cells of the vascular wall. By contrast, pravastatin is hydrophilic and acts mainly in the liver to modulate the plasma lipid profile, since it largely depends on transport by the organic anion transporter, but its effects on extrahepatic tissues are thought to be limited [162]. Nevertheless, the same lipophilicity-dependent effect of statins on vascular tone was reported in other studies, in PCAs [247], rat aorta [209] and bovine coronary arteries [188], with only lipophilic statins exhibiting vasorelaxant effects. In contrast with the present study, hydrophilic pravastatin was observed to induce an endothelium-dependent vasorelaxation effect in rat

aorta and mesenteric arteries [244, 245, 249]. The differences in responses to pravastatin are unclear and might be attributable to differences in species and/or vascular beds. However, the present data also indicated that 1 μM simvastatin inhibited PVAT-induced vasoconstriction only at baseline tone; this effect resembled the results obtained with indomethacin. The different (or opposite) effect of indomethacin and low concentration of simvastatin (1 μM) on the PVAT contraction at baseline tone compared to in the presence of U46619 may indicate that PVAT responds differently to different treatments in the presence of applied tone. However, more *in vitro* and *in vivo* investigations are needed to further validate these findings.

To determine whether the simvastatin-mediated inhibition of PVAT vasocontraction was through direct effects on PVAT-induced transferable factors or by acting on the PCA itself, a bioassay experiment was performed involving the transfer of PVAT-conditioned media to isolated PCAs. The results supported the release of transferable (paracrine) constricting factors from porcine coronary PVAT and showed that treatment with 10 μM simvastatin caused an inhibition of the contraction induced by these transferable factors. However, the changes in contraction seen with media incubated with PVAT in the presence or absence of simvastatin was about 4 % of KCl-induced contraction, whereas incubating the media with simvastatin only (no PVAT) caused a reduction in the contraction by 3 % relaxation compared to the vehicle control. Thus, these results suggest that the inhibition of PVAT-induced contraction caused by simvastatin may be due to the dual effects of simvastatin on the PCA itself as well as on the contractile factors released from PVAT (Figure 2.13). However, this must be viewed with caution,

as short-lived factors would not have been picked up by this method.

Although the role of Ca^{2+} in simvastatin-induced vascular effects is beyond the aim of this study, it is important that this is investigated because PVAT-induced vascular effects were also reported to depend on Ca^{2+} [208, 250]. In previous studies, a reduction in calcium influx has been proposed for the inhibition of vascular contraction by statins; for example, a previous study from the laboratory has shown that simvastatin inhibits calcium influx in isolated smooth muscle cells taken from PCAs [247]. Also, rosuvastatin has been reported to induce relaxation of rat aorta through the opening of Ca^{2+}-activated K^+ channels, which may lead to reduced calcium influx [186], while lovastatin has been shown to prevent calcium influx through directly inhibiting L-type calcium channels in rat basilar arteries [185]. Herein, the results were in line with these studies, since treatment with simvastatin significantly blocked the vasocontraction by Ca^{2+} reintroduction in PCAs. Next, the role of Ca^{2+} as a mediator of the simvastatin-induced inhibition of PVAT contraction was tested by the re-addition of PVAT with and without simvastatin in the presence or absence of extracellular Ca^{2+}. In the absence of Ca^{2+}, PVAT-induced contraction was significantly inhibited, while the presence of simvastatin in this case completely eliminated the contraction induced by PVAT re-addition. These results clearly indicated that PVAT's influences on vasomotor tone largely depend on the influx of Ca^{2+} from the extracellular environment, and simvastatin may inhibit PVAT-induced contraction by preventing Ca^{2+} entry. Similar results have been reported by other studies, in which PVAT-derived relaxing factors were shown to depend on extracellular Ca^{2+} [208, 250].

PVAT-induced release of adipokines is a key player in the ability of PVAT to regulate vascular functions; for example, PVAT-induced release of COX-derived thromboxane and prostaglandin was reported to augment arterial vasoconstriction in lean mice and, to a greater extent, in obese mice [77]. Also, PVAT-induced adiponectin release has a local protective effect that prevents vascular oxidative stress [251]. PVAT-induced chemerin release plays a potential role in hypertension and obesity-induced hypertension due to the ability of chemerin to induce contraction of vascular smooth muscles [94] and to regulate adipogenesis [116] and angiogenesis [112]. To study the possible effects of simvastatin on PVAT-derived thromboxane, prostaglandin, and chemerin release, an immunoassay technique was used whereby PVAT was incubated with 10 μM simvastatin for 2 h before quantifying the amount of these adipokines in the media. The data in the present study demonstrated that simvastatin significantly inhibited chemerin release from PVAT but had no effect on PVAT-induced release of thromboxane and prostaglandin. This finding is important because chemerin and chemerin receptors can be found throughout the human body, and there is evidence pointing towards chemerin playing a multifunctional role as a chemokine, adipokine, and possible growth factor [108]. Therefore, the mechanisms by which simvastatin affects PVAT-induced chemerin release will be investigated in the next chapter.

It should be noted that PVAT is capable of releasing different adipokines and cytokines, which in terms of vascular effect can induce both vasocontractile and vasorelaxant actions. In the current study, only three vasocontractile adipokines were tested; thus, more studies are needed to test the effect of

statins on other PVAT-derived contractile factors, such as leptin and vasorelaxant mediators like adiponectin, NO, and H_2S. Indeed, one study reported increased net H_2S production from PVAT in rats following treatment with a high dose of lipophilic atorvastatin, but not hydrophilic pravastatin, which enhanced the relaxant effect of PVAT [209]. This later study and the present investigation indicate a role of lipophilic statins in PVAT vascular biology towards inhibition of the vasocontraction effects of PVAT, but it remains to be determined whether these observations can be confirmed from clinical data obtained from patients using statins.

In summary, data from this chapter provides evidence that porcine coronary PVAT is capable of releasing transferable factors that initiate and potentiate contraction of coronary arteries through Ca^{2+}-dependent pathways. Treatment with lipophilic statins can lead to inhibition of this contraction through a direct effect on PCAs as well as on the release of chemerin from PVAT (see Figure 2.13).

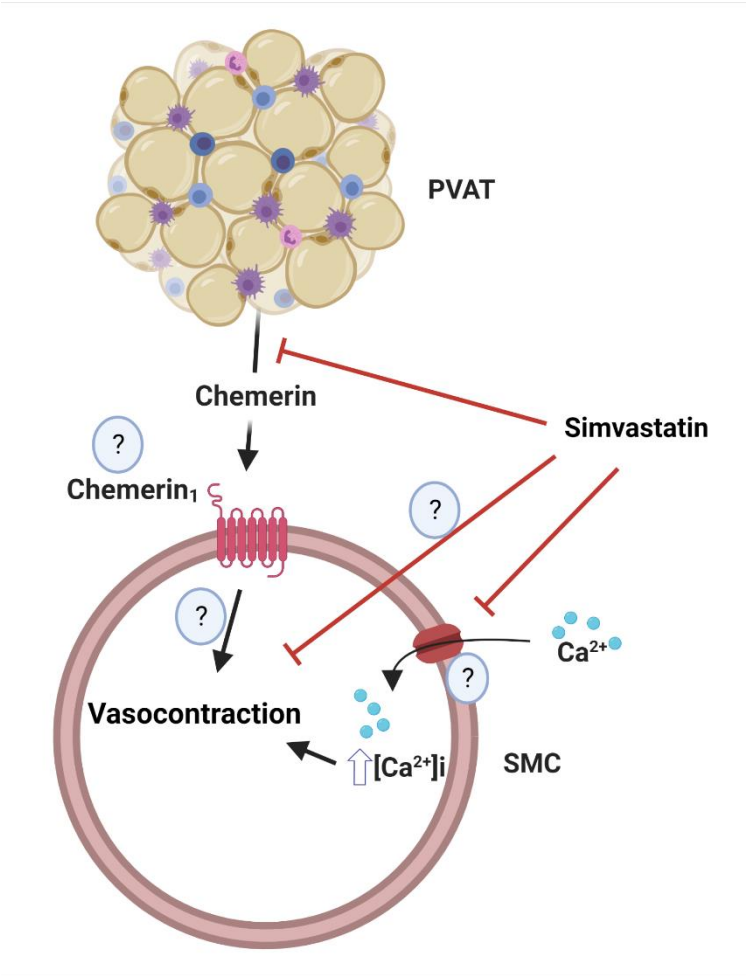


Figure 2.13. Hypothesized schematic diagram of the effect of simvastatin on PVAT-induced contraction in PCA. The present study demonstrated that simvastatin-induced inhibition of PVAT vasoconstriction was via a dual mechanism, involving direct vascular smooth muscle effects and an effect on release of chemerin from PVAT.

Chapter 3
Effects of statins on chemerin release from 3T3-L1 adipocytes and PVAT

3.1 Introduction

Chemerin, a novel adipokine, is highly expressed in adipose tissues, in the liver, and to a lesser extent in the lungs, skeletal muscles, kidneys, ovaries, endothelial cells, and heart [252]. Chemerin is secreted as prochemerin before undergoing further cleavage at various sites by serine and cysteine proteases, generating different isoforms of active chemerin [120]. The chemerin protein was initially described as a chemoattractant for immune cells, but subsequent studies indicated that chemerin is implicated in different physiological and pathophysiological processes, including adipogenesis, cardiovascular diseases (CVDs), inflammation, and metabolic disorders [105, 111].

Many studies have observed that circulating chemerin levels in humans are strongly and positively associated with body mass index, hypertension, atherosclerosis, and inflammatory cytokines [108, 123, 253]. In support of the several clinical studies that indicated higher chemerin serum concentrations in obese patients, chemerin is highly expressed in and released from 3T3-L1 adipocytes, and its knockdown impairs differentiation of 3T3-L1 preadipocytes, indicating its vital role in obesity and adipogenesis [113, 116]. Compared with healthy controls, subjects with hypertension were found to have significantly higher levels of chemerin in the serum, which were consistent with the ability of recombinant chemerin to induce vasoconstriction *in vitro* [94, 147]. Additionally, in human aortic and coronary arteries with atherosclerotic lesions, chemerin was expressed in perivascular adipose tissue (PVAT) and foam cells, both of which correlated positively with the severity of atherosclerosis [144]. Also, positive correlations of systemic chemerin have been found in chronic inflammatory diseases,

and the pro-inflammatory chemotactic effect of chemerin is well characterized *in vitro* by the transmigration of leukocytes and macrophages, suggesting a strong association between chemerin and inflammation [129, 130, 136].

As discussed in the General Introduction, statins have beneficial clinical effects (known as pleiotropic effects) that are not related to their ability to inhibit cholesterol synthesis; however, some of these pleiotropic effects might antagonise or counteract the previously mentioned pathological conditions associated with enhanced chemerin levels. For instance, simvastatin was shown to reduce blood pressure in hypertensive patients with normal cholesterol levels [180], atorvastatin inhibited adipogenesis in 3T3-L1 cells [205], statin treatment was associated with enhanced stability of atherosclerotic plaques [254], and vascular inflammation as well as the release of inflammatory cytokines were reduced by statins [178, 255]. These similarities might suggest that the pleiotropic effects of statins could be attributed, at least partially, to alterations in chemerin production.

Very little is currently known about the effects of statins on chemerin. One study reported a significant decrease in chemerin serum levels in patients with acute myocardial infarction treated with atorvastatin (80 mg/day) or rosuvastatin (40 mg/day) for 4 weeks [234]. Recently, in 2020, Guo *et al.* indicated an inhibitory effect of simvastatin on the adipogenesis of bone marrow-derived mesenchymal stem cells (BMSCs) through the downregulation of PPARγ and the PPARγ-mediated induction of chemerin mRNA expression [235]. However, to my knowledge, no studies have examined the effects of statins on adipocyte-induced chemerin release. The aim of this study, therefore, was to examine the ability of statins to inhibit

chemerin release from porcine coronary perivascular adipose tissue and 3T3-L1 adipocytes and to investigate the underlying mechanisms of this ability.

3.2 Materials and Methods

3.2.1 Determination of PVAT-induced chemerin release in the presence of simvastatin, pravastatin, hypoxia, and EFS

Levels of chemerin released by PVAT into Krebs–Henseleit solution were determined by ELISA. To mimic the conditions used in the contractile experiments in Chapter 2, 0.3 g PVAT was placed in a four-channel wire myograph as previously described in Chapter 2, section 2.2.3. To study the long-term effects of simvastatin and pravastatin treatment, the PVAT was incubated in the Krebs–Henseleit buffer with simvastatin (10 μM), a vehicle control (0.1 % v/v DMSO), or pravastatin (10 μM) for 4 h. All chambers in the wire myograph were covered with provided plastic covers as seen in Figure 2.1. In some experiments, 250 μM mevalonate was added to the bath with the application of simvastatin and pravastatin to study mevalonate dependency [256].

Little is known about how chemerin release from PVAT is stimulated. Therefore, to assess the ability of hypoxia to stimulate chemerin release from PVAT, the gas cylinder was set at 95 % N_2 and 5 % CO_2 for 30 min based on previous findings that 30 min of gassing with 95 % N_2 / CO_2 resulted in reduction of oxygen levels in the Krebs–Henseleit buffer to levels of 20-30 mmHg [257]. Likewise, electrical field stimulation (EFS) at 0.5–12 Hz, 60 V, 0.1 ms, and 30 s was applied to the PVAT to test the role of sensory nerve activation in PVAT-induced chemerin release. EFS at the used settings was shown to elicit PVAT-dependent vasorelaxation and enhanced PVAT-derived leptin release in rats' mesenteric arterial beds [65].

3.2.2 Differentiation of 3T3-L1 cells

3T3-L1 preadipocytes were maintained as fibroblasts (American Type Culture Collection, Manassas, USA) (passage 10–13) in

Dulbecco's Modified Eagle Medium (DMEM, Sigma D6546) supplemented with 10 % (v/v) newborn calf serum (NCS, Sigma N4637), 100 units/ml of penicillin and streptomycin (Sigma PO781), and 2 mM L-glutamine (Sigma G7513). Cells were incubated at 37 °C in a humidified atmosphere of 5 % CO_2 and were grown to 70-80 % confluence in T75 flasks. The cells were then washed with phosphate-buffered saline (PBS) prior to trypsinisation with 1 % trypsin and subcultured at a 1:5 ratio.

3T3-L1 fibroblasts intended for differentiation to 3T3-L1 adipocytes were seeded in a 12-well cell culture plate at a density of 3 x 10^4 cells/ml. Cells were counted using a BIO-RAD TC20™ automated cell counter with 50 % (v/v) Trypan Blue. 3T3-L1 fibroblasts were differentiated using the method outlined in [258]. The differentiation process initiated using a differentiation medium consisting of DMEM containing 10 % (v/v) fetal bovine serum (FBS, Sigma F9665), 100 units/ml of penicillin and streptomycin, 1 µg/ml insulin (Sigma 15523), 0.5 mM 3-isobutyl-1-methylxanthine (IBMX, Sigma 17018), 0.25 µM dexamethasone (Sigma D1756), and 2 µM rosiglitazone (Sigma R2408). After 48 h, the medium was replaced with DMEM containing 10 % FBS, 100 units/ml of penicillin and streptomycin, and 1 µg/ml insulin. The cells were incubated in this medium for 48 h before the medium was aspirated and replaced with DMEM containing 10 % FBS and 100 units/ml of penicillin and streptomycin, in which the cells were then maintained by changing the medium after 24 h and then every 48 h [258]. During the early stages of differentiation, the cells contained multiple small fat droplets. As differentiation progressed, the multiple droplets coalesced into a single large droplet, and the cells became macroscopic. At 12–13 days post-induction of differentiation, cells were used for experimentation.

3.2.3 3T3-L1 cells stained with oil red O stain

To confirm the presence and accumulation of lipid droplets following cell differentiation, differentiated and undifferentiated 3T3-L1 cells were stained with oil red O. Oil red O is a fat-soluble dye commonly used for the staining of triglycerides and neutral lipids [259].

3T3-L1 fibroblasts or adipocytes were seeded in a 6-well plate before the culture medium was removed and the cells were washed with PBS. Cells were then fixed with 4 % (w/v) paraformaldehyde for 15 min at room temperature. The fixative was discarded, and the cells were washed with PBS. A stock solution of oil red O (0.25 g in 40 ml of isopropanol) was prepared by shaking for 2 h, and a fresh working solution was then prepared by diluting 18 ml of stock solution in 12 ml of distilled water, then filtered through a 0.2 µm filter before use. Oil red O working solution was applied to the cells for 1 h at room temperature. The cells were then rinsed 3 times with PBS and incubated with 60 % isopropanol for 2 min. Finally, the 3T3-L1 cells were washed with PBS, and the stained lipid droplets were visualized under a light microscope.

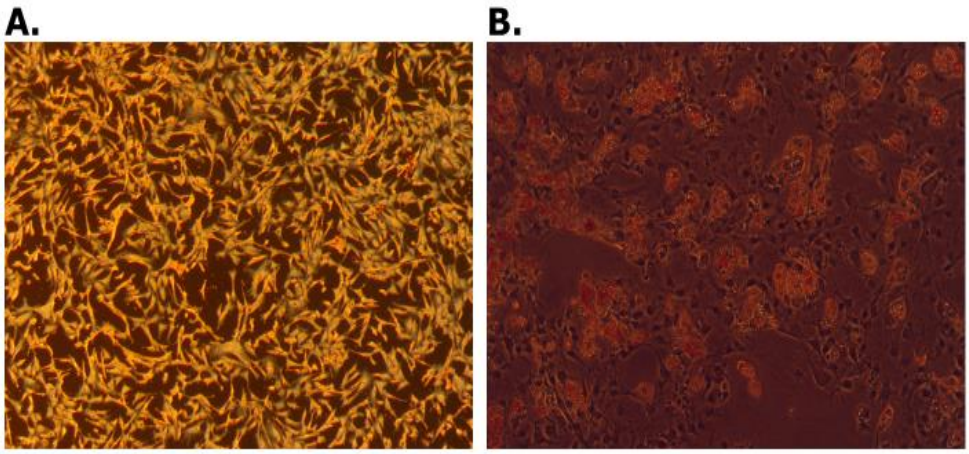


Figure 3.1. 3T3-L1 fibroblast before differentiation **(A)** and 13 days post-induction of differentiation **(B)** after oil red O staining, with lipid droplets stained in red.

3.2.4 Treatment of cultured 3T3-L1 adipocytes

At 12–13 days post-induction of differentiation, 3T3-L1 adipocytes were incubated with different drugs in serum-free DMEM containing 100 units/ml of penicillin and streptomycin, because the presence of serum could cause conflicting results because chemerin could be present in the serum which could interfere with the used ELSA kits. After treatment, the medium was collected and stored in -80 °C for ELISA study. Chemerin levels in the media were determined using a mouse chemerin ELISA Kit (ab204520, Abcam, Cambridge, UK) according to the manufacturer's instructions. The range of the standard curve was 14.06 pg/ml–900 pg/ml sensitivity: < 1.75 pg/ml. The results were expressed as picograms (pg) of chemerin released per ml of media solution.

Effects of simvastatin and pravastatin on chemerin released by cultured 3T3-L1 adipocytes

To examine the effects of simvastatin and pravastatin on 3T3-L1-induced chemerin release, 3 different concentrations of simvastatin and pravastatin (1, 10, and 100 μM) were added to

the medium, and cells were incubated for 24 h before collecting the media for ELISA study. A vehicle control for simvastatin received a similar amount of DMSO (0.1 % v/v and 1 % v/v for 100 µM simvastatin). 10 µM simvastatin was found to be the lowest concentration to cause inhibition in chemerin release; thus, 10 µM simvastatin was incubated with the cells for 48 h to examine its long-term effect. In some experiments, cells were also exposed to 250 µM mevalonate [256] with or without 10 µM simvastatin.

Effects of nifedipine and Bay K8644 on the simvastatin-mediated inhibition of chemerin released by cultured 3T3-L1 adipocytes:

To investigate the roles of Ca^{2+} channels in the simvastatin-mediated inhibition of chemerin released by 3T3-L1 adipocytes, cells were treated with 10 µM nifedipine or 10 µM Bay K8644—an activator of the voltage- dependent Ca^{2+} channels (VDCC)—in the presence or absence of simvastatin (10 µM) for 24 or 48 h. The vehicle control received a similar amount of DMSO (0.2 % v/v). The concentrations of nifedipine and Bay K8644 used in this study were based on published data from *in vitro* studies using adipocytes culture [260, 261].

Effects of TNF-α and LPS on the simvastatin-mediated inhibition of chemerin released by cultured 3T3-L1 adipocytes:

To study simvastatin's ability to reduce the release of chemerin from 3T3-L1 in an inflammatory condition, differentiated 3T3-L1 cells were incubated in serum-free DMEM with 1 ng/ml or 10 ng/ml TNF-α [262] or with 1µg/ml LPS [263] in the presence or absence of simvastatin (10 µM) over a period of 24 h. Lipopolysaccharides (LPS) used was from *Escherichia coli* (sigma L4516) and was dissolved in phosphate buffered saline

(PBS), while the vehicle control for TNF-α included an equal amount of DMSO (0.1 % v/v).

Effects of pinacidil and glibenclamide on the simvastatin-mediated inhibition of chemerin released by cultured 3T3-L1 adipocytes:

To investigate the roles of ATP-sensitive potassium channels (K_{ATP}) in the simvastatin-mediated inhibition of 3T3-L1-induced chemerin release, cells were treated with either 10 μM pinacidil [264], 1 μM glibenclamide [265], 10 μM pinacidil + 1μM glibenclamide, 10 μM pinacidil + 10 μM simvastatin, or 1 μM glibenclamide + 10 μM simvastatin for 24 h before the media were collected for ELISA study. The vehicle control received equal amounts of DMSO (0.2 % v/v).

Effect of rosiglitazone on the simvastatin-mediated inhibition of chemerin released by cultured 3T3-L1 adipocytes:

To study the role of peroxisome proliferator-activated receptor gamma (PPARγ) in simvastatin's inhibitory effect on the release of chemerin by 3T3-L1 adipocytes, cells were treated for 24 or 48 h with 1 μM rosiglitazone (a PPARγ agonist) in the presence or absence of 10 μM simvastatin [266]. The vehicle control received equal amounts of DMSO (0.2 % v/v).

3.2.5 MTT assay

Thiazolyl blue tetrazolium bromide (MTT) assay was performed to study the toxicity of simvastatin and other selected drugs used in this study on 3T3-L1 preadipocytes. Viable cells with active metabolism convert MTT into a purple formazan product that can be measured spectrophotometrically [267]. Cells were seeded in a 12-well cell culture plate at a density of 3 x 10^4 cells/ml. After 24 h, cells were treated with serum-free DMEM containing either DMSO (as a vehicle control), 10 μM

simvastatin, 10 µM nifedipine, 60 mM KCl, or 10 µg/ml LPS, then incubated for 24 h. MTT stock solution was prepared by dissolving 3 mg of MTT in 1 ml of PBS, which was then kept in a refrigerator. A working solution of 60 µg/ml MTT was formulated with 1 ml stock solution in 50 ml of the slightly heated DMEM. After incubation with the drugs, 2 ml of MTT solution were added to each well and incubated for 3 h at 37 °C in a humidified atmosphere of 5 % CO_2. The MTT solution was aspirated, and 3T3-L1 cells were washed twice with PBS before the addition of 2 ml isopropanol. Finally, 200 µl of isopropanol from each well was aliquoted in a 96-well plate prior to spectrophotometric measurement of the absorbance at 620 nm [267]. The results were expressed as percentages of the absorbance measured in the vehicle control cells.

3.2.6 Statistical analysis

All values were expressed as picograms (pg) of chemerin released per ml of culture media solution or Krebs–Henseleit buffer and were means ± SEM (standard error of the mean) from at least four independent experiments, with n representing the number of different passages of 3T3-L1 fibroblasts that differentiated into adipocytes. Statistical tests were performed using Graphpad Prism (version 7, GraphPad Software, La Jolla, California, USA) and differences between two groups were assessed using two-tailed, paired Student's *t*-test. Differences between three or more groups were assessed using one-way ANOVA in conjunction with a Sidak's *post-hoc* test. *p* values less than 0.05 ($p < 0.05$) were considered to be statistically significant. **** indicates $p < 0.001$, *** indicates $p < 0.001$, ** indicates $p < 0.01$, and * indicates $p < 0.05$.

3.2.7 Drugs and chemicals

All drugs were purchased from Sigma-Aldrich (Poole, UK), except for simvastatin, pravastatin, and Bay K8644, which were obtained from Tocris-Cookson (Bristol, UK). Stock solutions of pravastatin, TNF-α, and LPS were dissolved in distilled water. Stock solutions of all the remaining chemicals were dissolved in dimethyl sulfoxide (0.1 % v/v DMSO). All further stock solution dilutions were formulated using distilled water except for simvastatin, which was further diluted with 0.1 % v/v DMSO. All stock solutions were kept frozen at -20 °C, except for glibenclamide, which was kept at 4 °C.

3.3 Results

3.3.1 Effects of simvastatin on chemerin production by cultured 3T3-L1 adipocytes

The ELISA results indicated that 3T3-L1 adipocytes were able to release chemerin in the adipocyte media. To determine whether simvastatin could inhibit 3T3-L1-induced chemerin release, the cells were incubated with 3 concentrations (1, 10, and 100 μM) of simvastatin for 24 h (Figure 3.2). 1 μM simvastatin had no effect on the chemerin release, but 10 μM and 100 μM significantly inhibited 3T3-L1-induced chemerin release in a concentration-dependent manner. In the presence of 10 μM simvastatin, the chemerin concentration in the media was found to be 733 ± 119 pg/ml, compared to 1041 ± 56 pg/ml in the vehicle control (0.1 % v/v DMSO). 100 μM simvastatin reduced chemerin release in the cultured 3T3-L1 adipocytes from 577 ± 67 pg/ml in vehicle control (1 % v/v DMSO) to 114 ±16 pg/ml.

10 μM simvastatin was used for further assessment to examine the time-dependent inhibition of simvastatin. 48 h incubation with 10 μM simvastatin further inhibited chemerin release from 3T3-L1 adipocytes at levels of 794 ± 58 pg/ml in vehicle control (0.1 % v/v DMSO) to 230 ± 86 pg/ml in the presence of 10 μM simvastatin (Figure 3.3). As seen in figure 3.3, 48 h incubation with 10 μM simvastatin resulted in 3.5-fold drop in chemerin concentration compared to 1.5-fold after 24 h incubation with 10 μM simvastatin.

The ability of mevalonate to reverse simvastatin's inhibitory effect was examined. As Figure 3.4 shows, 250 μM mevalonate had no effect on the 3T3-L1-induced chemerin release or on the simvastatin-mediated inhibition of chemerin release by 3T3-L1 adipocytes.

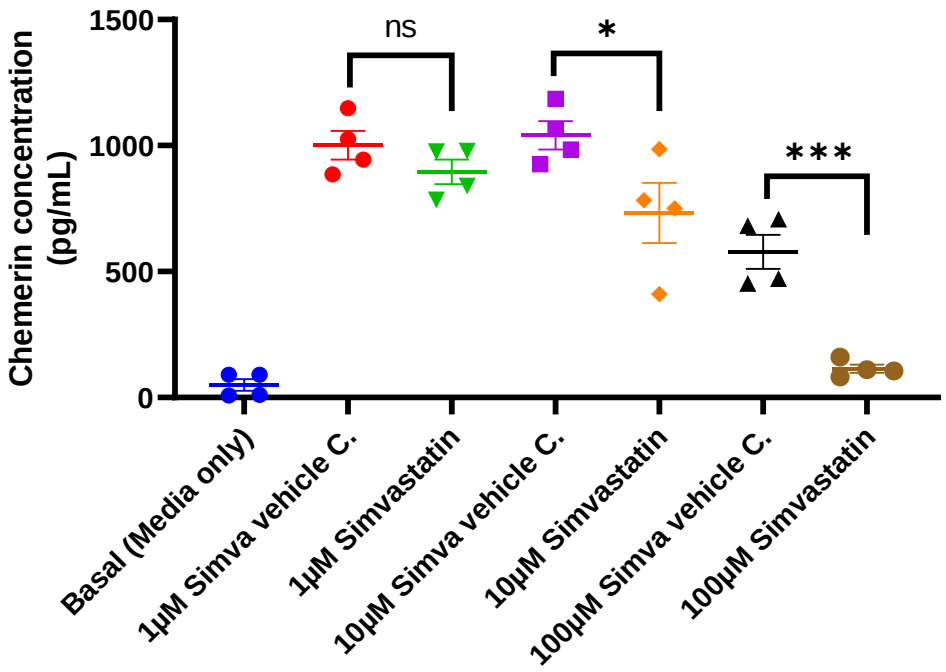


Figure 3.2. The levels of chemerin released from cultured 3T3-L1 adipocytes into the media in the presence or absence of 1, 10, and 100 µM simvastatin compared to their relative vehicle control (0.1 % v/v DMSO for 10 µM simvastatin and 1 % v/v DMSO for 100 µM simvastatin). Data are expressed as pg of chemerin released per ml of media and are means ± SEM (n = 4). *$p < 0.05$, ***$p < 0.001$ using one-way ANOVA followed by a Sidak's *post-hoc* test.

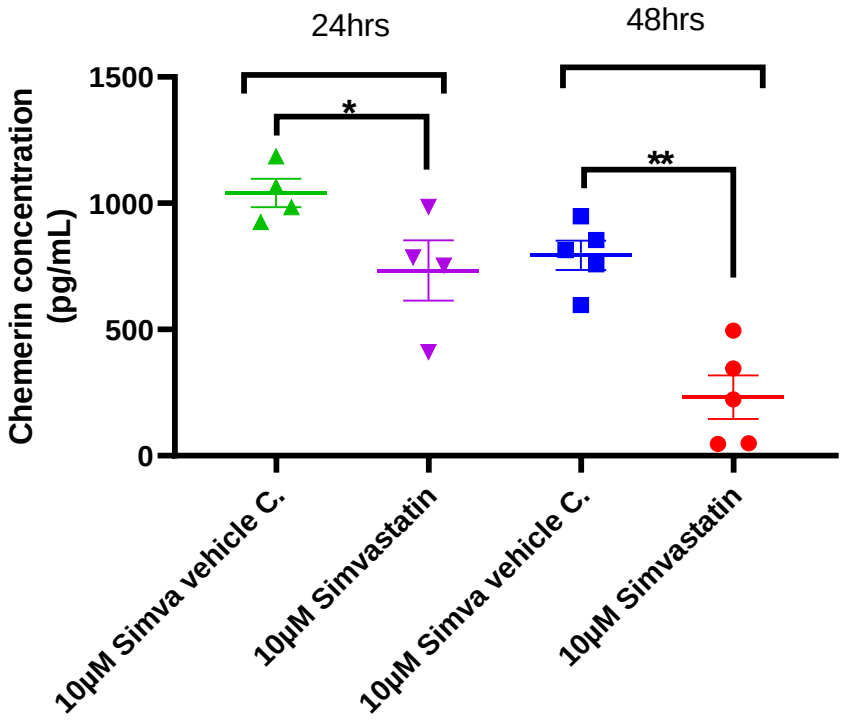


Figure 3.3. The levels of chemerin in the 3T3-L1 adipocyte media after 48 h of incubation with 10 μM simvastatin. Data for 24 h incubation with 10 μM simvastatin were adapted from Figure 3.2 for comparison. Data are expressed as pg of chemerin released per ml of media and are means ± SEM n = 5 for 48 h and n = 4 for 24 h. *$p < 0.05$, **$p < 0.01$, 2-tailed, paired Student's *t*-test vs. paired vehicle controls (0.1 % v/v DMSO).

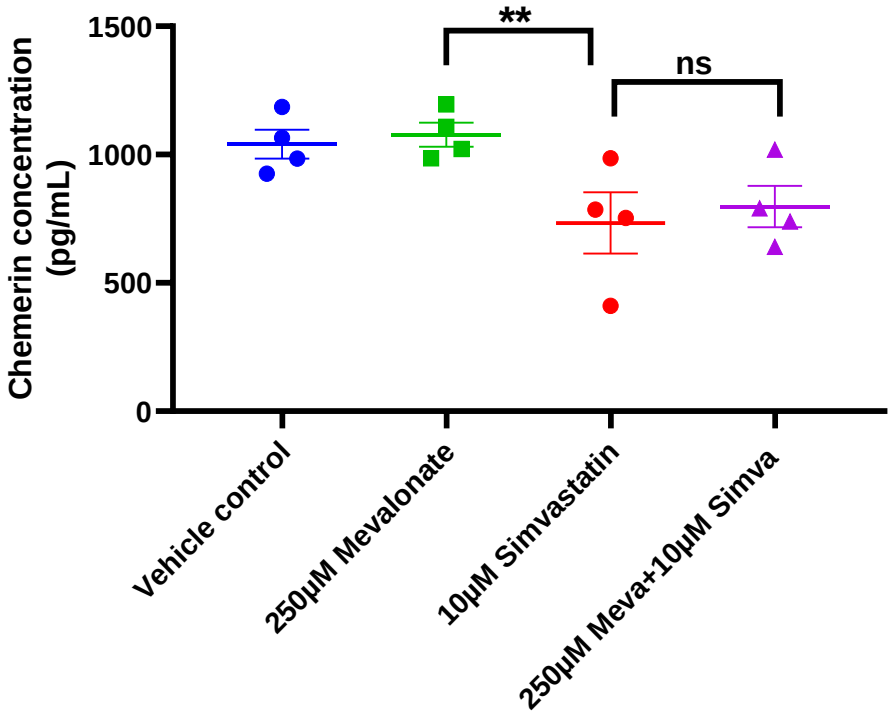


Figure 3.4. The levels of chemerin released from 3T3-L1 adipocytes into the media in the presence or absence of 250 μM mevalonate, 10 μM simvastatin, or 250 μM mevalonate + 10 μM simvastatin, or vehicle control (0.2 % v/v DMSO). Data are expressed as pg of chemerin released per ml of media and are means ± SEM (n = 4). $^{**}p < 0.01$ using one-way ANOVA followed by a Sidak's *post-hoc* test.

3.3.2 Effects of simvastatin on chemerin production by PVAT

The ability of simvastatin to inhibit PVAT-induced chemerin release was investigated. As Figure 3.5A shows, 2 h of incubation with 10 μM simvastatin resulted in significant inhibition of chemerin release from 0.3 g of PVAT. The chemerin concentration in the Krebs–Henseleit buffer decreased from 791 ± 113 pg/ml to 645 ± 86 pg/ml in the presence of 10 μM simvastatin. To determine the time- and mevalonate-dependent inhibition of simvastatin, 10 μM simvastatin was incubated with 0.3 g PVAT in the presence or absence of 250 μM mevalonate for 4 h. However, there was no significant

change in chemerin release by PVAT after 4 h incubation with simvastatin. Also, 250 μM mevalonate had no effect on PVAT-induced chemerin release or on the simvastatin-mediated inhibition of chemerin release by PVAT (Figure 3.5B).

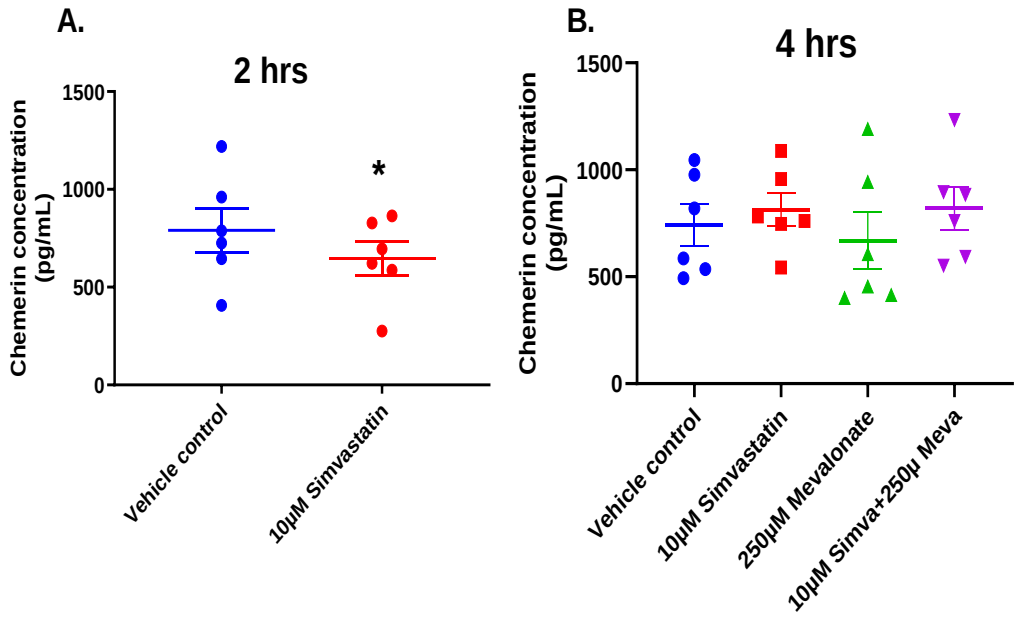


Figure 3.5. **(A)** The levels of chemerin released from 0.3 g PVAT into the Krebs–Henseleit buffer in the presence of 10 μM simvastatin or vehicle control (0.1 % v/v DMSO) after 2 h of incubation. **(B)** The levels of chemerin released from 0.3 g PVAT into the Krebs–Henseleit buffer following 4 h of incubation with 10 μM simvastatin, 250 μM mevalonate, 10 μM simvastatin + 250 μM mevalonate, or vehicle control (0.2 % v/v DMSO). Data are expressed as pg of chemerin released per ml of Krebs–Henseleit buffer and are means ± SEM (n = 6). *$p < 0.05$, using a Student's two-tailed, paired t-test for **A** and one-way ANOVA for **B**.

3.3.3 Effects of pravastatin on chemerin production by cultured 3T3-L1 adipocytes

To test whether hydrophilic statins could inhibit cultured 3T3-L1-induced chemerin release, the cells were incubated with 3

concentrations (1, 10, and 100 μM) of pravastatin for 24 h (Figure 3.6). Only 100 μM pravastatin showed a significant effect as the concentration of chemerin in the media decreased from 1,047 ± 20 pg/ml to 735 ± 34 pg/ml. However, even with performing addition five n number for 10 μM pravastatin, this concentration of pravastatin still had no effect on cultured 3T3-L1 adipocyte-induced chemerin release, since chemerin levels were 729 ± 107 pg/ml in the control adipocytes and 649 ± 90 pg/ml in the presence of 10 μM pravastatin (Figure 3.7).

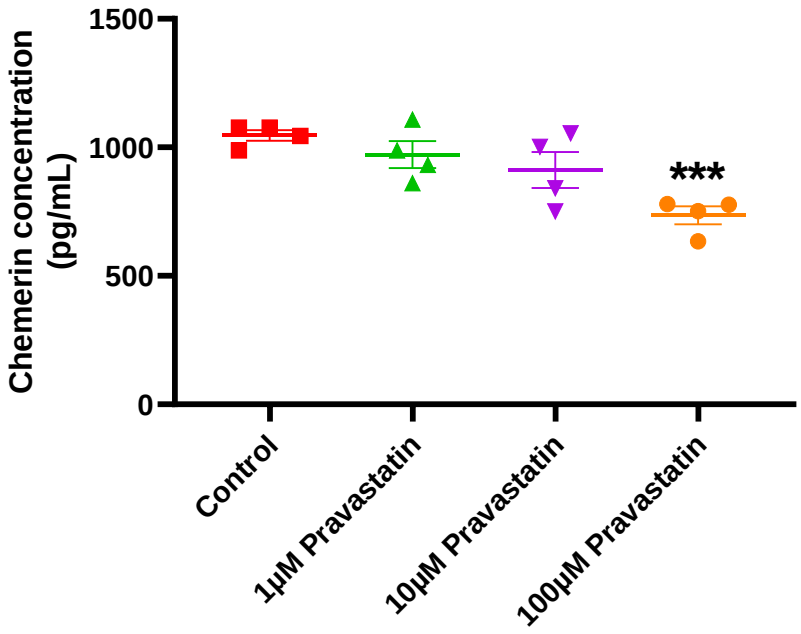


Figure 3.6. The levels of chemerin released from cultured 3T3-L1 adipocytes into the media in the presence or absence of 1, 10, and 100 μM pravastatin. Data are expressed as pg of chemerin released per ml of media and are means ± SEM (n = 4). ***$p < 0.001$ using one-way ANOVA followed by a Sidak's *post-hoc* test.

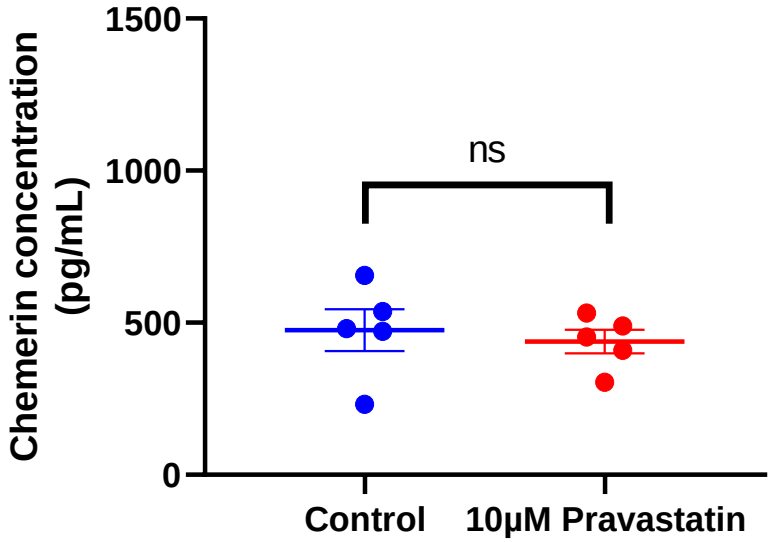


Figure 3.7. Comparison of the levels of chemerin in the 3T3-L1 adipocyte media after 24 h of incubation with 10 μM pravastatin across five independent experiments. Data are expressed as pg of chemerin released per ml of media and are means ± SEM (n = 5). Data were analysed using a Student's two-tailed, paired *t*-test.

3.3.4 Effects of pravastatin on chemerin production by PVAT

Unlike cultured 3T3-L1 cells, 10 μM pravastatin reduced chemerin release in freshly isolated PVAT after 2 h of incubation from 1,233 ± 72 pg/ml to 573 ± 66 pg/ml as shown in Figure 3.8A. Four hours of incubation with 10 μM pravastatin or 250 μM mevalonate had no effect on the chemerin release by PVAT (Figure 3.8B).

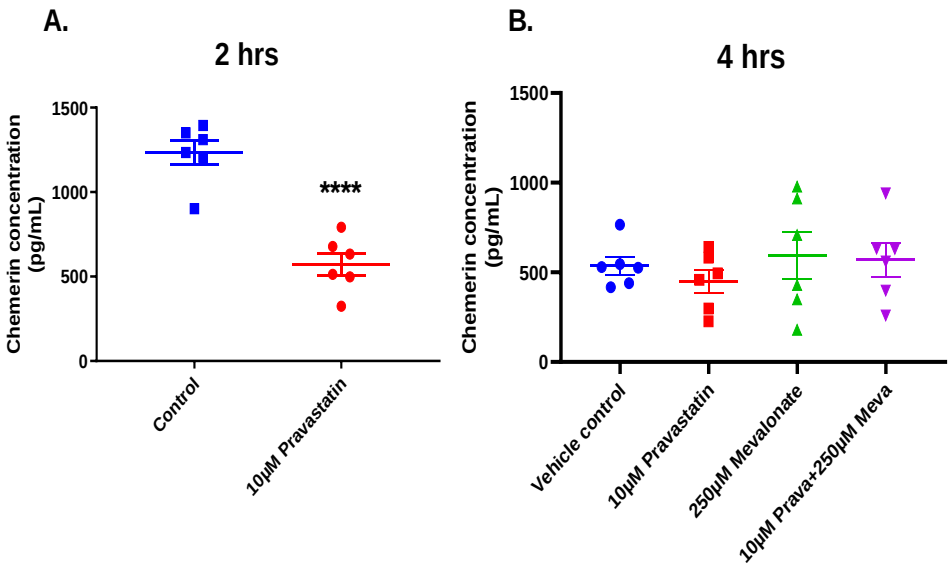


Figure 3.8. **(A)** The levels of chemerin released from 0.3 g PVAT into the Krebs–Henseleit buffer in the presence or absence of 10 μM pravastatin after 2 h of incubation. **(B)** The levels of chemerin released from 0.3 g PVAT into the buffer solution following 4 h of incubation with 10 μM pravastatin, 250 μM mevalonate 10 μM pravastatin + 250 μM mevalonate or vehicle control (0.1 % v/v DMSO). Data are expressed as pg of chemerin released per ml of Krebs–Henseleit buffer and are means ± SEM (n = 6). ****$p < 0.0001$, using a Student's two-tailed, unpaired *t*-test for **A** and one-way ANOVA followed by a Sidak's *post-hoc* test for **B**.

3.3.5 Role of Ca^{2+} in the simvastatin-mediated inhibition of chemerin release by cultured 3T3-L1 adipocytes

Simvastatin was reported to inhibit Ca^{2+} entry [268]. Therefore, to investigate the role of Ca^{2+} channels in chemerin release and the simvastatin-mediated inhibition of chemerin release by cultured 3T3-L1 adipocytes, cells were incubated with 10 μM nifedipine (an L-type Ca^{2+} blocker) and 10 μM Bay K8644 (a Ca^{2+} channel opener) for 24 h. Nifedipine resulted in inhibition of chemerin release from 466 ± 78 pg/ml to 309 ± 38 pg/ml,

while Bay K8644 had no effect on the levels of chemerin in cultured media (Figures 3.9A and 3.10). Since nifedipine had an inhibitory effect on chemerin release, it was tested with simvastatin. However, incubation with 10 μM nifedipine and 10 μM simvastatin produced a similar inhibitory effect of chemerin concentrations at 433 ± 50 pg/ml and 522 ± 38 pg/ml for nifedipine and simvastatin, respectively, compared to 757 ± 29 pg/ml for the vehicle control. Also, the dual presence of nifedipine and simvastatin further inhibited chemerin production by cultured 3T3-L1 adipocytes at a level of 229 ± 19 pg/ml (Figure 3.9B).

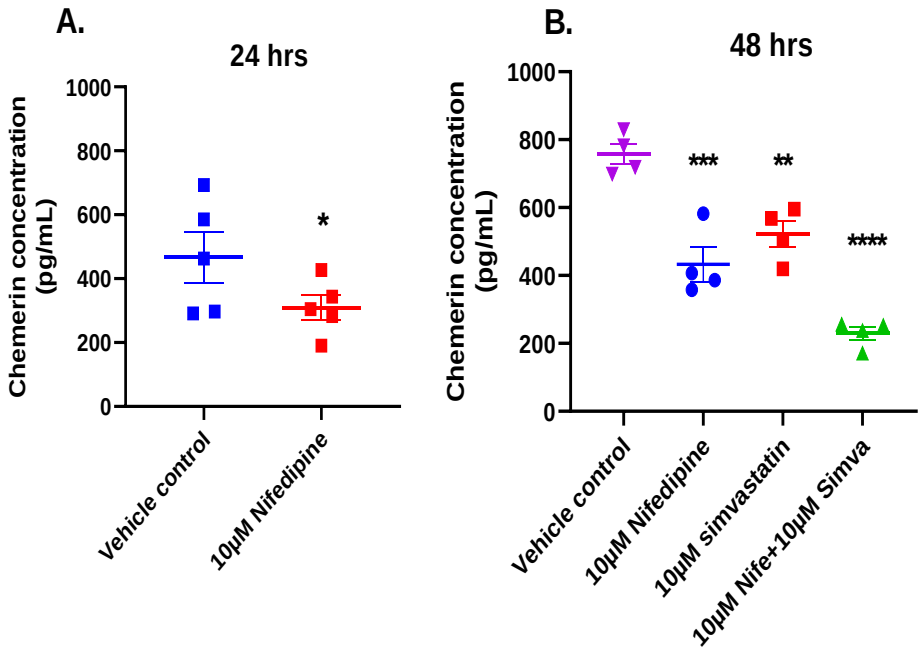


Figure 3.9. **(A)** The levels of chemerin released from cultured 3T3-L1 adipocytes into the media in the presence of 10 μM nifedipine or vehicle control (0.1 % v/v DMSO) after 24 h of incubation. **(B)** The levels of chemerin released from 3T3-L1 adipocytes following 48 h of incubation with 10 μM nifedipine, 10 μM simvastatin or 10 μM nifedipine + 10 μM simvastatin, or vehicle control (0.2 % v/v DMSO). Data are expressed as pg of

chemerin released per ml of media and are means ± SEM (n = 5 for **A** and n = 4 for **B**). *$p < 0.05$, **$p < 0.01$, ***$p < 0.001$, and ****$p < 0.0001$ using a Student's two-tailed, paired *t*-test for **A** and one-way ANOVA followed by a Sidak's *post-hoc* test vs. the vehicle control for **B**.

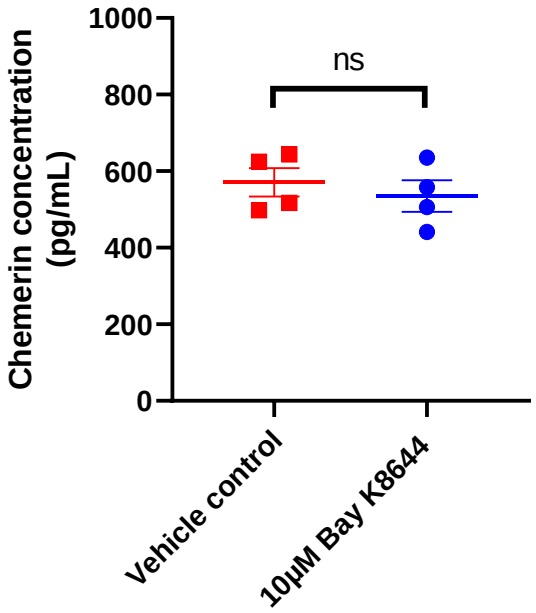


Figure 3.10. **(A)** The levels of chemerin released from cultured 3T3-L1 adipocytes into the media in the presence of 10 μM Bay K8644 or vehicle control (0.1 % v/v DMSO) after 24 h of incubation. Data are expressed as pg of chemerin released per ml of media and are means ± SEM (n = 4). Data were analysed using a Student's two-tailed, paired *t*-test.

3.3.6 Role of LPS in the simvastatin-mediated inhibition of chemerin release by cultured 3T3-L1 adipocytes

To investigate the effects of inflammation on chemerin release by 3T3-L1 adipocytes and the ability of simvastatin to alter chemerin release during inflammation, the adipocytes were incubated with 1 μg/ml LPS in the presence or absence of 10 μM simvastatin. 1 μg/ml LPS significantly increased chemerin release from 512 ± 39 pg/ml in the vehicle control to 763 ± 50

pg/ml. 10 μM simvastatin inhibited the overall release of chemerin and the enhanced release in the presence of LPS, the chemerin levels reduced to 231 ± 37 pg/ml in the presence of 10 μM simvastatin alone, and to 383 ± 38 pg/ml in the dual presence of 10 μM simvastatin and 1 μg/ml LPS (Figure 3.11).

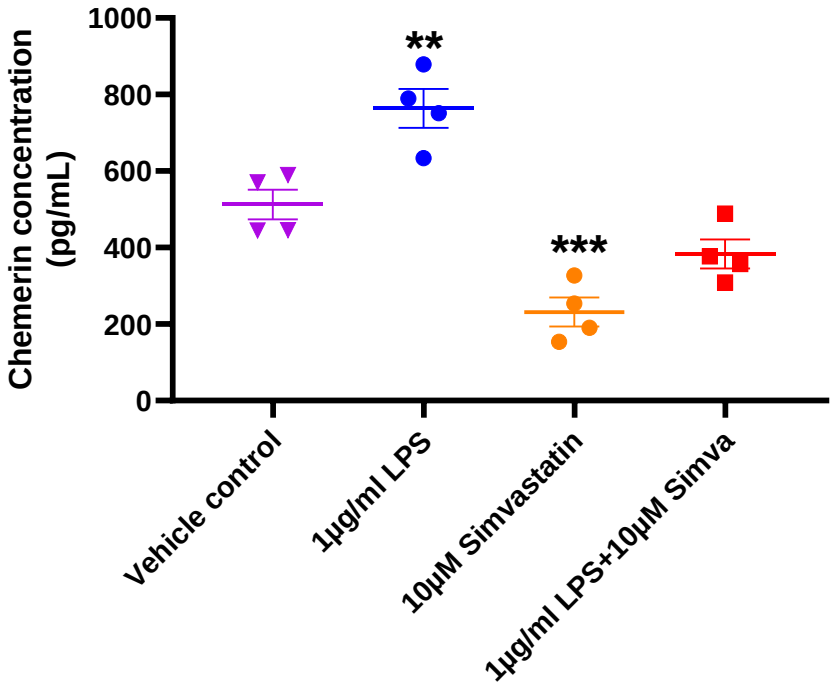


Figure 3.11. The levels of chemerin released from 3T3-L1 adipocytes following 24 h of incubation with 1 μg/ml LPS, 10 μM simvastatin, 1 μg/ml LPS + 10 μM simvastatin, or vehicle control (0.1 % v/v DMSO). Data are expressed as pg of chemerin released per ml of media and are means ± SEM (n = 4). $**p < 0.01$ and $***p < 0.001$ using one-way ANOVA followed by a Sidak's *post-hoc* test vs the vehicle control.

3.3.7 Role of TNF-α on chemerin production by cultured 3T3-L1 adipocytes

TNF-α has been reported to increase chemerin release in 3T3-L1 cells [262]; therefore, cells were incubated with 1 ng/ml or 10 ng/ml TNF-α for 24 h in the presence or absence of 10 μM

simvastatin. As Figure 3.12 shows, TNF-α had no effect on 3T3-L1 cultured adipocyte-induced chemerin release or on simvastatin-mediated inhibition of chemerin release by 3T3-L1 cells.

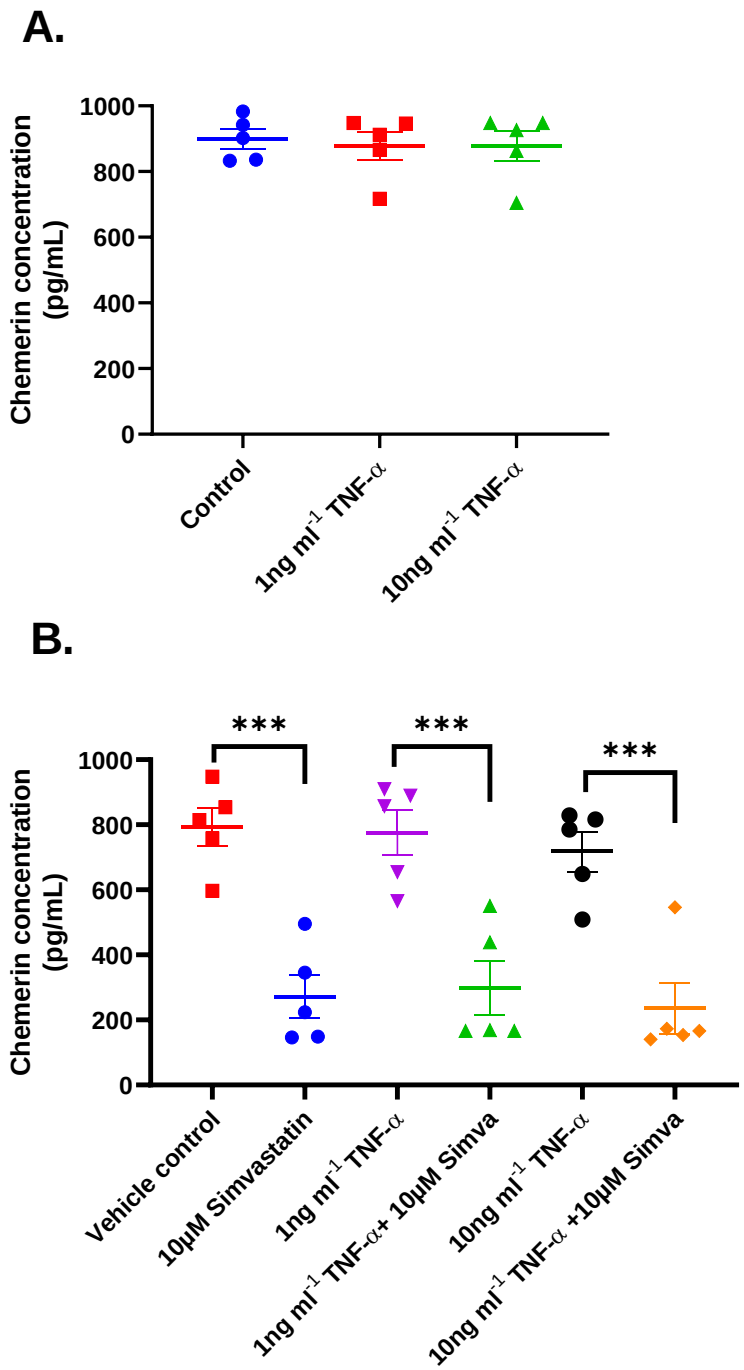


Figure 3.12. **(A)** The levels of chemerin released from cultured 3T3-L1 adipocytes into the media in the presence of 1 ng/ml or

10 ng/ml TNF-α after 24 h of incubation. **(B)** The levels of chemerin released from 3T3-L1 adipocytes after 24 h of treatment with 1 or 10 ng/ml TNF-α in the presence or absence of 10 μM simvastatin. Vehicle control cells received 0.1 % v/v DMSO. Data are expressed as pg of chemerin released per ml of media and are means ± SEM (n = 5). ***$p < 0.001$ using one-way ANOVA followed by a Sidak's *post-hoc* test.

3.3.8 Role of K_{ATP} in the simvastatin-mediated inhibition of chemerin release by cultured 3T3-L1 adipocytes

To study the role of ATP-sensitive potassium channels (K_{ATP}) in the simvastatin-induced inhibition of chemerin release, the effects of pinacidil and glibenclamide on chemerin production by 3T3-L1 in the presence or absence of simvastatin were determined (Figure 3.13). 10 μM pinacidil enhanced chemerin release from 401 ± 15 pg/ml in the vehicle control to 597 ± 31 pg/ml. This effect of pinacidil was inhibited in the presence of 1 μM glibenclamide as the chemerin concentration decreased to 370 ± 21 pg/ml in the dual presence of 10 μM pinacidil and 1 μM glibenclamide, while glibenclamide alone had no effect on the levels of chemerin release from 3T3-L1 adipocytes (393 ± 35 pg/ml in the presence of 1 μM glibenclamide vs. 401 ± 15 pg/ml in the vehicle control). Similar to glibenclamide, 10 μM simvastatin inhibited pinacidil-induced chemerin release, but treatment with simvastatin and glibenclamide had no further inhibitory effect on chemerin production by 3T3-L1 adipocytes. The concentrations of chemerin in the media were 231 ± 38 pg/ml, 374 ± 35 pg/ml, and 254 ± 48 pg/ml in the presence of 10 μM simvastatin, 10 μM simvastatin + 10 μM pinacidil, and 10 μM simvastatin + 1 μM glibenclamide, respectively.

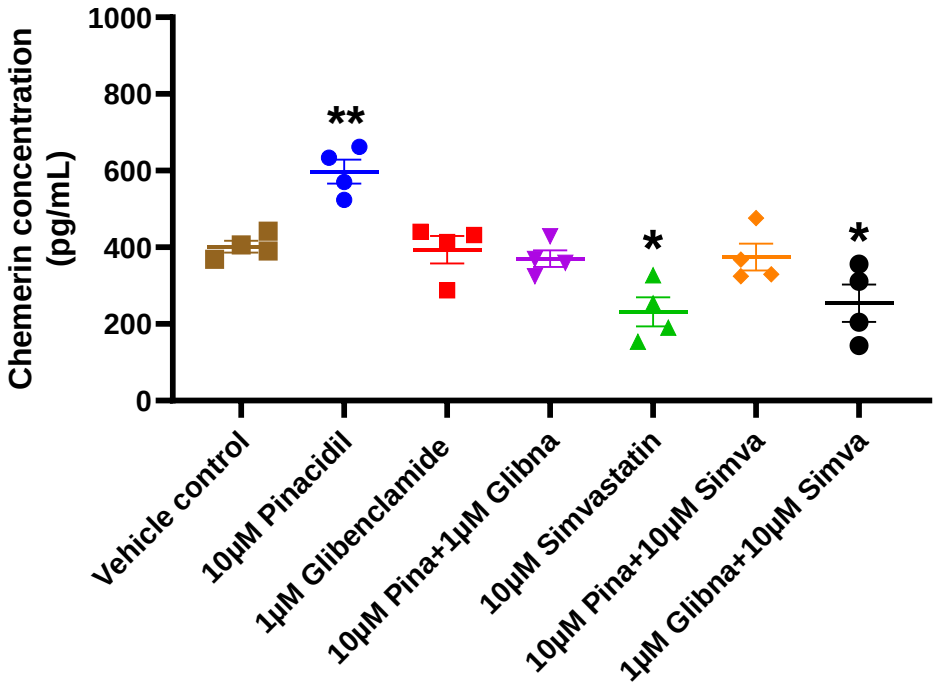


Figure 3.13. The levels of chemerin released from cultured 3T3-L1 adipocytes into the media in the presence or absence of 10 μM pinacidil, 1 μM glibenclamide, 10 μM pinacidil + 1 μM glibenclamide, 10 μM simvastatin, 10 μM simvastatin + 10 μM pinacidil, 10 μM simvastatin + 1 μM glibenclamide, or vehicle control (0.2 % v/v DMSO). Data are expressed as pg of chemerin released per ml of media and are means ± SEM (n = 4). *$p < 0.05$, **$p < 0.01$ using one-way ANOVA followed by a Sidak's *post-hoc* test vs. the vehicle control.

3.3.9 Role of PPARγ in the simvastatin-mediated inhibition of chemerin release by cultured 3T3-L1 adipocytes

To determine whether the inhibitory effect of simvastatin on chemerin release was mediated through peroxisome proliferator-activated receptor gamma (PPARγ), 3T3-L1 adipocytes were incubated for 24 or 48 h with 1 μM rosiglitazone in the presence or absence of 10 μM simvastatin (Figure 3.14A and B). 1 μM rosiglitazone increased 3T3-L1-induced chemerin release only after 48 h of incubation, where the chemerin

concentration increased to 1,075 ± 105 pg/ml compared to 746 ± 57 pg/ml in the vehicle control. 48 h treatment (but not 24 h treatment) with 1μM rosiglitazone prevented the simvastatin-mediated inhibition of chemerin release from 3T3-L1 adipocytes (Figure 3.14 B). In the presence of 10 μM simvastatin, the level of released chemerin decreased to 333 ± 28 pg/ml and the addition of 1 μM rosiglitazone eliminated this inhibitory effect; chemerin concentration increased to the level of 1,051 ± 151 pg/ml.

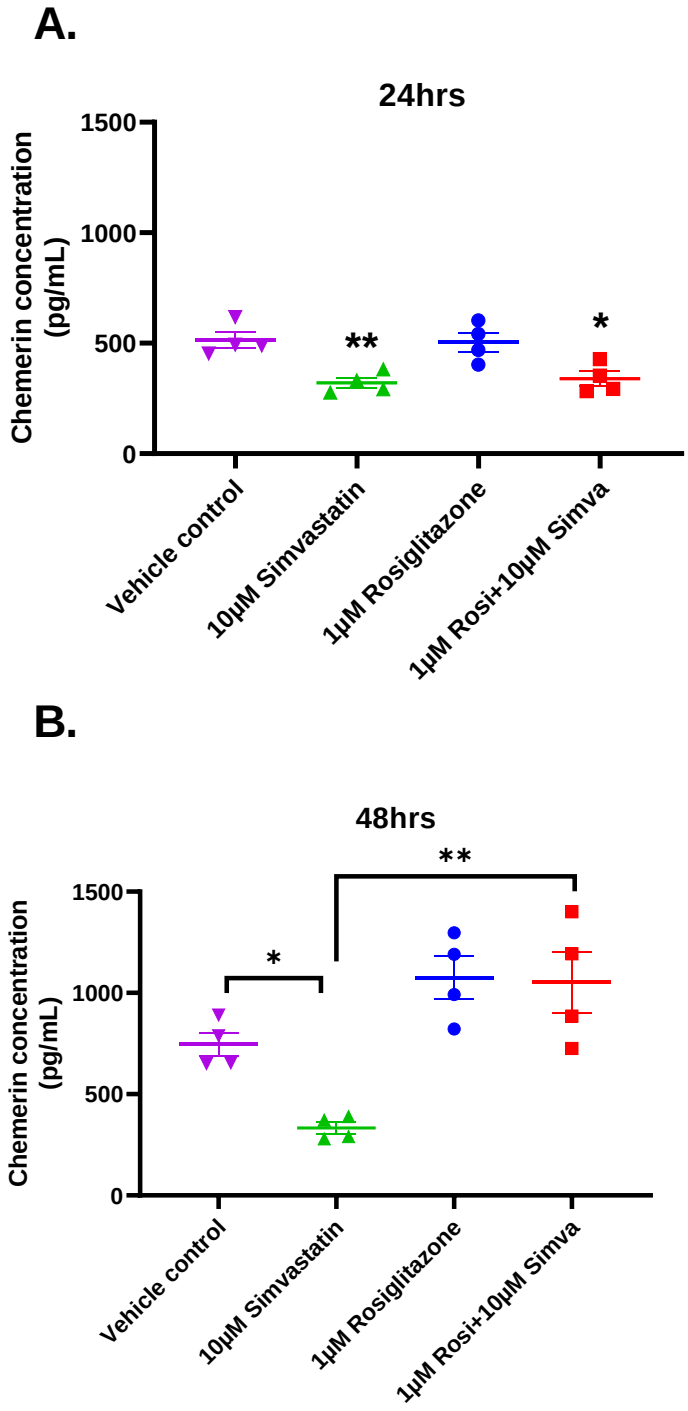


Figure 3.14. The levels of chemerin released from 3T3-L1 adipocytes following 24 h **(A)** or 48 h **(B)** of incubation with 1 μM rosiglitazone in the presence or absence of 10 μM simvastatin. Vehicle control cells received 0.2 % v/v DMSO. Data are expressed as pg of chemerin released per ml of media

and are means ± SEM (n = 4). *$p < 0.05$ and **$p < 0.01$ using one-way ANOVA followed by a Sidak's *post-hoc* test.

3.3.10 Effects of hypoxia and EFS on chemerin release by PVAT

In isolated PVAT, hypoxia (95 % N_2 and 5 % CO_2) caused a reduction in chemerin released from PVAT into the Krebs–Henseleit buffer. The concentration of chemerin reduced from 1,233 ± 72 pg/ml to 944 ± 60 pg/ml under hypoxic conditions. EFS (0.5–12 Hz, 60 V, 0.1 ms, 30 s) had no effect on PVAT-induced chemerin release (Figure 3.15).

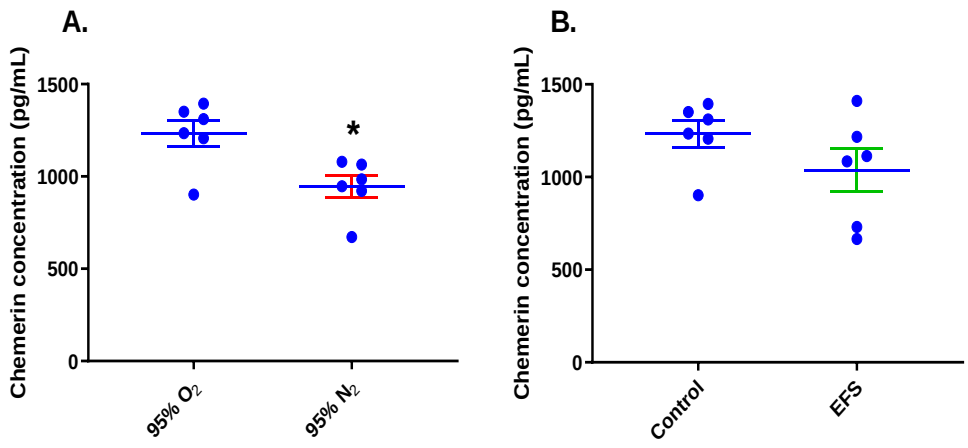


Figure 3.15. **(A)** The levels of chemerin released from 0.3 g PVAT into the Krebs–Henseleit buffer under hypoxic conditions (95 % N_2 and 5 % CO_2) compared to gassing with 95 % O_2 and 5 % CO_2. **(B)** The levels of chemerin released from 0.3 g PVAT into the buffer solution after electrical field stimulation (EFS; 0.5–12 Hz, 60 V, 0.1 ms, 30 s) was applied to PVAT. Data are expressed as pg of chemerin released per ml of Krebs–Henseleit buffer and are means ± SEM (n = 6). *$p < 0.05$, using a Student's two-tailed, paired *t*-test.

3.3.11 MTT assay of simvastatin

To study the toxicity of simvastatin on 3T3-L1 adipocytes, MTT assays were performed (Figure 3.16). The cells viabilities were circa 100 % following incubation with 10 µM simvastatin and 10 µM nifedipine. In the presence of 60 mM KCl and 10 µg/ml LPS, the cells viabilities were about 80 % and 90 %, respectively.

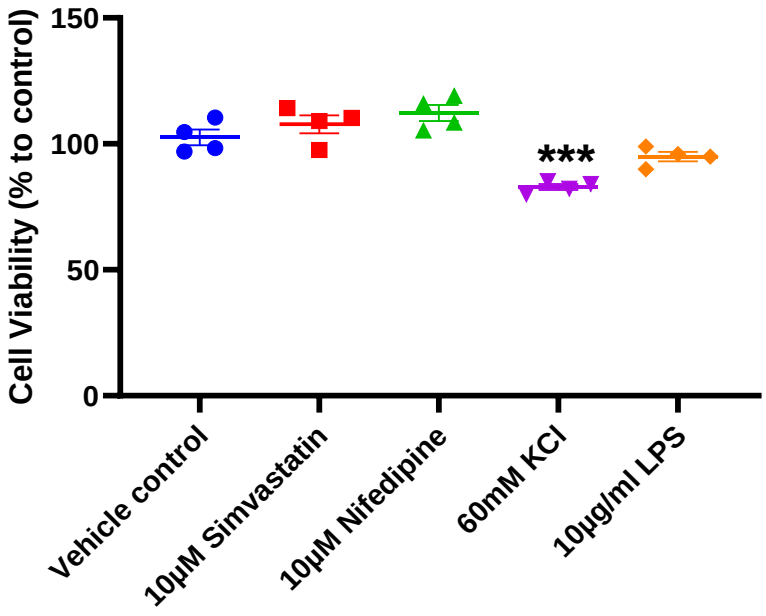


Figure 3.16. The cell viabilities of 3T3-L1 cells after 24 h of incubation with 10 µM simvastatin, 10 µM nifedipine, 60 mM potassium chloride (KCl), 10 µg/ml LPS, or vehicle control (0.2 % v/v DMSO) as determined by MTT assays. The results are expressed as percentages of the absorbance measured in the vehicle control cells and are means ± SEM (n = 4). ***$p < 0.001$ using one-way ANOVA followed by a Sidak's *post-hoc* test (n = 4).

3.4 Discussion

Chemerin plays an important role in inflammation, and chemerin gene expressions and circulating levels positively correlate with increased BMI, obesity-related biomarkers, and hypertension. Statins, on the other hand, exhibit unexplained beneficial effects such as vasodilatation and anti-inflammatory effects in patients with hypercholesterolemia, as well as in those with normal cholesterol levels. Understanding the relationship between statins and chemerin could provide insight into the mechanisms that underpin statins' pleiotropic effects. The key observations in this chapter (summarised in Figure 3.17) are that (1) both lipophilic simvastatin and hydrophilic pravastatin inhibited chemerin release from porcine coronary PVAT and 3T3-L1 adipocytes, (2) simvastatin reduced the enhancement of chemerin release during inflammation and after stimulation of K_{ATP} channels in 3T3-L1 adipocytes, (3) PPARγ agonist rosiglitazone could elevate chemerin levels and reverse simvastatin-mediated inhibition of chemerin release from cultured 3T3-L1 adipocytes and (4) induction of hypoxia reduced chemerin release from PVAT.

In this study, 10 μM simvastatin consistently inhibited the release of chemerin from both porcine coronary PVAT and 3T3-L1 adipocytes through a mevalonate-independent pathway. In 3T3-L1 adipocytes, simvastatin's inhibitory effect appeared to be concentration-dependent; 1 μM simvastatin had no effect, 10 μM and 100 μM simvastatin resulted in 30 % and 80 % inhibition of chemerin release, respectively. Also, longer incubation of 3T3-L1 cells for 48 h with 10 μM simvastatin produced a further decrease in chemerin concentrations, indicating simvastatin's time-dependent effect. By contrast, 4 h treatment of PVAT with 10 μM simvastatin had no effect on

PVAT-induced chemerin release compared to 40 % inhibition following 2 h incubations. This lack of effect of simvastatin in PVAT after 4 h of incubation could be explained in two ways. First, simvastatin may act differently on the tissue and only inhibit chemerin release in the short term. Second, the physiological buffer that covers PVAT in the myograph channels tends to evaporate after about 3 h of incubation, leaving some parts of the PVAT tissue with no oxygen supply and preventing interaction between simvastatin and PVAT. The latter idea was supported by the results for simvastatin in 3T3-L1 adipocytes, in which longer incubation produced greater inhibition, and by other published data that indicated a time-dependent effect of simvastatin on human white adipocyte-induced leptin release [269].

The hydrophilic statin (pravastatin) caused inhibition in PVAT and 3T3-L1-induced chemerin release at different concentrations. In porcine coronary PVAT, 10 μM pravastatin inhibited chemerin production by about 55 % after 2 h, while longer incubation for 4 h had no significant effect. The lack of effect after 4 h of treatment can be attributed to the same reasons previously given for simvastatin. However, in 3T3-L1 adipocytes, only a high concentration of pravastatin (100 μM) had an inhibitory effect on chemerin levels, while 10 μM (unlike in PVAT) had no effect. Although further studies are needed to clarify this, one possible explanation for the opposite effect of 10 μM pravastatin in PVAT and 3T3-L1 cells is the differential expression of the organic anion transporters required for cellular uptake of hydrophilic statins, which are unlikely to be expressed in 3T3-L1 cells. Similarly, other researchers reported that pravastatin had no effect in 3T3-L1 cells, while other

lipophilic statins had a significant effect on the glucose uptake and gene expressions of different proteins [205, 270, 271].

Statin concentrations detected in patients' plasma were found to be in the nanomolar range [272]. Indeed, the statin concentrations required to induce inhibition of chemerin release in this study were considerably higher than those for human plasma, but statins and lipophilic statins, in particular, could build up in different tissues due to their ability to diffuse through the cell membrane [273]. Accumulation of statins is more likely with chronic use, and statins are usually prescribed for life; therefore, statins' plasma concentrations may not necessarily reflect concentrations at the tissue level. Supporting the accumulation of lipophilic statins, one study demonstrated a higher concentration of simvastatin, but not pravastatin, in rats' liver tissue compared to plasma concentrations following 3 days of treatment [274]. However, Tunçez *et al.* (2019), reported a similar inhibitory effect of atorvastatin (80 mg/day) and rosuvastatin (40 mg/day) on serum chemerin levels in patients with acute myocardial infarction [234]. This latter study suggested that the results of the present investigation could reflect the effect of statins in humans, at least regarding chemerin serum concentrations; thus, 10 μM simvastatin was used for further investigation to study the mechanisms of statin-induced inhibition of the release of chemerin from adipocytes.

To investigate the mechanisms underpinning the inhibitory effect of simvastatin on chemerin release, it was important to examine the proven effects of simvastatin and any potential interactions between simvastatin and possible promotion of chemerin production by adipocytes. In this vein, different lipophilic statins have been reported to inhibit calcium influx

through multiple mechanisms, including the inhibition of L-type channels [185, 247]. Herein, blockage of L-type calcium channels by nifedipine resulted in a time-dependent inhibition of chemerin release from 3T3-L1 adipocytes, suggesting that calcium influx through L-type Ca^{2+} channels is important for adipocytes' ability to release chemerin. However, the dual presence of nifedipine and simvastatin significantly inhibited chemerin production from adipocytes compared to simvastatin alone, indicating that simvastatin-induced reduction of chemerin release may involve other pathways, independent of L-type calcium channels. To the best of my knowledge, this is the first report to show a direct inhibitory effect of Ca^{2+} channel blockers on chemerin release, which may provide opportunities for future clinical or *in vivo* investigations into the possible effects of these anti-hypertensive drugs on chemerin serum levels.

The Ca^{2+} channel opener Bay K8644 acts to promote Ca^{2+} influx most likely through voltage-gated calcium channels (VGCCs) [275]. Based on the nifedipine results, an effect of Bay K8644 on increasing intracellular Ca^{2+} was expected to enhance 3T3-L1-induced chemerin release, but the data indicated no further increase in chemerin concentrations by Bay K8644. The reason for this lack of effect is unclear, but there could be many explanations. One possibility is that the 3T3-L1 adipocytes had reached their maximum capacity for chemerin production and were unable to release further chemerin following treatment with Bay K8644. Alternatively, VGCCs may not be present in 3T3-L1 adipocytes or may have a very low functional density and the observed effects of nifedipine would be due to non-specific effects on other Ca^{2+} influx pathways. Another study reported an absence of effect for Bay K8644 to enhance

intracellular Ca^{2+} in 3T3-L1 cells [276], this latter study may outweigh the proposed hypothesis that 3T3-L1 adipocytes lacks a functional VGCCs.

Another question addressed in the current study was whether simvastatin could affect chemerin release under inflammatory conditions. LPS from *Escherichia coli* was used to study the effect of inflammation on 3T3-L1 adipocytes. LPS has been extensively used in models for studying inflammation because of its ability to stimulate the production of different proinflammatory cytokines, such as TNF-α and IL-6 in adipocytes [277]. LPS could strongly trigger the release and production of various inflammatory factors and cytokines in 3T3-L1 cells by activating toll-like receptor 4 signalling pathways [278]. 3T3-L1 adipocytes in the present study increased chemerin production by more than 30 % after 24 h of incubation with 1 µg/ml LPS—an effect that was blocked by treatment with 10 µM simvastatin. The LPS effect reported here was consistent with previous studies indicating elevated levels of chemerin due to LPS application *in vivo* and *in vitro* [279-281]. Also, lovastatin and simvastatin were found to inhibit LPS-induced NO and TNF-α in different cell lines [282, 283]. To test whether the LPS enhancement of chemerin release was mediated through LPS-induced TNF-α, TNF-α was directly applied to 3T3-L1 cultured adipocytes, but it had no effect on chemerin levels or the simvastatin-mediated inhibition of chemerin release. The concentrations (1 ng/ml or 10 ng/ml) and incubation times of TNF-α used in the current study were consistent with those of other studies that observed increased chemerin release and expression in 3T3-L1 adipocytes and bovine differentiated adipocytes due to the addition of TNF-α [262, 284]. The reason for the lack of effect of TNF-α is unclear

and needs further investigation, but LPS may directly increase chemerin production and/or increase other proinflammatory cytokines, such as IL-6, to stimulate chemerin release. Nevertheless, it is well documented that chemerin levels are elevated in obesity, and adipose tissue dysfunction is often associated with an increased release of proinflammatory cytokines. The current study demonstrated a strong association between adipose tissue inflammation and chemerin production and proposes a new pleiotropic effect of simvastatin in preventing LPS-induced enhanced chemerin release from adipocytes.

Activation of ATP-sensitive potassium channels (K_{ATP}) was reported to enhance chemerin release in cultured rat aortic endothelial cells and the release of other adipokines, such as resistin and visfatin, in 3T3-L1 adipocytes [265, 285]. In contrast, simvastatin has been shown to inhibit K_{ATP} channel activity in various studies, including vascular activity in porcine coronary arteries from our lab and others, where simvastatin significantly inhibited relaxation of the K_{ATP} channel opener pinacidil [286, 287]. In the present study, incubation of 3T3-L1 adipocytes with 10 μM pinacidil caused about a 50 % increase in chemerin production; this effect was blocked by simvastatin and/or glibenclamide. However, this study demonstrated that the blocker of K_{ATP} channels (glibenclamide) alone had no effect on the basal chemerin release in 3T3-L1 adipocytes. Therefore, this would seem to rule out inhibition of K_{ATP} channels as a mechanism by which simvastatin inhibits basal release of chemerin.

PPARγ agonists, including rosiglitazone, are effective for the regulation of adipogenesis and adipokine release [288, 289]. One study reported increased serum chemerin levels in mice

treated with rosiglitazone, which were associated with elevated chemerin mRNA levels in adipose tissue [290]. Studies of the potential effects of statins on PPARγ have produced conflicting results; for example, simvastatin was shown to prevent bone marrow adipogenesis by downregulating PPARγ [291], but another study reported that atorvastatin increased PPARγ activation in primary human monocytes [292]. Such differences in the effects of statins on PPARγ could relate to the diversity of different cell lines or the types of statins used [293]. In the current study, unlike 24-h incubation, treatment with 1 μM rosiglitazone for 48 h increased cultured 3T3-L1-induced chemerin release by 30 % and eliminated the inhibitory effect of simvastatin treatment.

The findings for rosiglitazone differed from those for nifedipine, LPS, or pinacidil in that rosiglitazone was able to reverse simvastatin's inhibitory effect on chemerin levels (see Figure 3.17), and these results could be interpreted in different ways. First, it is possible that at least the long-term inhibition of chemerin release observed for simvastatin treatment was mediated through the inhibition of PPARγ, and rosiglitazone's activity on PPARγ reversed this inhibitory effect of simvastatin. Second, rosiglitazone and simvastatin may induce opposite effects through unidentified mechanisms that are important in 3T3-L1-induced chemerin release. Additionally, since rosiglitazone had no effect on chemerin levels after 24 h of incubation and only increased chemerin release with prolonged treatment for 48 h, this may suggest that rosiglitazone's effect is due to the enhancement of chemerin gene expression in 3T3-L1 adipocytes. It is possible that simvastatin acts through a distinct mechanism, and the increase in chemerin gene expression induced by rosiglitazone led to enhancement of

chemerin production to a level that simvastatin was unable to prevent. However, the current investigation was supported by a recent study conducted by Guo *et al.*, in 2020, which found simvastatin to have an inhibitory effect on the differentiation process of bone marrow-derived mesenchymal stem cells (BMSCs) through the downregulation of PPARγ and the PPARγ-mediated induction of chemerin mRNA expression [235]. In the same study, the authors obtained similar results to the present findings, with rosiglitazone treatment partially reversing the negative regulatory effects of simvastatin on chemerin mRNA expression. Taken together, these results may suggest that rosiglitazone is capable of inhibiting the beneficial pleiotropic effects of simvastatin in reducing chemerin release from adipocytes, although more investigations are required to examine whether these findings can be verified at the clinical level.

Rosiglitazone is an effective antidiabetic drug that has been withdrawn from the market due to adverse cardiovascular events, including myocardial infarction, heart failure, stroke, and weight gain [294, 295]. Considering chemerin's well-known pro-adipogenesis effect and the different studies indicating a positive correlation between chemerin and previously mentioned CV complications, it seems fair to suggest that the ability of rosiglitazone to enhance chemerin release from adipocytes in the present study (and others [235, 290]) may explain the increased weight gain and CV side effects caused by rosiglitazone treatment [101, 127]. However, more studies—especially clinical observations—are needed to form definitive conclusions about the effects of rosiglitazone on serum chemerin levels and how they may be connected to CV incidents caused by rosiglitazone.

In summary, these data showed the ability of simvastatin and pravastatin to inhibit chemerin release from PVAT and cultured 3T3-L1 adipocytes, and this effect may explain some statins' pleiotropic effects. The results in this chapter propose a new effect of simvastatin by preventing enhanced chemerin release from adipocytes during inflammation and the activation of K_{ATP} channels. This study suggests rosiglitazone as a promoter of chemerin release from 3T3-L1 adipocytes and hypoxia as an inhibitor of PVAT-induced chemerin release.

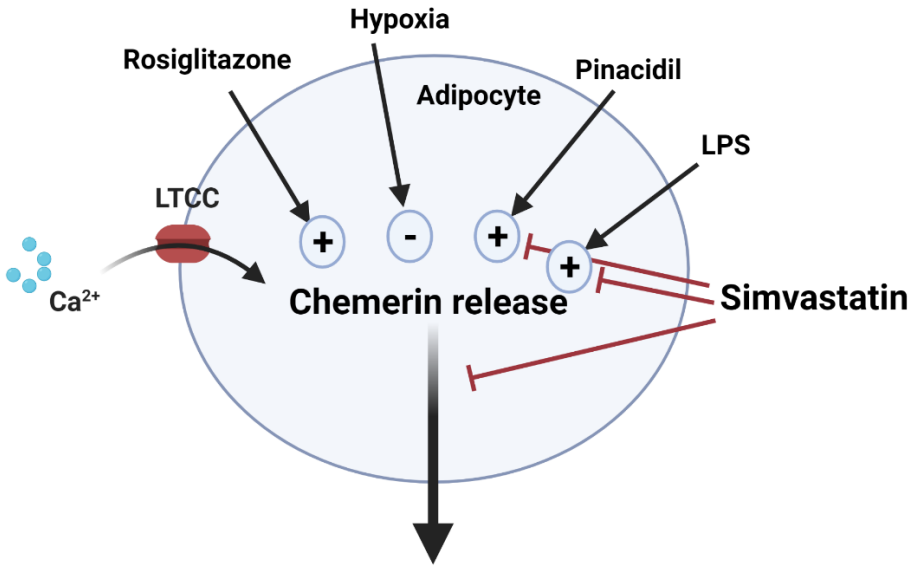


Figure 3.17. Hypothesized schematic diagram of the effect of simvastatin on total chemerin release from adipocyte. The present study demonstrated that simvastatin inhibited the basal release of total chemerin as well as prevented enhanced chemerin release from adipocytes following incubation with lipopolysaccharide (LPS) or the K_{ATP} channels opener, pinacidil. This study suggests rosiglitazone as a promoter of chemerin release from adipocytes and hypoxia as an inhibitor of chemerin release.

Chapter 4
Effects of precontraction with the thromboxane mimetic U46619 on chemerin-induced contraction in porcine coronary arteries

4.1 Introduction

Perivascular adipose tissue (PVAT) is the fat deposit that surrounds most systemic blood vessels. Owing to its unique location and secretome profile, PVAT has received particular attention recently, with studies demonstrating a clear role of PVAT in vascular physiology and pathophysiology. PVAT releases many factors that stimulate vasodilatation and vasoconstriction and, hence, plays a key role in the regulation of vascular tone. These factors include adipokines such as leptin, adiponectin, thromboxane, and chemerin, as well as vital cytokines including interleukins, tumour necrosis factor α (TNFα), and gaseous molecules like H_2S (for more information, see Chapter 1 and [29, 43]). Although studies have demonstrated the effects of individual adipose-derived compounds on vascular tone, less is known about whether these PVAT-derived compounds might act synergistically.

Chemerin is a small adipokine (a 16kDa protein) secreted from hepatocytes and adipocytes [253]. Three G protein-coupled receptors (GPCRs) are currently known to bind chemerin: chemerin receptor 1 (also known as ChemR23 and CMKLR1) [109, 110], chemerin receptor 2 (GPR1) [104], and C-C chemokine receptor-like 2 (CCRL2) [107]. The vascular effects of chemerin appear to be mediated through activation of chemerin receptor 1 ($Chemerin_1$) [94, 108]. $Chemerin_1$ is expressed in human endothelial cells [112], vascular smooth muscle cells (VSMCs) [94], adipocytes [152], and immune cells, including dendritic cells, monocytes, macrophages, and natural killer (NK) cells [253]. PVAT-induced chemerin release plays a potential role in hypertension due to chemerin's ability to induce contraction of vascular smooth muscles, and the proximity of PVAT to vasculature may reinforce this action of chemerin

[108]. Also, chemerin could play a key role in obesity-induced hypertension as a result of the high amount of chemerin released from the excess adipose tissue typical of obesity [94, 296]. Thus, chemerin is considered a biomarker for obesity since its increased level is strongly attributed to high body mass index (BMI) and metabolic syndrome [123, 297], whereas weight loss causes a reduction in chemerin levels [141, 143].

Chemerin, either as chemerin-9 or full-length recombinant peptide, causes contraction of isolated arteries in rats and humans [93, 94]. Also, chemerin was reported to potentiate the effect of established vasocontractile agents; for instance, one study found that chemerin-9 potentiated phenylephrine- and endothelin-1-induced contraction in rat aorta through an ERK-MAPK pathway [152]. Also, a study demonstrated that pre-treatment with chemerin-9 amplifies electrical field-stimulated contraction in isolated rat superior mesenteric arteries [151]. None of these studies, however, indicated any role of these contractile agents in amplifying chemerin's vascular effect.

$Chemerin_1$ is a Gi protein-coupled receptor [111]. Previous studies in our laboratory have demonstrated that activation of the thromboxane receptors (TP) in blood vessels can lead to enhanced contractile responses to α_2-adrenoceptor activation and neuropeptide Y_1-receptor activation, both of which are Gi protein-coupled receptors [298, 299]. Since chemerin and thromboxane are both released from PVAT [92, 145, 151], I hypothesised that they might act synergistically to produce enhanced contraction.

VSMC contraction plays an important role in the regulation of vascular tone. Contraction in VSMCs is triggered by an increase in intracellular free Ca^{2+} concentration ($[Ca^{2+}]_i$) which could be increased in two ways: by Ca^{2+} release from the intracellular

stores in the smooth sarcoplasmic reticulum and/or by Ca^{2+} entry from the extracellular space through the plasma membrane Ca^{2+} channels, particularly voltage-dependent L-type Ca^{2+} channels. In the cytosol, Ca^{2+} binds calmodulin to form a Ca^{2+}–calmodulin complex that activates myosin light chain (MLC) kinase. This in turn causes MLC phosphorylation and thus enables a cross-bridge formation with actin, resulting in VSM contraction [300]. Activation of Rho kinase can lead to further enhancement of VSM contraction through inhibition of MLC phosphatase, thereby preventing dephosphorylation of MLC [301]. Activation of extracellular regulated kinase (ERK) is another important pathway in vascular tone regulation. ERK is thought to cause vasoconstriction through phosphorylation and inhibition of the actin-binding protein caldesmon [302], which is responsible for the direct inhibition of myosin ATPase activity. Myosin ATPase hydrolyses ATP to provide energy for actin-myosin cross-bridging [303].

As shown in Chapter 2, section 2.3.1, PVAT-induced contraction is significantly enhanced in the presence of the thromboxane mimetic U46619, suggesting that U46619 could initiate a series of events in PVAT that amplify the release of vasoconstrictor adipokines and/or enhanced receptors that mediate contraction within PCA, including the Gi Chemerin$_1$. This latest hypothesis is reinforced by the ability of simvastatin to inhibit both the enhanced PVAT-induced contraction in the presence of U46619 and the release of chemerin from PVAT. This is also supported by earlier research in our laboratory, which found that the enhanced contraction to Gi α_2-adrenoceptor activation in the presence of a thromboxane receptor agonist in blood vessels is mediated through enhanced activation of Rho kinase and ERK [304]. Therefore, the aims of this chapter were to determine

the effect of TP activation on chemerin-induced contraction of porcine coronary arteries (PCAs) and to determine the signalling pathways that underlie this process.

4.2 Materials and Methods

4.2.1 Tissue preparation

Tissues were set up as previously described in Chapter 2, section 2.2.1.

4.2.2 Experimental protocol

As previously described in Chapter 2, section 2.2.2, vessels of distal PCAs were set up in a wire myograph initially pre-tensioned to 3 g and then left to equilibrate for approximately 45 min. Once a stable baseline was attained, two consecutive responses to 60 mM KCl were obtained for standardisation before test compounds were added to the bath. In some experiments, the endothelium of the PCA vessels was removed mechanically by rubbing the lumen gently with forceps. The denuding of the endothelium was confirmed by a lack of relaxation to 100 nM substance P. It has been noticed that denuded PCA showed no response at all for substance P when precontracted with KCl, therefore, denuded vessels that induced even minor relaxation response to substance P were discarded.

Effects of precontraction with U46619 on chemerin-induced contraction

To determine whether precontraction with U46619 altered the contractile response to chemerin, tissues were precontracted with U46619 to a level between 10–20 % of the maximum second KCl response [298] or (in different experiments) to a lower level of KCl response. After the contraction had reached a plateau, a single concentration of chemerin-9 (1, 10, or 30 μM) was added. In control tissues, chemerin-9 was added to the tissues under baseline conditions. In tissues precontracted with U46619, the change in tone was recorded from the point

where chemerin-9 was added to the bath. To examine the effect of hypoxia, the gas cylinder was quickly swapped to 95 % N_2 and 5 % CO_2 for 30 min before or (in different experiments) after the addition of U46619. When a stable U46619 precontraction level was reached, chemerin-9 was added during gassing with 95 % N_2 and 5 % CO_2. To determine the endothelium-dependent effects of U46619 precontraction on chemerin-9-induced vasocontraction, endothelium-denuded rings were used and compared to endothelium-intact vessels as a control. To study the role of chemerin in U46619 contraction, PCA segments were exposed to 10 µM chemerin-9 before the addition of cumulative concentrations of U46619. In a different set of experiments, tissues were precontracted with either KCl or the calcium channel activator BAY K8644 to a level between 10–20 % of the 60 mM KCl before the addition of chemerin-9.

Roles of Rho kinase, ERK MAP kinase, PI3 kinase, Nox1 inhibitor, and L-type calcium channels in chemerin-induced contraction

Distal PCA rings from the same animal were set up in wire myographs as described above. Tissues were exposed to the following compounds for 1 h: PD98059 (50 µM) to inhibit ERK MAP kinase activity [305], Y-27632 (10 µM) to inhibit Rho kinase [306], LY294002 (10 µM) to inhibit phosphoinositide 3-kinase (PI3 kinase) [306], 2-acetylphenothiazine (ML171) (100 µM) as a selective NADPH oxidase-1 (NOX1) inhibitor [307], and the L-type calcium channel blocker verapamil (10 µM). Ethanol (0.1 % v/v) was used as a vehicle control for PD98059, Y-27632, LY294002, ML171, and verapamil. Tissues were then treated with 10 µM of chemerin-9, with or without precontraction by U46619. The U46619 concentrations required to induce contraction in tissues exposed to the previous

compounds were different, and the concentrations of U46619 were adjusted (as indicated in the results section) to ensure a similar level of precontraction in each tissue.

Role of extracellular calcium in chemerin-induced contraction

To determine whether extracellular calcium was involved in enhanced vasoconstriction in response to chemerin-9 in the presence of U46619, the Krebs–Henseleit buffer was replaced with calcium-free Krebs–Henseleit buffer in which the calcium chloride had been replaced with 2 mM EGTA, before precontracting the PCA rings with U46619 to a level between 10–20 % of KCl response and the addition of 10 μM chemerin-9. A higher concentration of U46619 was required to induce contraction in the absence of extracellular calcium, and the concentrations of U46619 were adjusted as indicated in the results section.

4.2.3 Determination of PVAT-induced chemerin release in the presence of U46619 by ELISA

To investigate whether U46619 could enhance the release of chemerin from PVAT, the level of total chemerin released by PVAT into the Krebs–Henseleit solution was determined by ELISA in the presence or absence of U46619. As previously described in Chapter 2, section 2.2.3, 0.3 g PVAT was incubated in the Krebs–Henseleit buffer with or without 5 nM U46619 for 60 min to maintain consistency with the functional studies. Total chemerin levels in the Krebs–Henseleit solution were then determined using a pig chemerin ELISA Kit (abx257462, Abbexa, Cambridge, UK) according to the manufacturer's instructions. The results were expressed as picograms (pg) of total chemerin released per ml of Krebs–Henseleit solution.

4.2.4 Estimation of total and phosphorylated ERK and MYPT-1 expression in PCA by immunoblotting

SDS-polyacrylamide gel electrophoresis (SDS-PAGE) and Western blotting, followed by immunoblotting, were carried out to determine the expression of phosphorylated and total extracellular signal-regulated kinase (ERK) or total and phosphorylated myosin phosphatase target subunit 1 (MYPT1) in PCA segments after contraction with chemerin-9, either at the baseline tone or in the presence of U46619. PCA segments were mounted in a wire myograph as described previously. Four distal PCA vessels from the same animal were exposed to either (a) 10 μM chemerin-9 at the baseline, (b) 10 μM chemerin-9 after U46619 precontraction, (c) U46619 precontraction only, or (d) a control segment that was not exposed to any compound (baseline conditions). When the vessel tone reached a plateau, the segments were quickly removed from the tissue baths and immediately frozen on dry ice. Frozen segments were then homogenised on ice with 75 μl of homogenisation buffer (80 mM sodium β-glycerophosphate, 20 mM imidazole, 1 mM dithiothreitol, and 1 mM sodium fluoride (pH 7.6)) containing a protease inhibitor cocktail (Caliche, VWR International Ltd, Lutterworth, Leicestershire, UK). Estimation of the protein content of each sample was performed using a Bradford protein assay. Homogenised samples were diluted 1:1 in 2x Laemmli solubilisation buffer before heating at 100 ^{o}C for 5 min and centrifuged at 13,000 rpm in a bench-top centrifuge for 1 min. Five μg of each sample were separated using a 4–20 % gradient SDS-PAGE gel (Bio-Rad, Hemel Hempstead, Hertfordshire, UK) and then transferred onto nitrocellulose membrane (GE Healthcare, Little Chalfont, Buckinghamshire, UK) by Western blotting.

Nitrocellulose membranes were then blocked with 5 % bovine serum albumin (BSA) in Tris-buffered saline containing 0.1 % Tween 20 (TBST) at room temperature for 1 h. The membranes were then probed overnight with either rabbit anti-phosphorylated ERK antibody (1:1,000; #4370, Cell Signaling Technology, MA, USA), mouse anti-total ERK antibody (1:1,000; #9107, Cell Signaling Technology, MA, USA), rabbit anti-phosphorylated MYPT1 antibody (1:1,000; Ser507 #3040, 1:1,000; Ser668 #3048, 1:1,000; Thr853 #4563, and 1:1,000; Thr696 #5163 Cell Signaling Technology, MA, USA) or rabbit anti-MYPT1 antibody (1:1,000; #2634, Cell Signaling Technology, MA, USA). The following day, the blot was washed in TBST 3 times every 15 min for 1 h. After washing, blots were incubated with IRDye 800CW goat anti-rabbit or IRDye 680CW goat anti-mouse secondary antibodies (both at 1:10,000 dilution; IRDye, LI-COR, Cambridge, UK) for 1 h before being washed again in TBST. The immunoblot was then visualised using an Odyssey system, and bands were analysed by densitometry using Odyssey Image Studio (LI-COR).

4.2.5 Statistical analysis

All values are expressed as means ± SEM (standard error of the mean) from at least six independent experiments, with n representing the number of different animals. Time-response curves were obtained graphically using Graphpad Prism (version 7, GraphPad Software, La Jolla, California, USA). The contractile responses were expressed as percentages (%) of the contraction induced by 60 mM KCl. ELISA results were expressed as picograms (pg) of chemerin released per ml of Krebs–Henseleit buffer. Western blot results were expressed as percentages of the relative protein expression in control segments (baseline tone) based on the intensities of the bands

using Odyssey Image Studio (LI-COR). Statistical tests were performed using a two-tailed, paired Student's *t*-test to compare differences between two groups. Differences between three or more groups were assessed using one-way ANOVA or two-way ANOVA in conjunction with a Sidak's *post-hoc* test. *p* values less than 0.05 ($p < 0.05$) were considered to be statistically significant. Asterisks (*) indicate the differences between each group. **** indicates $p < 0.001$, *** indicates $p < 0.001$, ** indicates $p < 0.01$, and * indicates $p < 0.05$.

4.2.6 Drugs and chemicals

All drugs were purchased from Tocris-Cookson (Bristol, UK), except for chemerin-9, which was purchased from GenScript (RP20248; Piscataway, NJ, USA). Stock solutions of chemerin and KCl were dissolved in distilled water and U46619 stock solution was dissolved in dimethyl sulfoxide (0.1 % v/v DMSO), while stock solutions of all other drugs were dissolved in absolute ethanol. All further dilutions of the stock solutions were made using distilled water. Stocks were kept frozen at -20 °C, except for KCl, which was kept at room temperature.

4.3 Results

4.3.1 The level of PVAT-derived chemerin in the presence of U46619

As the data in Chapter 2 (section 2.3.1) showed, PVAT-induced contraction is amplified in the presence of U46619; hence, these studies examined whether the thromboxane mimetic U46619 could enhance PVAT-derived chemerin release. The ELISA results indicated no difference in the levels of total chemerin released from PVAT in the presence or absence of U46619. Total chemerin concentrations released from PVAT were 743 ± 76 pg/ml in the absence of U46619 and 640 ± 125 pg/ml in the presence of 5 nM U46619. However, there was a significant difference between the levels of released chemerin in the presence of PVAT and those measured in a blank sample which were about 3 ± 1 pg/ml (no tissue present; Figure 4.1).

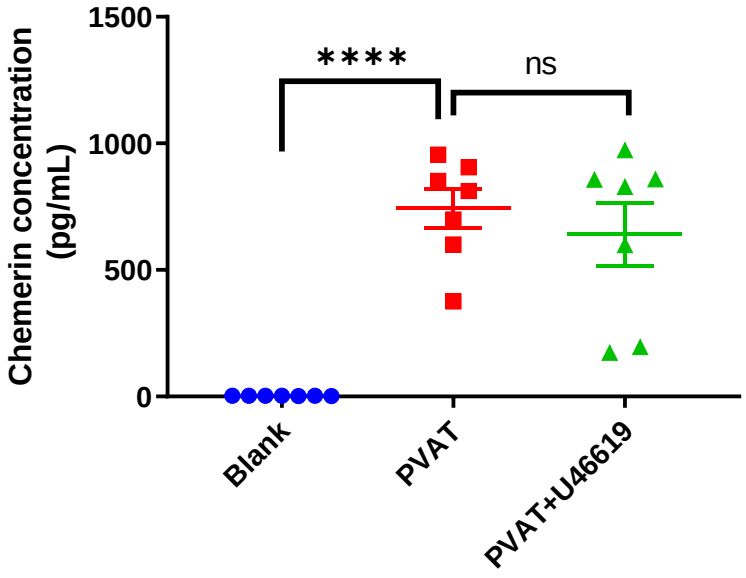


Figure 4.1. The levels of chemerin released from 0.3 g PVAT into the Krebs-Henseleit buffer in the presence or absence of 5 nM U46619. Data are expressed as pg of chemerin released per ml and are means ± SEM (n = 8): ****$p < 0.0001$ using one-way ANOVA followed by a Sidak's *post-hoc* test.

4.3.2 Effects of U46619 precontraction on the response to chemerin in PCA

Since no difference was identified in PVAT-induced chemerin release in the presence of U46619, it was determined whether pre-treatment of the PCA segments with U46619 could enhance chemerin-9-induced contraction. Chemerin-9 is the activate fragment of the full peptide chemerin. Precontraction with U46619 to a level between 10–20 % of KCl response significantly enhanced chemerin-9-induced contraction for all the concentrations used. The addition of 1 μM chemerin-9 produced a vasocontraction of 4 ± 1 % (of KCl response) at baseline tone, whereas in vessels precontracted with U46619, the contraction was 12 ± 2 %. With 10 and 30 μM chemerin-9, contractions at baseline tone were 10 ± 1 % and 11 ± 2 %, respectively, while in the presence of U46619, their vasoconstrictions were enhanced to 21 ± 2 % and 38 ± 6 %, respectively (Figure 4.2A and Figure 4.3). The concentration of U46619 needed to induce 10– 20 % contraction of the maximum KCl response was 1-5 nM. A similar enhanced contraction for 10 μM chemerin-9 was seen in the presence of a low U46619 concentration (0.2-1 nM), producing about 3 % of KCl response (Figure 4.2B). Furthermore, there was no difference in contractile response to chemerin-9 in the presence of U46619 between endothelium-intact and endothelium-denuded vessels (Figure 4.2C).

By contrast, pre-incubation of PCAs with 10 μM chemerin-9 had no effect on the subsequent addition of cumulative concentrations of U46619 (Figure 4.4).

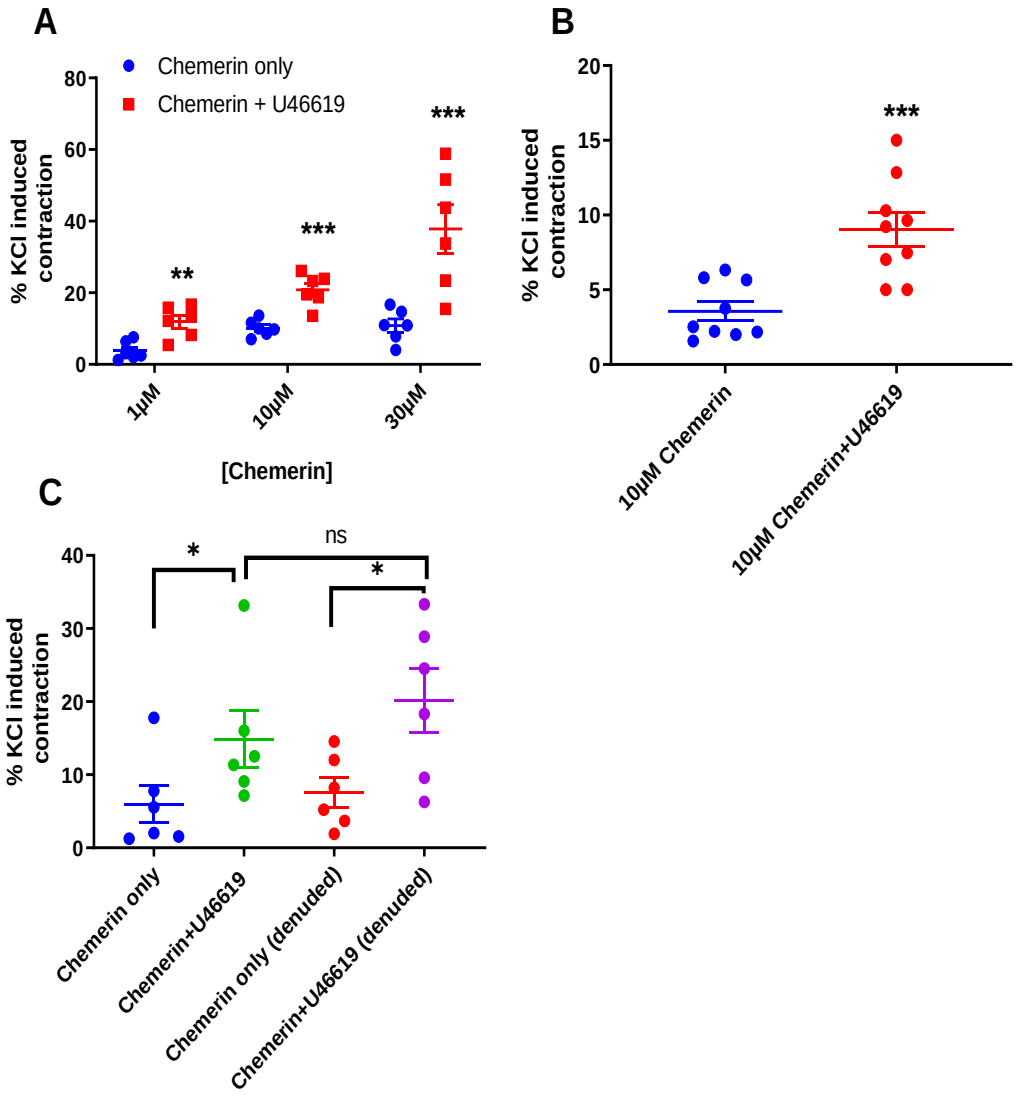


Figure 4.2. (A) Effects of 1, 10, and 30 µM chemerin-9 on contractile responses in PCAs at baseline tone (chemerin only) and after precontraction with the thromboxane agonist U46619 (1-5 nM) to a level between 10 % and 20 % of 60 mM KCl-induced contraction (chemerin + U46619). **(B)** Effects of 10 µM chemerin-9 in the presence or absence of a low U46619 concentration (0.2-1 nM) producing tone equivalent to about 3 % of the KCl response. **(C)** Effects of 10 µM chemerin-9 in the presence or absence of U46619 in endothelium-intact or endothelium-denuded PCAs. All data are expressed as percentages of the contraction induced by 60 mM KCl and are

means ± SEM (n = > 6). Asterisks compare the significant differences with values obtained from the control: *$p < 0.05$, **$p < 0.01$, ***$p < 0.001$ using a two-tailed, paired student's *t*-test for **A** and **B** or one-way ANOVA followed by a Sidak's *post-hoc* test for **C**.

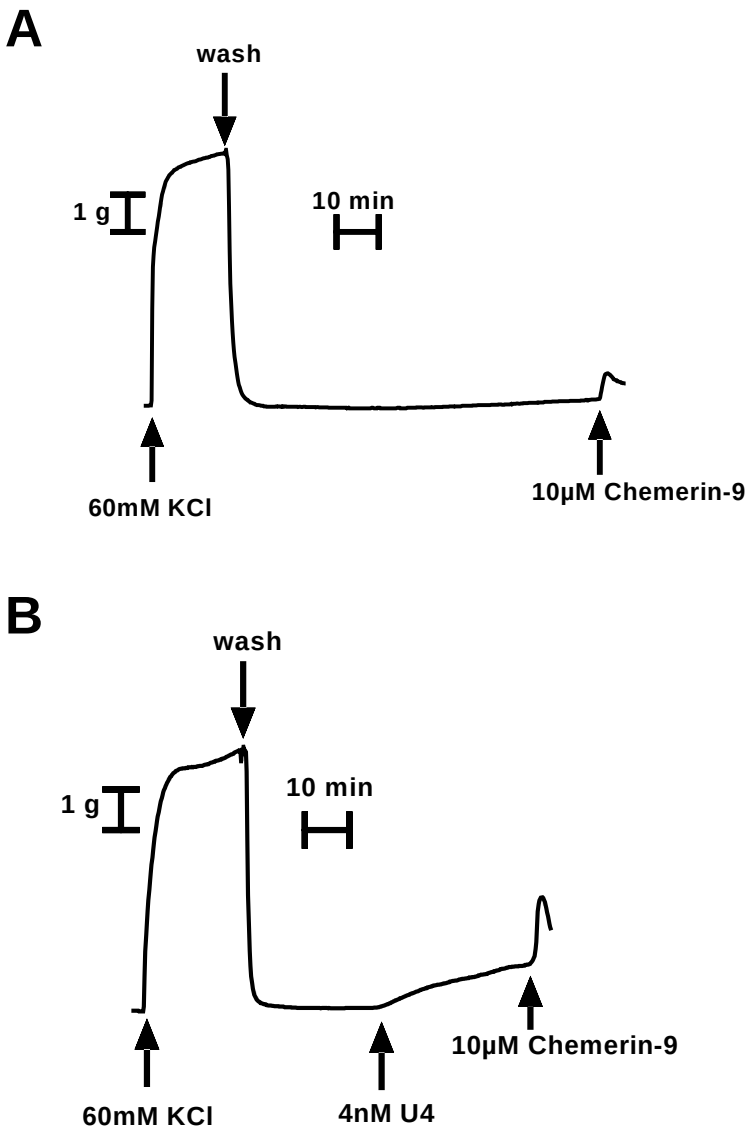


Figure 4.3. Original traces showing the responses of PCA to chemerin-9 at baseline tone **(A)** and in vessels precontracted with U46619 to a level between 10–20 % of KCl response **(B)**.

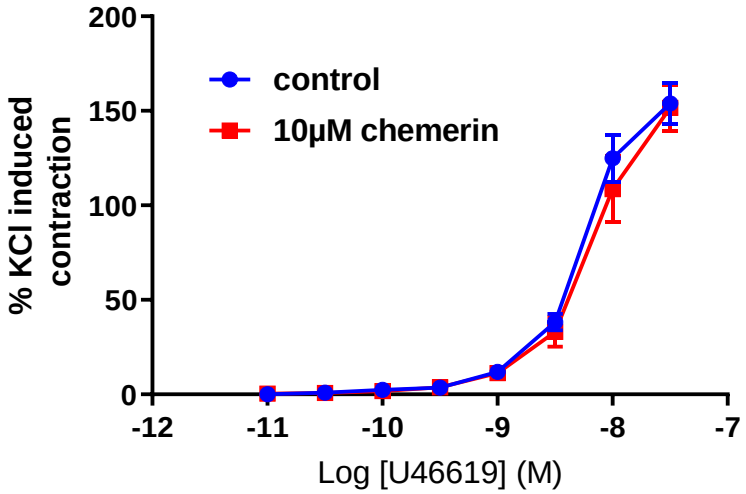


Figure 4.4. Effect of pre-incubation of PCAs with 10 μM chemerin-9 on the contractile response to cumulative additions of U46619. Data are expressed as percentages of the contraction induced by 60 mM KCl and are means ± SEM (n = 6).

4.3.3 Effects of Ca^{2+}-free buffer and L-type calcium channels on chemerin-induced contraction in PCA

In the absence of extracellular calcium, the contractile response to 10 μM chemerin-9 was reduced to the same level with both the presence and absence of U46619 at a level of 2 % of the KCl response (Figure 4.5A). A higher concentration of U46619 was required to induce contraction in tissues exposed to calcium-free buffer (10–20 nM in calcium-free buffer compared to 1–5 nM in normal buffer). However, the L-type Ca^{2+} channel blocker verapamil (10 μM) inhibited the direct contraction induced by 10 μM chemerin-9 and prevented enhanced contraction in the presence of U46619 (Figure 4.5B). At baseline tone, chemerin-9 contraction was 9 ± 2 %, and in the presence of verapamil, it was 3 ± 0.3 %. In U46619 precontracted vessels, chemerin-9 contraction was 16 ± 2 % and decreased to 3 ± 1 % in the presence of verapamil. In

tissues that were exposed to verapamil, a higher concentration of U46619 was required to produce the same level of precontraction (10–20 % of 60 mM KCl response) obtained in control tissues (10–30 nM in the presence of 10 µM verapamil compared to 1–5 nM in control tissues).

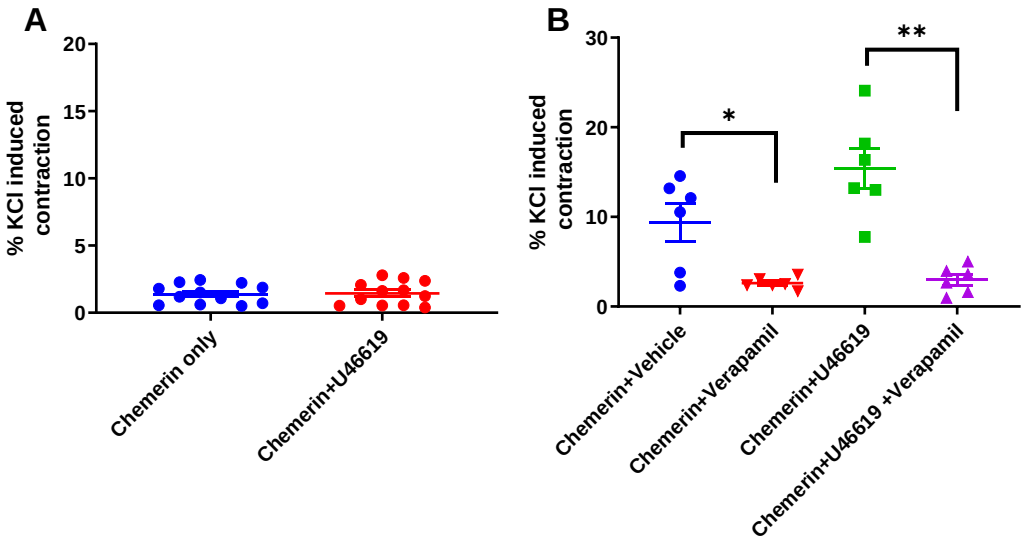


Figure 4.5. (A) Contractile responses to 10 µM chemerin-9 in PCAs at baseline tone (chemerin only) or after precontraction with U46619 in the absence of extracellular Ca^{2+}. **(B)** Effects of 10 µM chemerin-9 in the presence or absence of U46619 with 10 µM verapamil or vehicle control (0.1 % v/v ethanol). Data are expressed as percentages of the contraction induced by 60 mM KCl and are means ± SEM (n = 6) : $*p < 0.05$, $**p < 0.01$, using a two-tailed, paired Student's *t*-test for **A** or one-way ANOVA followed by a Sidak's *post-hoc* test for **B**.

4.3.4 Role of ERK in chemerin-induced contraction in PCA

The MEK inhibitor PD98059 inhibited the contractile response to chemerin-9 at baseline tone from 10 ± 2 % to 5 ± 1 %. Although chemerin-9 contraction in the presence of U46619 decreased from 18 ± 2 % to 13 ± 1 % in the presence of PD98059, tissues pre-treated with U46619 still indicated

enhanced vasocontraction due to chemerin-9 compared with baseline tone even in the presence of PD98059 (Figure 4.6). In tissues exposed to PD98059, a slightly higher concentration of U46619 was needed to produce the same level of precontraction obtained in control tissues (3–20 nM of U46619 in the presence of PD98059 compared to 1–9 nM in control tissues).

Expression of ERK1/2 in the PCA was determined by Western blotting following treatment of the segments with 10 μM chemerin-9 in the absence or presence of U46619. Bands of both total and phosphorylated ERK1/2 were detected at the predicted molecular weight of 44 kDa for ERK1 and 42 kDa for ERK2 (Figure 4.7A and C). However, quantitative analysis based on band intensities indicated no significant differences between PCAs treated with chemerin-9 only, U46619 only, chemerin-9 after U46619 precontraction, and control PCAs (baseline conditions; Figure 4.7B and D). In this thesis, the whole blots are presented in the appendices.

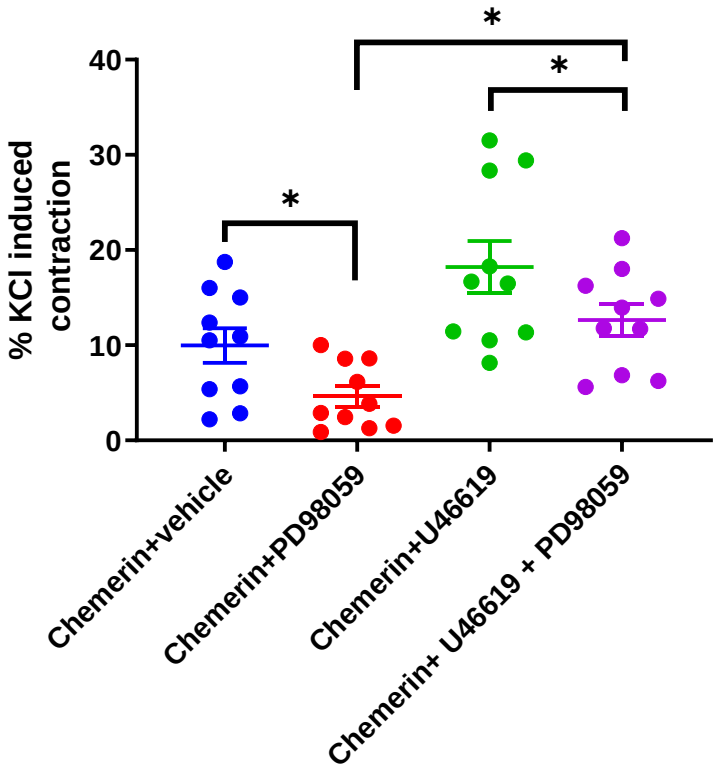


Figure 4.6. Effects of 50 μM PD98059 or vehicle (0.1 % v/v ethanol) on contraction induced by 10 μM chemerin-9 at baseline tone and in the presence of U46619. Data are expressed as percentages of the contraction induced by 60 mM KCl and are means ± SEM (n = 10): *$p < 0.05$, **$p < 0.01$, using one-way ANOVA followed by a Sidak's *post-hoc* test.

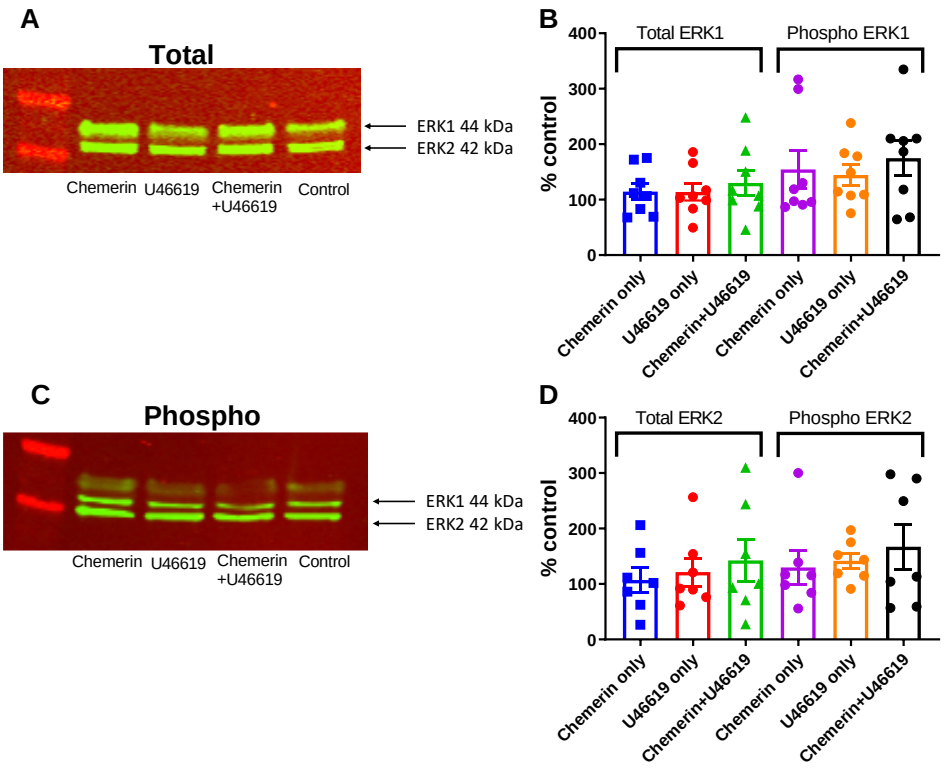


Figure 4.7. Example Western blots showing expression of **(A)** total and **(C)** phosphorylated ERK1/2 levels in 5 µg of coronary arteries under baseline conditions (control) or following treatment with 10 µM chemerin-9 only, U46619 only, and 10 µM chemerin-9 after U46619 precontraction (for the whole blots, see the appendices). **(B-D)** Bar chart showing expression levels of phosphorylated and total ERK1/2 as percentages of the expression in control segments (baseline tone) based on the intensities of their bands: means ± SEM (n = 5).

4.3.5 Role of Rho kinase in chemerin-induced contraction in PCAs

The direct contractile responses to chemerin-9 in PCAs were completely inhibited by the Rho kinase inhibitor Y-27632 (10 µM). In the presence of U46619, 10 µM Y-27632 inhibited the contractile response to chemerin-9 from 19 ± 3 % to 7 ± 1 %. Again, even though the enhanced contraction induced by chemerin-9 in the presence of U46619 was reduced by Y-27632

(10 μM), the contraction was still enhanced compared to the baseline tone (Figure 4.8). In vessels incubated with Y-27632 for 1 h, a higher concentration of U46619 was needed to produce the same level of precontraction obtained in control tissues (30–70 nM in the presence of Y-27632 compared to 1–5 nM in control tissues).

To confirm these results, the levels of phosphorylated and total MYPT-1 were measured by Western blot. In tissues contracted by chemerin-9 alone or U46619 alone, there was no increase in phosphorylated MTPT-1 compared to the control (baseline conditions), while in the enhanced response to chemerin-9 in the presence of U46619, there was a significant increase in the level of phosphorylated MYPT-1 at Ser507 (Figure 4.9C and D). The level of phosphorylated MYPT-1 at Ser668, Thr853, and Thr696 were tested and no bands were detected at these sites. Levels of total MYPT-1 were similar under all conditions (Figure 4.9A and B). The whole blots are presented in the appendices.

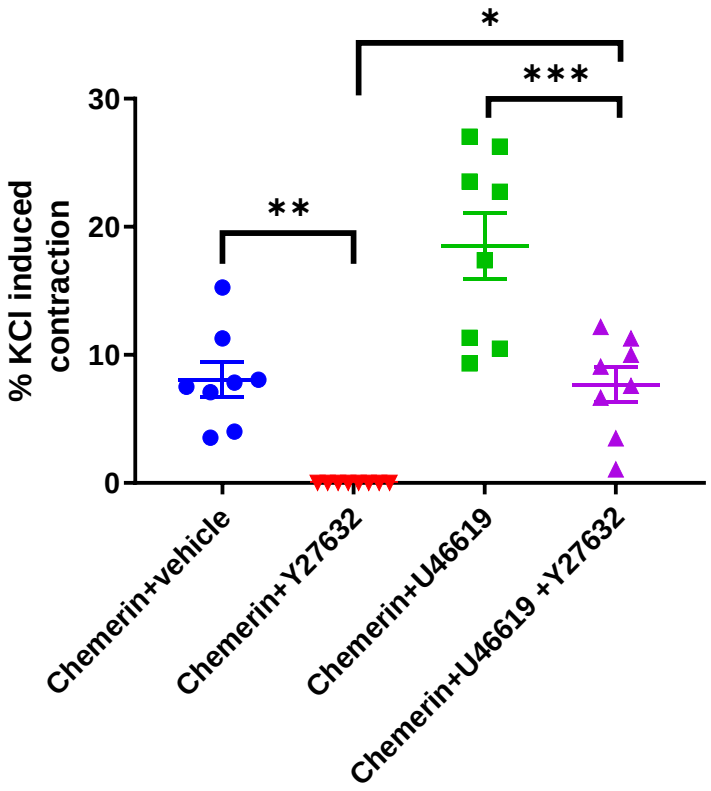


Figure 4.8. Effects of 10 μM Y-27632 or vehicle (0.1 % v/v ethanol) on contraction induced by 10 μM chemerin-9 at the baseline and in the presence of U46619. Data are expressed as percentages of the contraction induced by 60 mM KCl and are means ± SEM (n = 8): *$p < 0.05$, **$p < 0.01$, and ***$p < 0.001$, using one-way ANOVA followed by a Sidak's *post-hoc* test.

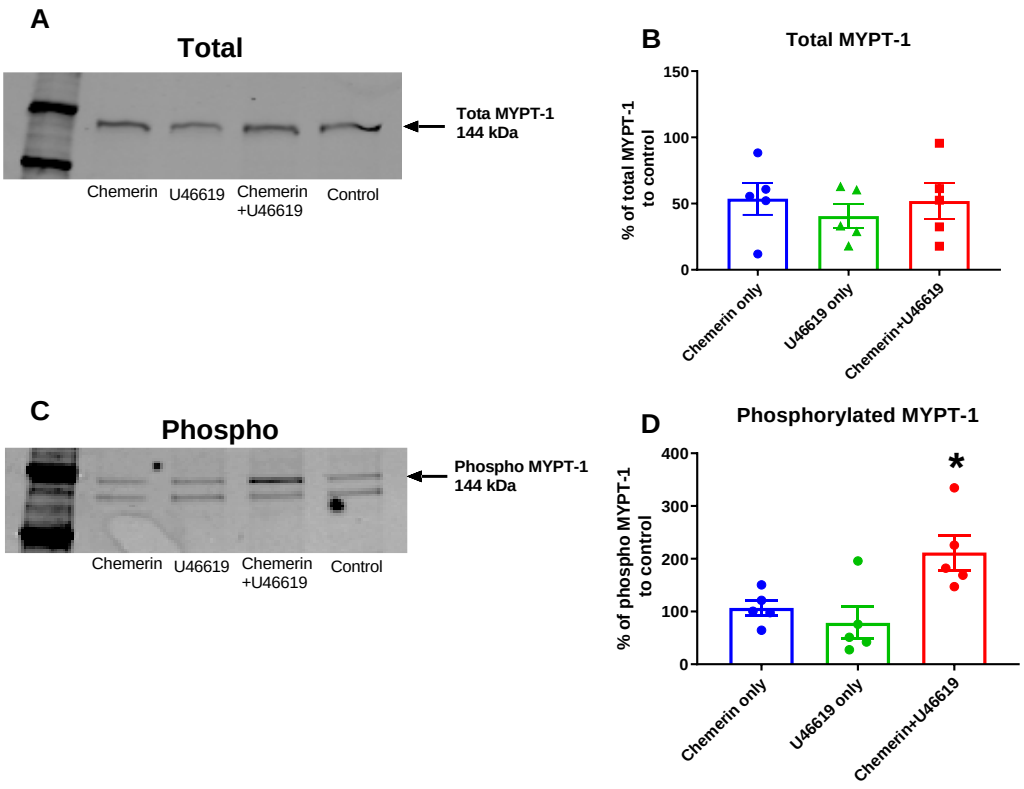


Figure 4.9. Example Western blots showing **(A)** total MYTP-1 and **(C)** phosphorylated MYPT-1 levels in 5 µg of coronary arteries under baseline conditions (control) or following treatment with chemerin-9 only, U46619 only, and chemerin-9 after U46619 precontraction (for the whole blots, see the appendices). **(B-D)** Bar chart showing expression levels of phosphorylated and total MYPT-1 as percentages of the expression in control segments based on the intensities of their bands: *$p < 0.05$, one-way ANOVA followed by a Sidak's *post-hoc* test vs control values; means ± SEM (n = 5).

4.3.6 Role of PI3 kinase and Nox1 in chemerin-induced contraction in PCA

Incubation of PCA segments with the phosphoinositide 3-kinase (PI3 kinase) inhibitor LY294002 (10 µM) caused an inhibition of the direct vasocontractile responses to chemerin-9 from 5 ± 1 % to 1 % and of the enhanced contraction from 18 ± 2 % to 9 ± 2 %. Again, the chemerin-9 contraction in the presence of

U46619 was still enhanced compared with the baseline tone regardless of the presence of LY294002 (Figure 4.10A). Pre-treatment with the Nox1 selective inhibitor ML171 (100 μM) had no effect on chemerin-9-induced contraction in the presence or absence of U46619 (Figure 4.10B). Unlike ML171, in segments pre-treated with 10 μM LY294002, a higher concentration of U46619 was needed to produce the same level of precontraction obtained in control tissues (40–70 nM in the presence of Y-27632 compared to 1–3 nM in control tissues).

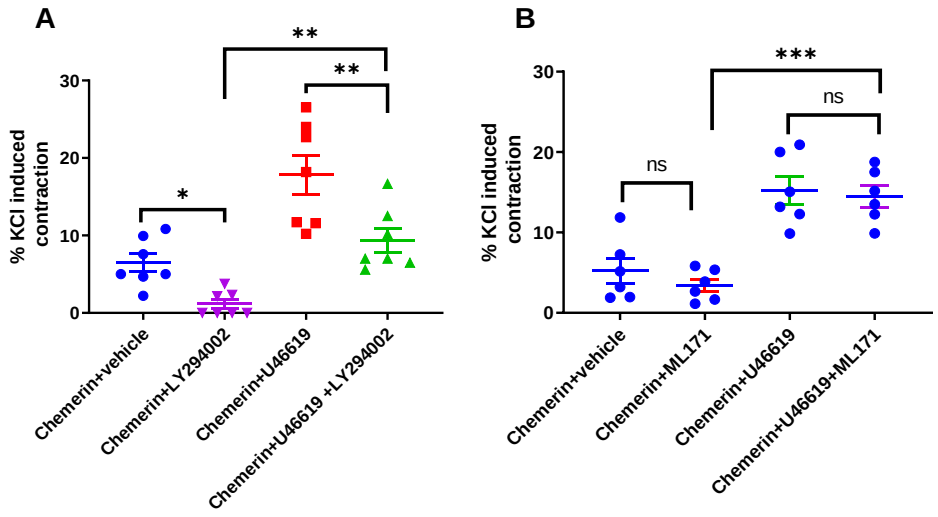


Figure 4.10. (A) Effects of 10 μM LY294002 or vehicle (0.1 % v/v ethanol) on the chemerin-9-induced contraction of PCA at baseline tone and in the presence of U46619. **(B)** Effects of the Nox1 inhibitor ML171 (100 μM) or vehicle (0.1 % v/v ethanol) on contraction induced by 10 μM chemerin-9 in the absence or presence of U46619. Data are expressed as percentages of the contraction induced by 60 mM KCl and are means ± SEM (n = >6): *$p < 0.05$, **$p < 0.01$, and ***$p < 0.001$, using one-way ANOVA followed by a Sidak's *post-hoc* test.

4.3.7 Effects of KCl and BAY K8644 precontraction on the response of PCA to chemerin

To investigate the ability of other contractile agents to enhance the contraction induced by chemerin-9, PCAs were precontracted separately with KCl or BAY K8644 (L-type Ca^{2+} channel opener) to a level between 10–20 % of KCl response prior to the addition of chemerin-9 (10 μM). Both KCl and BAY K8644 precontraction enhanced the chemerin-9-induced contraction of PCA (Figure 4.11). KCl precontraction produced a similar enhancement of chemerin-9-induced contraction to that observed with U46619 precontraction, since the chemerin-9-induced contraction increased from 9 ± 1 % to 20 ± 3 % (n = 8) in vessels precontracted with KCl. BAY K8644 precontraction also significantly enhanced the chemerin-9 response to a level of 48 ± 12 % compared to 9 ± 2 % (n = 6) at the baseline level.

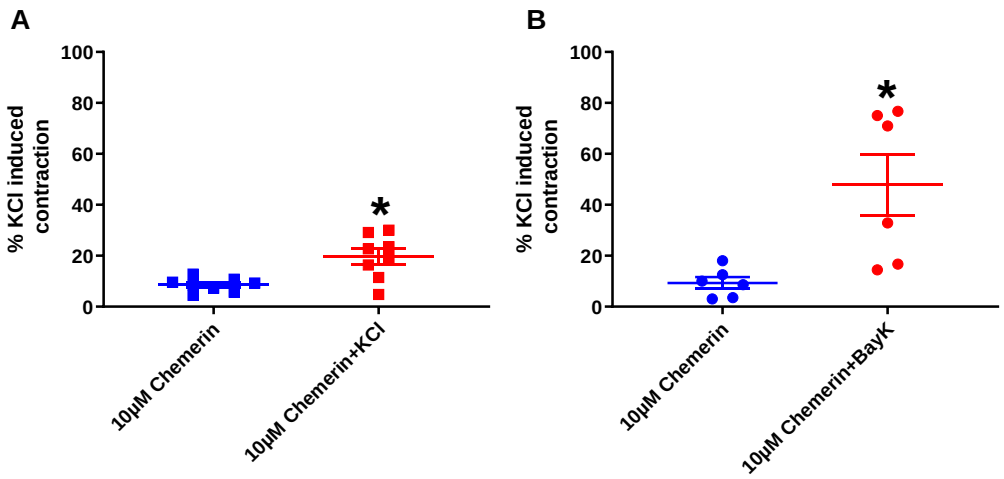


Figure 4.11. (A) Contractile responses to 10 μM chemerin-9 at baseline tone and in the presence of KCl precontraction. **(B)** Contractile effects of 10 μM chemerin-9 at baseline tone and in the presence of BAY K8644 precontraction. Data are expressed as percentages of the contraction induced by 60 mM KCl and

are means ± SEM (n = 8 for **A** and n = 6 for **B**): $*p < 0.05$, using a Student's two-tailed, paired *t*-test.

4.3.8 Effects of hypoxia on direct and enhanced chemerin-induced contraction in PCA

To examine the ability of U46619 to enhance chemerin-9-induced vasocontraction under hypoxic conditions, U46619 precontracted segments were gassed with 95 % N_2 for 30 min before the addition of 10 µM chemerin-9. Induction of hypoxia promoted a slight contraction followed by considerable relaxation to baseline levels. The addition of chemerin-9 in the presence of U46619 still produced enhanced contraction compared with baseline tone, since chemerin-9-induced contraction was 6 ± 1 % at the baseline and 17 ± 4 % in precontracted vessels under hypoxia (Figure 4.12 and Figure 4.13). In a cross-sectional study, no significant difference was noticed in the extent of chemerin-9-induced contraction in the presence of U46619 when gassed with 95 % O_2, 95 % N_2, or air. The same applied for chemerin-9 at baseline tone.

In different sets of experiments, PCA segments were exposed to hypoxia before the precontraction with U46619 and the addition of chemerin-9. In this case, chemerin-9 still produced amplified contraction in the presence of U46619 (Figure 4.14). Interestingly, under these conditions, higher concentrations of U46619 were needed to reach the required level of contractile tone (10–20 nM of U46619 under hypoxia compared to 1–5 nM under 95 % O_2 gassing conditions). This contrasted with chemerin at baseline tone, for which the same concentration (10 µM) induced similar contraction under both gassing conditions.

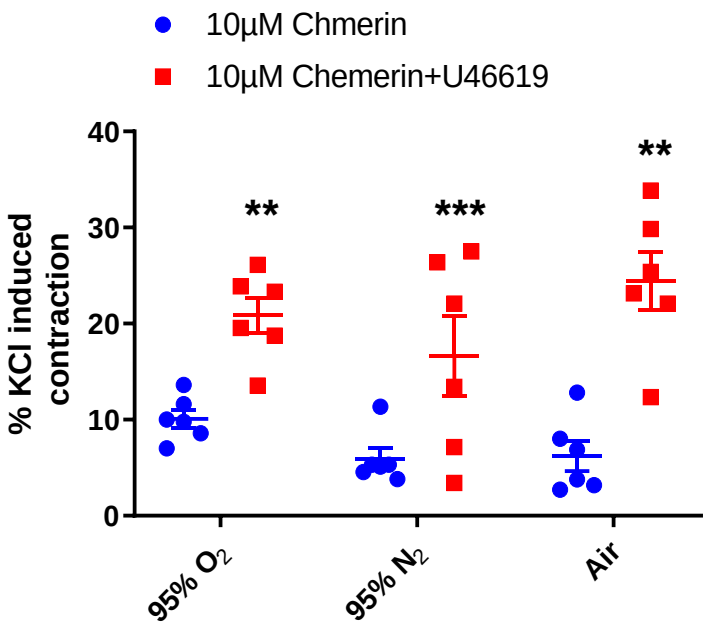


Figure 4.12. 10 µM Chemerin-9-induced contraction in the presence or absence of U46619 under 95 % O_2, 95 % N_2, or air. Data are expressed as percentages of the contraction induced by 60 mM KCl and are means ± SEM (n = >6). Asterisks compare the significant differences with values obtained from the relevant control: $^{**}p < 0.01$, $^{***}p < 0.001$ using a two-tailed, paired Student's *t*-test.

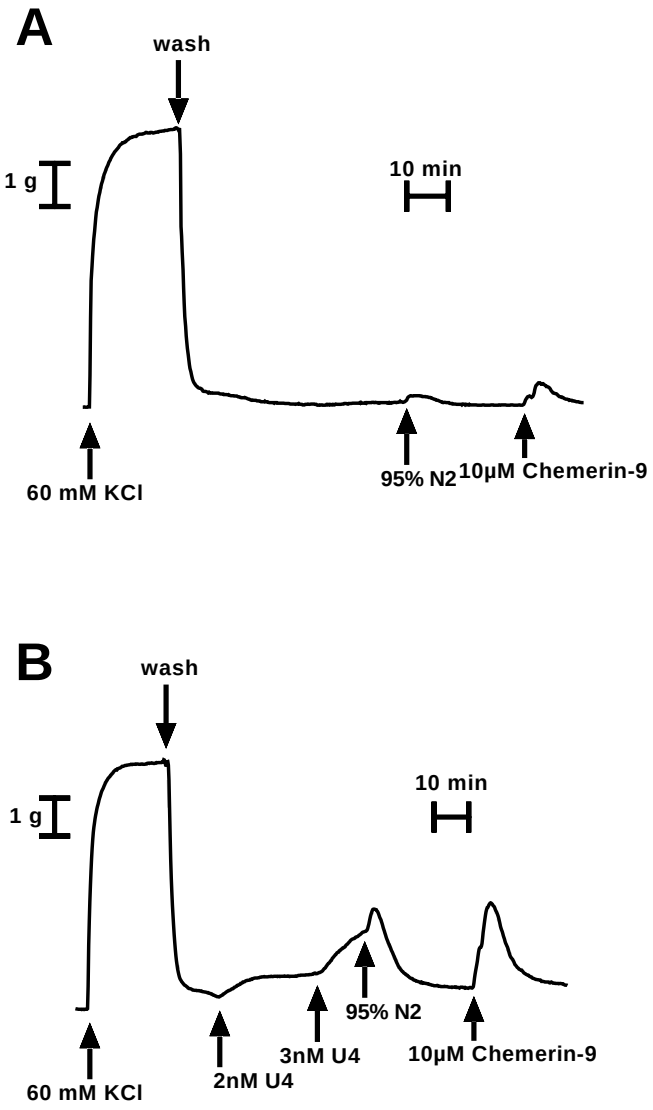


Figure 4.13. Original traces showing the responses of PCA to chemerin-9 at baseline tone **(A)** and in vessels precontracted with U46619 **(B)** under hypoxic conditions.

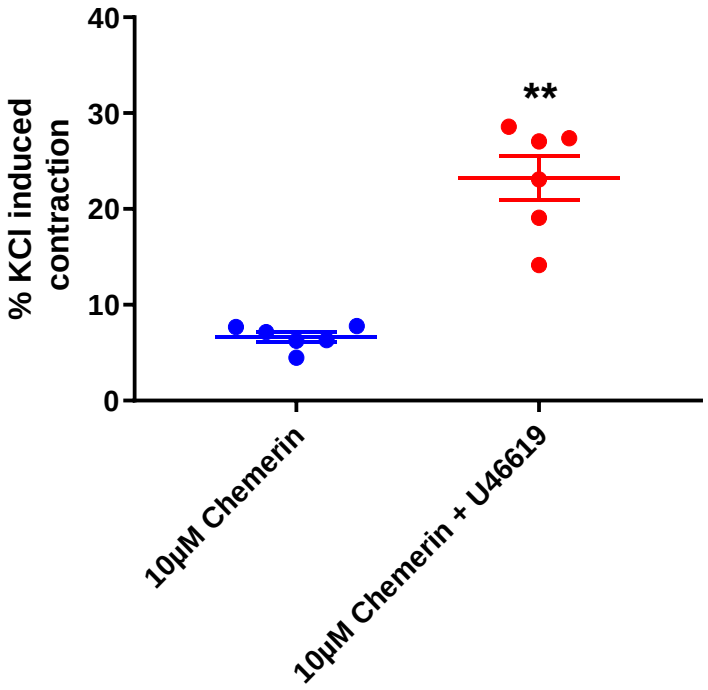


Figure 4.14. Vasocontraction in response to 10 μM chemerin-9 in the presence or absence of U46619 when hypoxia (gassing with 95 % N_2) was induced prior to the addition of U46619. Data are expressed as percentages of the contraction induced by 60 mM KCl and are means ± SEM (n = 6). Asterisks indicate $^{**}p < 0.01$ using a two-tailed, paired Student's *t*-test.

4.4 Discussion

The principal observation of the present chapter was that precontraction of PCAs with the thromboxane mimetic U46619 enhanced the contraction induced by chemerin-9. This finding is important because it indicates a new mechanism by which chemerin can affect vascular tone, especially when both chemerin and thromboxane are co-released from PVAT. Although chemerin is reported to be released from the liver, because of the proximity of PVAT to the blood vessels, PVAT should be regarded as a potential source of chemerin-induced vascular tone. Interestingly, a recent study by Ferland *et al.*, (2019) indicated that chemerin released from adipose tissues (rather than from the liver) was the key player in chemerin-induced hypertension in rats fed a high-fat diet [150].

As previously presented in Chapter 2, the presence of U46619 amplified PVAT-induced contraction compared to control vessels. Therefore, it was hypothesised that the enhanced contraction in response to PVAT re-addition in the presence of U46619 could be due to amplification of the response to chemerin released from fat. Although PVAT is expected to release more than one vasocontractile factor that could enhance PCA contraction, two reasons suggest that the enhanced contraction due to PVAT re-addition in the presence of U46619 could be attributable to chemerin. First, the sharp and rapid contraction seen with PVAT addition in the presence of U46619 (Figure 2.4) resembled the contraction observed with the addition of exogenous chemerin. Second, the similarity between simvastatin-induced inhibition of the enhanced contractile response to PVAT (in the presence of U46619) and simvastatin-induced inhibition of chemerin release from PVAT may indicate

that chemerin is the factor responsible for this enhanced contraction (Figure 2.5B and Figure 2.12).

Although chemerin release from PVAT could be detected in the buffer by ELISA, this was not altered by the presence of U46619, indicating that the effect of the thromboxane mimetic in enhancing chemerin-9-induced contraction was not due to enhanced release of chemerin from fat, but may be due to an enhanced contractile response within the blood vessel itself. Indeed, in the presence of U46619, the contraction induced by chemerin-9 was significantly enhanced in PCAs. The chemerin-9-induced contraction was transient; therefore, only a single concentration of chemerin-9 was used rather than cumulative concentrations. To avoid conflicting results, vessels with PVAT removed were used to avoid complications due to the release of endogenous chemerin. A study reported a similar amplification of chemerin-9-induced contraction in rats, with pre-incubation with phenylephrine, PGF2α, and KCl producing enhanced chemerin-9-induced contraction that was inhibited by Chemerin$_1$ receptor antagonist (CCX832) [94].

Notably, at baseline tone, increasing the concentration of chemerin-9 from 10 to 30 μM produced a similar extent of contraction. However, in the presence of U46619, the contractile effect of chemerin-9 almost doubled as the concentration increased from 10 to 30 μM. Also, the level of tone induced by U46619 did not seem to be important in this synergistic effect, as enhanced chemerin-9-induced contraction was still seen in tissues precontracted with U46619 to a very low level of KCl-induced contraction (circa 3 % of KCl-induced contraction). These results suggest that it may be important to take thromboxane concentrations and TP activation into account when exploring chemerin's vasoactive effect.

Since chemerin and TXB_2, the metabolite of TXA_2 (see Chapter 2, section 2.3.9) could both be detected in the buffer in the presence of PVAT, the data indicated that thromboxane and chemerin were both released from the PVAT, and therefore the contractile response to PVAT was likely to be caused by a combined action of these compounds, potentially acting in a synergistic manner (see Figure 4.15). This finding may be particularly important in inflammatory states characterised by high thromboxane and chemerin concentrations; for instance, serum TXB_2 levels were found to be significantly higher in obese subjects [308], and obesity is reported to augment prostanoid-dependent vasoconstriction as well as markedly increase the gene expression of vascular TPs in rats [309]. In parallel with this, there is a positive association between obesity and serum chemerin levels [253, 310]. Furthermore, bariatric surgery-induced weight loss resulted in a decrease in chemerin levels in human [138, 142]. Therefore, the elevation of both thromboxane and chemerin in obesity could result in an even larger vasocontractile response, which may explain, at least in part, the increase in blood pressure associated with obesity. Moreover, this synergistic effect of thromboxane and chemerin might also be important in platelet activation. A study reported that chemerin is stored in platelet granules and is released upon platelet activation by different platelet-activating factors [311]. It is well known that activation of platelets releases thromboxane, which causes vasoconstriction during haemostasis; therefore, the ability of platelets to release chemerin might enhance this vasoconstriction.

Both the direct and enhanced chemerin-9 contraction was endothelium-independent, since denudation of the endothelium did not affect the responses of PCAs. These findings

contradicted previously published observations by other investigators claiming that endothelium removal potentiated chemerin vasocontraction effects in rat aortic rings [152] and rat pulmonary arteries [153]. Such differences could be attributed to differences in vascular beds, considering the expected low or different role of endothelium vasoactive roles in conduit blood vessels, such as aorta, or in vessels exposed to deoxygenated blood, such as pulmonary arteries.

Even though U46619 enhanced chemerin-9-induced contraction, the results in this chapter indicated that chemerin-9 precontraction had no effect on U46619-induced contraction in PCAs. Similar findings with phenylephrine were seen by Darios *et al.,* (2016), in which chemerin precontraction failed to enhance phenylephrine-induced contraction in rat mesenteric arteries, whereas in their previous study, phenylephrine precontraction augmented chemerin's vasoconstrictive effect in the same vascular bed [94, 151]. The incapability of chemerin-9 to amplify U46619-induced contraction could be attributed to the transient nature of chemerin-9-induced vasocontraction, and U46619 may require a stable tone to be affected by chemerin-9. Alternatively, for this synergistic action to be effective, it may require activation of the TP receptor prior to application of chemerin-9. This, however, could raise another question regarding the order by which PVAT releases these different adipokines.

Inducing hypoxia after the tissue had been precontracted with U46619 reduced the tone to the baseline level, but application of chemerin-9 still produced enhanced contraction. These data may indicate that the enhancement of chemerin contraction seen in the presence of U46619 was due to activation of the TPs by U46619 rather than rising of vascular tone. Also, under

hypoxic conditions, there was a need for higher concentrations of U46619 (10 nM-18 nM compared with 1 nM-4 nM) to produce the same effect as that seen under gassing with 95 % O_2 or air (that is, 10 % to 20 % of KCl response). This contrasted with the chemerin experiments, in which the same concentration of chemerin-9 (10 μM) produced similar responses under all three gassing conditions. These data may suggest that, unlike U46619, chemerin-induced direct and enhanced contraction is not sensitive to hypoxia. It is well known that peripheral vessels dilate in response to low oxygen to increase blood supply to meet the energy demands of the affected organs [312]. Since chemerin-9-induced contraction is not affected by hypoxia, this may suggest that chemerin could interrupt this physiological response, especially in obese subjects where high levels of chemerin serum concentrations are found. However, more comparisons with the effect of other PVAT-derived vasoactive agents on VSMC levels are needed to elucidate the role of chemerin released from PVAT in hypoxic conditions.

The chemerin receptor is a Gi-coupled receptor [111, 119]. Previous studies in the laboratory have demonstrated that U46619 enhances α_2-adrenoceptor-mediated contraction, which is also a Gi protein-coupled receptor [298]. This enhanced contraction involves activation of ERK-MAP kinase and Rho kinase signalling [304]; therefore, the current study determined whether the enhanced contraction due to chemerin-9 also involved these pathways. Inhibition of ERK activation by the MEK inhibitor PD98059 and inhibition of Rho kinase by Y-27632 both caused a reduction in the direct contraction due to chemerin-9 and the enhance contraction in the presence of U46619 (Figure 4.15). However, in both cases, there was still a greater contraction in the presence of U46619, indicating that

neither inhibitor affected the mechanism underlying the enhanced contraction.

Although PD98059 inhibited the contractile response, immunoblotting results showed no difference in the phosphorylation of ERK (an indication of ERK activity), suggesting no detectable increase in ERK activity. Although the functional study indicated a minor role for ERK in chemerin-9-induced contraction, this small effect may be hard to detect by Western blotting, particularly as the homogenate of the blood vessel contains different cell types, which might result in dilution of the phosphorylated ERK within the VSMCs. The link between ERK-MAP kinase and the actions of chemerin has been discussed in the literature, but mostly regarding chemerin's effect in angiogenesis [313], adipogenesis [116], and chemotaxis [131]. The limited available data are controversial regarding the involvement of ERK-MAPK in chemerin-induced vascular contraction. For instance, one study found that chemerin potentiated phenylephrine- and endothelin-1-induced contraction in rat aorta through an ERK-MAPK pathway [152]. Another study reported that the ERK-MAPK pathway had no effect on chemerin signalling in rat aorta and that chemerin functions through activation of L-type Ca^{2+} channels and Rho kinase [119]. Unlike the second study, the first did not challenge PD98059's action against direct chemerin-9 contraction, but rather examined the role of ERK-MAPK in the ability of chemerin pre-treatment to potentiate phenylephrine- and endothelin-1-induced contraction. Therefore, differences between these two studies could be attributed to the different experimental protocols used. Indeed, the evidence from this investigation suggests that ERK-MAPK plays a role in chemerin-9-induced contraction in PCAs; more investigations are needed

to draw conclusions regarding the role of ERK-MAPK in chemerin's vascular effect.

The effects of chemerin on MYPT1 phosphorylation was investigated to determine changes in Rho kinase activity. MYPT1 is a subunit of myosin phosphatase that is phosphorylated by Rho kinase, leading to inhibition of myosin phosphatase activity [314]. In tissues contracted with chemerin-9 in the presence of U46619, there was a significant increase in the level of phosphorylated MYPT1 compared to chemerin-9 alone, U46619 alone, or the control (baseline conditions), suggesting an enhancement of Rho kinase activity in the presence of U46619, which may play a role in the enhanced chemerin-induced contraction. The contractile study, however, indicated that the contraction by chemerin-9 was still enhanced in vessels pre-treated with U46619, regardless of the presence of the Rho kinase inhibitor Y-27632, suggesting that other pathways may also be involved.

The PI3-K/Akt pathway was reported to be involved in U46619-enhanced α_2-adrenoceptor-mediated contraction and in the ability of chemerin to promote migration and cell proliferation of ECs [298, 315]. In this study, inhibition of PI3 kinase by LY294002 showed similar results to those for ERK inhibitor PD98059. Again, although the direct and enhanced contractile effect of chemerin-9 was inhibited by LY294002, the contraction in the presence of U46619 was still enhanced compared to the baseline tone. Also, the results for ML-171 (a commonly used Nox enzyme inhibitor) suggest that Nox inhibition plays no role in chemerin-induced direct and enhanced vasocontraction.

In the current study, three different protein kinase inhibitors were used: PD98059 (50 μM) to inhibit ERK MAP kinase activity, Y-27632 (10 μM) to inhibit Rho kinase activity, and LY294002

(10 μM) to inhibit PI3 kinase activity. Several studies have detailed the high selectivity of these protein kinase inhibitors at the used concentrations for inhibiting activation of their related protein kinases without a significant effect on a variety of other protein kinases important for signal transduction [306]. However, Y-27632 and LY294002 have been reported to act as ATP competitive inhibitors, which may indicate conflicting results regarding PCA vascular contraction, considering the important role of ATP in actin-myosin cross-bridging [316, 317]. Thus, Western blotting was used to study the change in Rho kinase phosphorylation following chemerin-9 treatment, and the results confirmed the findings obtained with Y-27632, which (as previously described) indicated a role of Rho kinase activity in chemerin-9 enhanced vasoconstriction. Although PD98059 showed no effect on ATP binding sites, it has been reported to inhibit cyclooxygenases 1 and 2 (the rate-limiting enzymes in the production of prostaglandins), but this effect of PD98059 is expected to play no significant role in the vasomotor of PCA with the method used, which may give more reliable results regarding the role of ERK activity in chemerin-9-induced direct and enhanced contraction [318].

Chemerin-9-induced contraction was also inhibited by verapamil, indicating that calcium influx through L-type calcium channels is important in both direct and enhanced contraction (Figure 4.15). Unlike other inhibitors, the vasocontractile effect of chemerin-9 was similar in the presence of verapamil at both baseline tone and after precontraction with U46619, suggesting that the enhancement of the contractile response depends on calcium influx. Precontraction with KCl, which caused contraction through influx of extracellular calcium and the L-type calcium channel opener BAY K8644, also enhanced the

chemerin-9-induced contraction, confirming the importance of calcium influx in this response. The role of calcium in both direct and enhanced chemerin-induced contraction was further supported by the removal of extracellular calcium, since the enhanced chemerin-9-induced contraction was eliminated under these conditions. The chemerin receptor and chemerin signalling have been linked to L-type voltage gated Ca^{2+} channels in rat aortic rings [119], mesenchymal stem cells [319], and immune cells [320]. However, a novel finding in this chapter is that the enhanced contraction due to chemerin-9 in the presence of U46619 also depended on extracellular calcium influx and L-type Ca^{2+} channels.

In summary, these data have demonstrated that precontraction with U46619, KCl, and BAY K8644 enhances chemerin-9-induced contraction of isolated PCAs. Chemerin-9-induced contraction involves ERK, Rho kinase, and calcium influx, with a role for calcium influx, in particular, in the enhancement of the contraction in the presence of U46619 (Figure 4.15). This study suggests that the co-release of thromboxane and chemerin from PVAT plays a crucial role in the effect of PVAT on vascular functioning, and this may be important in the control of adipose tissue-induced vascular alterations in obesity and related diseases.

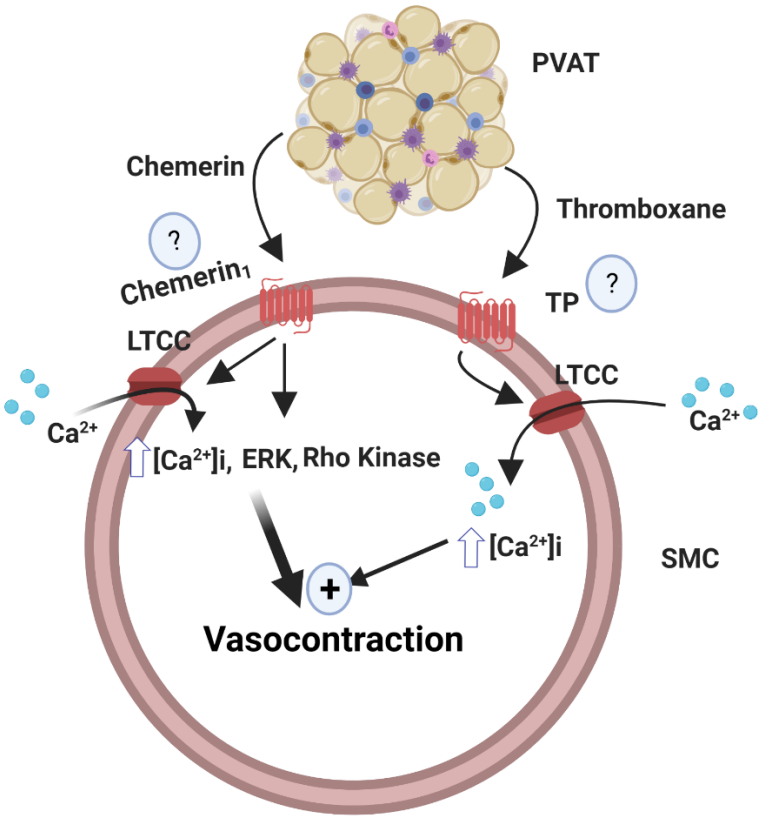


Figure 4.15. Hypothesized schematic diagram of the effect of precontraction with the thromboxane mimetic U46619 on chemerin-induced contraction in porcine coronary arteries. The present chapter demonstrated that chemerin-9-induced contraction involves ERK, Rho kinase, and calcium influx and the presence of U46619 enhances this contraction potentially through increasing intracellular calcium.

Chapter 5
General Discussion

Perivascular adipose tissue (PVAT) was considered as a supporting component of blood vessels and a protective cushion for the vessel wall from the neighbouring tissues during relaxation and contraction. Three decades of extensive research following Soltis and Cassis' initial study in 1991 has led to the knowledge that adipose tissue around blood vessels plays vital roles in vascular homeostasis and in vascular dysfunctions associated with obesity, hypertension, inflammation, and coronary ischaemic disease [50]. The understanding of PVAT's roles in physiology and pathophysiology has identified this fat deposit as a promising drug target for many diseases, including obesity and obesity-associated CVDs, yet the interaction between PVAT and currently available cardiovascular drugs is very limited. Considering the well-documented pleiotropic effects of statins that are unrelated to their ability to inhibit cholesterol biosynthesis, this study initially set out to illustrate the possible influences of statins on PVAT vasomotor regulation in porcine coronary arteries (PCAs).

Chapter 2 provided evidence that porcine coronary PVAT has the capacity to act in a paracrine manner by releasing transferable factors that can induce contraction of coronary arteries through Ca^{2+}-dependent pathways, and precontraction with U46619 augmented the vasocontraction of PVAT. These data support the findings reported by Owen *et al.* (2013), who observed that porcine coronary PVAT increases baseline tension and potentiates constriction of isolated coronary arteries to $PGF_{2\alpha}$—an effect that is inhibited by nifedipine [240]. However, this study indicated a role for contractile prostanoids in PVAT-induced contraction, since thromboxane and $PGF_{2\alpha}$ were detected in a buffer incubated with PVAT, and the release of these prostanoids and the vasocontraction effect due to PVAT

were all inhibited by the cyclooxygenase inhibitor, indomethacin. This finding was consistent with previous studies: one by our group indicating the release of thromboxane and $PGF_{2\alpha}$ from PVAT in proximal PCA [92], and another by Meyer *et al.* (2013) demonstrating the same in rat aortic and small mesenteric PVAT [77].

Currently, simvastatin, pravastatin, and lovastatin are approved for the treatment of hypercholesterolemia in humans [321]. The findings from Chapter 2 showed that lipophilic simvastatin and lovastatin, but not hydrophilic pravastatin, caused significant inhibition of the ability of PVAT to induce contraction in PCAs at baseline levels, as well as on artery segments precontracted with the thromboxane mimetic U46619. The inability of pravastatin to change PVAT vascular response could be attributed to its lipid solubility, which might prevent pravastatin from diffusing through the cell membrane of PVAT and/or PCA. This possibility is supported by the work of other investigators who reported lipophilicity-dependent effects of statins on vascular tone in different vascular beds, including PCA from our laboratory [209, 247]. In the current thesis, simvastatin was chosen to further investigate the mechanisms underlying statin-mediated inhibition of PVAT-induced vasocontraction, since simvastatin is one of the most widely prescribed statins. The maximal recommended dose of simvastatin is 80 mg/day and the concentrations detected in patients' plasma were found to be in the nanomolar range [272, 322]. Simvastatin concentrations used throughout this thesis were considerably higher than those for human plasma, but statins and lipophilic statins like simvastatin could build up in different tissues including adipocytes due to their ability to diffuse through the cell membrane [273]. Thus, plasma

concentrations of simvastatin (and other statins) may not necessarily reflect concentrations at the tissue level. However, the main conclusion from Chapter 2 was that simvastatin's inhibitory effects on PVAT-induced contraction seemed to be mediated through a direct Ca^{2+}-dependent effect on PCA and on the ability of PVAT to release vasocontractile chemerin (see Figure 2.13).

The findings from Chapter 2 formed the basis for Chapters 3 and 4. Firstly, although immunoassay was used to test the ability of simvastatin to inhibit three known PVAT-derived vasocontractile factors—thromboxane, prostaglandin, and chemerin—but only chemerin was inhibited by simvastatin treatment. This selective inhibitory effect of simvastatin on chemerin release from PVAT is important because chemerin has well-documented positive roles in pathophysiological conditions, such as inflammation, hypertension, and atherosclerosis [323]. Interestingly, some reported statins' pleiotropic actions had anti-inflammatory, anti-hypertensive, and anti-atherosclerotic effects [182]; thus, it was meaningful to assume that the protective effects of statins could be exerted through the inhibition of chemerin release from PVAT, and this was the main hypothesis underpinning Chapter 3. Notably, when Chapter 3 was being prepared, no study in the literature linked the pleiotropic effects of statins to chemerin; however, two articles were published later (in 2019 and 2020) and both supported the results of the present study, in finding that statin treatment inhibited chemerin serum levels in patients and downregulated chemerin mRNA expression in bone marrow-derived mesenchymal stem cells [234, 235]. Secondly, data from Chapter 2 also indicated that the re-addition of PVAT to PCA vessels precontracted with U46619 caused significantly

enhanced contraction compared to the re-addition of PVAT at baseline tone. Simvastatin inhibited the enhancement of PVAT-induced contraction in the presence of U46619 and, as previously described, the release of chemerin from PVAT. Therefore, the main hypothesis underpinning Chapter 4 was that the activation of thromboxane receptors by U46619 could enhance chemerin-induced contraction in PCAs. This interaction between thromboxane and chemerin might be important considering the ability of PVAT to release both molecules, which could act synergistically on the underlying vessels.

The Chapter 3 results showed that the release of total chemerin from PVAT and cultured 3T3-L1 adipocytes was inhibited by the application of simvastatin and pravastatin; it also found that simvastatin-mediated inhibition of 3T3-L1-induced chemerin release was in a time- and concentration-dependent manner. In an attempt to determine the mechanisms by which simvastatin caused inhibition of chemerin release from 3T3-L1 adipocytes, the role of L-type Ca^{2+} channels was tested by incubating cells with nifedipine in the presence or absence of simvastatin. The results indicated a further decrease in total chemerin release in the dual presence of simvastatin and nifedipine, which suggested that simvastatin-induced inhibition of total chemerin release involves other pathways that are independent of L-type Ca^{2+} channels. Also, these data showed, for the first time, the ability of nifedipine to inhibit total chemerin release from adipocytes and may provide opportunities for future research into the possible effects of these anti-hypertensive drugs on chemerin biology. This study was then extended to examine whether simvastatin mediated inhibition of 3T3-L1-induced chemerin release through the inhibition of K_{ATP} channel activity, because simvastatin was reported to significantly inhibit

vascular relaxation induced by the K_{ATP} channel opener, pinacidil, in different vascular beds, including PCAs from our laboratory [286, 287]. The data from Chapter 3 showed that pinacidil was able to enhance total chemerin production by cultured 3T3-L1 adipocytes—an effect that was blocked by simvastatin and/or glibenclamide. Similarly, activation of K_{ATP} channels was reported to enhance chemerin release from cultured rat aortic endothelial cells [265]. Nevertheless, because the well-known blocker of K_{ATP} channels (glibenclamide) alone indicated no further decrease in basal chemerin release from 3T3-L1 adipocytes, this would seem to rule out inhibition of K_{ATP} channels as a mechanism by which simvastatin inhibited the basal release of total chemerin.

In humans, adipocytes have the highest levels of PPARγ expression, and PPARγ agonists, including rosiglitazone, are effective for the regulation of adipogenesis and adipokine release [288, 289]. Serum chemerin levels were found to be elevated in mice treated with rosiglitazone and associated with increased chemerin mRNA in adipose tissue [290]. This latter study was supported by the results from Chapter 3, showing that treatment with rosiglitazone for 48 h increased cultured 3T3-L1-induced total chemerin release and, more importantly, reversed the inhibitory effect of simvastatin treatment on total chemerin production. Although the change in chemerin mRNA expression was not examined in this study, rosiglitazone-induced increase of chemerin production was thought to be through enhancement of chemerin gene expression in 3T3-L1 adipocytes, because rosiglitazone had no effect after 24 h incubation and was only effective following long treatment for 48 h. It is possible that simvastatin's long-term inhibition of total chemerin basal release could have been mediated through

the inhibition of PPARγ; otherwise, rosiglitazone might have led to enhancement of chemerin production to a level that simvastatin was unable to prevent. The early hypothesis was supported by recent findings indicating that simvastatin had an inhibitory effect on the differentiation process of bone marrow-derived mesenchymal stem cells (BMSCs) through the downregulation of PPARγ and the PPARγ-mediated induction of chemerin mRNA expression [235]. Notably, rosiglitazone was withdrawn from the market due to its connection with adverse cardiovascular events, such as stroke and myocardial infarction. Considering the reported positive correlation between chemerin and these CV complications, it might be speculated that the ability of rosiglitazone to enhance chemerin release from adipocytes, at least partially, is behind rosiglitazone's CV side effects [294]. Taken together, the results from Chapter 3 suggested that rosiglitazone may induce increased CV complications through elevated chemerin release and may inhibit some beneficial effects of simvastatin on reducing chemerin levels.

Pathophysiological conditions like obesity led to the development of an inflammatory phenotype in PVAT, resulting in an imbalance in favour of vasoconstriction and the release of pro-inflammatory substances [324]. Chemerin is no exception since its plasma levels are strongly associated with BMI, and serum chemerin levels are significantly elevated in morbidly obese patients, but reduced by weight loss after bariatric surgery [325]. To study the effects of inflammation on 3T3-L1-induced total chemerin release and the ability of simvastatin to interfere with this process, lipopolysaccharide (LPS) from *Escherichia coli* was used. 3T3-L1 adipocytes in this study increased total chemerin production by more than 30 % after

24 h of incubation with LPS—an effect that was blocked by treatment with simvastatin. These results were aligned with previous findings indicating elevated levels of chemerin due to LPS application in 3T3-L1 adipocytes [281]. However, these results from Chapter 3 proposed a new pleiotropic effect of simvastatin in preventing enhanced chemerin release from adipocytes during inflammation, which might explain, at least partially, some of the anti-inflammatory benefits of statins.

As explained earlier, the presence of U46619 caused amplification of the contraction due to PVAT re-addition compared to control vessels. PVAT-induced chemerin release was a potential candidate in this enhanced contraction because chemerin was the only tested vasocontractile agent that was inhibited by simvastatin, which also inhibited the amplified contraction. Thus, the main hypothesis for Chapter 4 was that the presence of U46619 may increase chemerin release from PVAT and/or enhance the vasocontractile effect of chemerin on PCAs. The ELISA results indicated no further increase in chemerin production from PVAT in the presence of U46619. However, the application of chemerin-9 to vessels precontracted with U46619 resulted in a significant amplification of chemerin-9-induced contraction, suggesting that these two adipokines may act synergistically when they are co-released from PVAT. This synergistic interaction between thromboxane and chemerin in the current study was remarkable in many ways. Firstly, the increased chemerin-9 concentration from 10 μM to 30 μM produced a relatively similar contractile effect at baseline tone, while in the presence of U46619, the size of PCA contraction doubled with the same increase in chemerin-9 concentration. Secondly, chemerin-9-induced enhanced contraction was still evident in tissues

precontracted with U46619 to a very low level of KCl-induced contraction. Additionally, the induction of hypoxia after the PCA rings had been precontracted with U46619 resulted in reduced tone to baseline levels, but chemerin-9 application still induced amplified contraction, suggesting that the level of tone induced by U46619 was not the key player in this synergistic effect, but instead the activation of thromboxane receptors by U46619. The ability of thromboxane treatment to enhance chemerin-induced contraction could be particularly important in obesity and obesity-related diseases, since high concentrations of both thromboxane and chemerin serum levels are found in obese subjects [253, 308]. Therefore, the elevation of thromboxane and chemerin in obesity—especially their release from PVAT—could result in an even greater vasocontractile response, which may explain, at least partially, the increase in blood pressure associated with obesity.

In an attempt to determine the mechanisms by which U46619 enhanced chemerin-9-induced vasocontraction in PCAs, the involvement of ERK-MAP kinase and Rho kinase were tested, because a previous study from the laboratory found that these pathways are important for the ability of U46619 to enhance α_2-adrenoceptor-mediated contraction [304]. In the current contractility study, inhibition of ERK activation by the MEK inhibitor PD98059 and inhibition of Rho kinase activity by Y-27632 both caused a reduction in the direct contraction to chemerin and the enhanced contraction in the presence of U46619. However, in both cases, there was still a greater contraction to chemerin-9 in the presence of U46619, indicating that neither inhibitor affected the mechanism underlying the enhanced contraction. However, immunoblotting results supported a role for Rho kinase in the enhanced chemerin-9-

induced contraction, because there was a significant increase in the level of phosphorylated MYPT1 in PCA tissues treated with chemerin-9 and U46619 compared to chemerin-9 alone, U46619 alone, or the control (basal conditions). Additionally, findings from Chapter 4 indicated a strong role for extracellular Ca^{2+} influx in the enhanced contraction to chemerin-9 in the presence of U46619. The treatment with verapamil and the removal of extracellular Ca^{2+} were the only two conditions under which the vasocontractile effect of chemerin-9 was similar at both basal tone and after precontraction with U46619, suggesting that the amplification of chemerin-9 contractile response depended on calcium influx. Also, the ability of KCl and Bay k8644 precontraction (which both cause contraction through influx of extracellular calcium) to amplify chemerin-9-induced contraction might confirm the importance of calcium influx in this response.

Hypoxic coronary vasodilatation is an important pathophysiological response that increases blood flow to the heart and, therefore, oxygenation of the ischaemic myocardium. Regarding the role of PVAT-induced chemerin release and the ability of chemerin to induce vasoconstriction during hypoxia, the current study indicated two important points. Firstly, in Chapter 3, the data showed that the basal release of total chemerin from porcine coronary PVAT significantly decreased under hypoxic conditions. Secondly, the Chapter 4 data showed that the same concentration of chemerin-9 (10 μM) produced similar contractile responses in PCA under gassing conditions with 95 % N_2, 95 % O_2, or air, which contrasted with the U46619 experiments in which, after the induction of hypoxia, there was a need for higher concentrations of U46619 to produce the same effect as that

seen under gassing with 95 % O_2 or air. Taken together, these findings suggest that chemerin-induced direct and enhanced contraction is not sensitive to hypoxia, but PVAT in hypoxic conditions could change its secretome by reducing chemerin production. Previously, a study reported that PVAT augments hypoxic relaxation of coronary arteries through a mechanism involving increased release of the vasodilator H_2S, and the current study may add to these findings that PVAT-induced release of the vasocontractile chemerin is reduced during hypoxia, which may complete the picture for the possible protective role of PVAT in regulating coronary blood flow during hypoxia [70]. Indeed, the increase of the adipocyte area that occurs in obesity leads to hypoxia in adipose tissues [326], and based on the current findings, it would be expected to result in lower chemerin release from adipose tissue, but, in fact, many studies have found higher chemerin concentrations in obese subjects. This could be simply explained by the significant increase in adipocyte mass, which might result in high chemerin production even though the release of chemerin from a single adipocyte would be reduced. Additionally, inflammation within adipose tissue and PVAT during obesity should be considered since, as described above, inflammation may result in high chemerin release from adipocytes.

On a larger scale, the findings from the current thesis might be relevant in hypertension and obesity-related hypertension, which involve high levels of chemerin due to excess adipose tissue, including PVAT. Both hypertension and obesity are independently associated with a significantly higher incidence of CVDs [327]. Currently, there are no specific treatments for obesity-related hypertension because the mechanisms by which obesity contributes to BP elevation are complex and not fully

understood. Also, resistant hypertension, which is defined as uncontrolled BP despite the treatment with optimal doses of three different antihypertensive drugs, has been estimated to account for over 10 % of hypertensive patients in the UK [328]. Thus, clearly there are urgent demands for new approaches to solve these pathological conditions. Antagonism of chemerin production or function could therefore be a new strategy for the treatment of hypertension and obesity-related hypertension. Understanding the mechanisms by which chemerin can cause vasocontraction and by which simvastatin mediates inhibition of PVAT-induced chemerin release could facilitate such a strategy.

5.1 Conclusions

The results presented in this thesis support and contribute to the plethora of evidence indicating a strong role of PVAT in the regulation of vascular biology and show, for the first time, the ability of statins to inhibit chemerin release from PVAT and cultured 3T3-L1 adipocytes. Results from Chapter 2 showed that porcine coronary PVAT is capable of releasing transferable factors that initiate and potentiate contraction of coronary arteries through Ca^{2+}-dependent pathways and that treatment with lipophilic statins can result in inhibition of PVAT contraction through direct effects on PCAs and the release of chemerin from PVAT. In Chapter 3, the data provided evidence that simvastatin was able to inhibit the basal release of total chemerin from 3T3-L1 adipocytes and prevent enhanced chemerin release during inflammation and the activation of K_{ATP} channels. Also, the results proposed rosiglitazone as a promoter of chemerin release from 3T3-L1 cells and hypoxia as an inhibitor of PVAT-induced chemerin release. Chapter 4 demonstrated that precontraction with U46619 enhanced chemerin-9-induced contraction of isolated PCA, and that vasocontraction due to

chemerin-9 involves ERK, Rho kinase, and calcium influx, with a role for calcium influx, in particular, in the enhancement the contraction by U46619.

It is important to consider that the proposed findings in this thesis were based on *in vitro* studies; thus, the physiological and clinical relevance of the results remains to be further investigated. However, the current findings provide meaningful data to justify follow-up *in vivo* studies to evaluate the role of statins in chemerin release and the mechanisms underlying this effect, which might provide a novel therapeutic target for obesity-related CVDs.

Appendices

A. Immunoblots

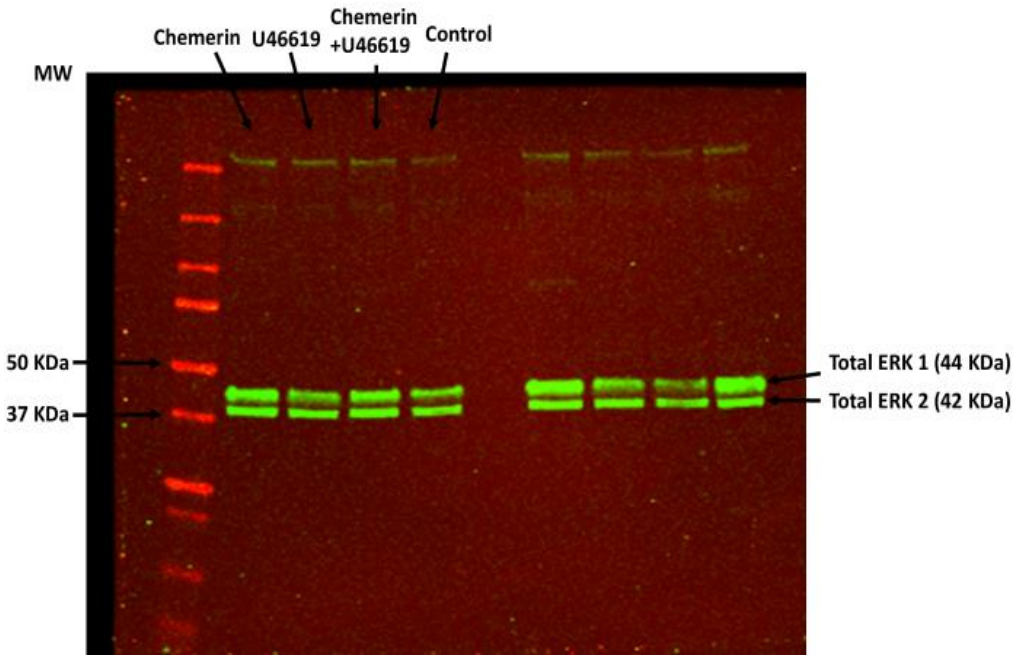


Figure 1. Full immunoblot showing expression of total ERK 1 and 2 in 5 µg of PCA following treatment with chemerin-9 only, U46619 only, chemerin-9 in the presence of U46619 (chemerin + U46619) or control (basal condition). (see Figure 4.6).

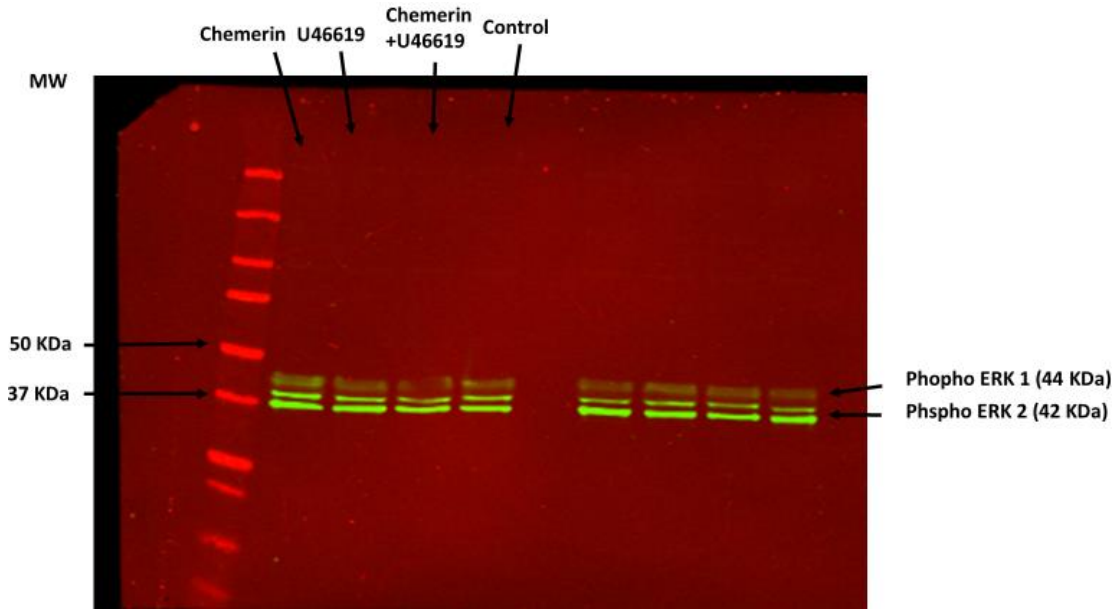


Figure 2. Full immunoblot showing expression of phosphorylated ERK 1 and 2 in 5 µg of PCA following treatment with chemerin-9 only, U46619 only, chemerin-9 in the presence of U46619 (chemerin + U46619) or control (basal condition). (see Figure 4.6).

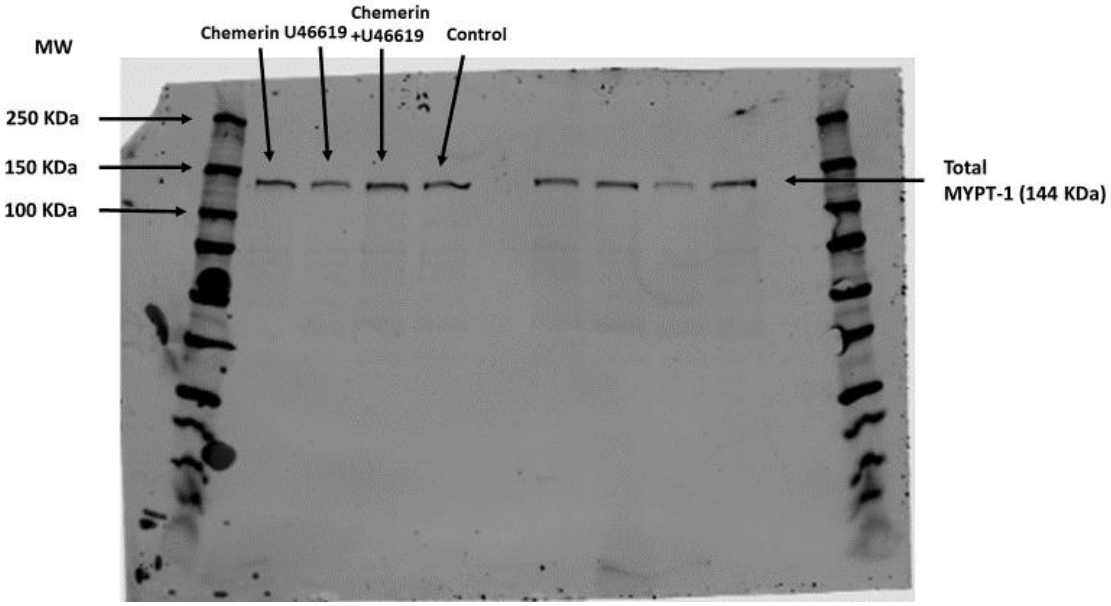


Figure 3. Full immunoblot showing expression of total MYPT-1 in 5 µg of PCA following treatment with chemerin-9 only, U46619 only, chemerin-9 in the presence of U46619 (chemerin + U46619) or control (basal condition). (see Figure 4.8).

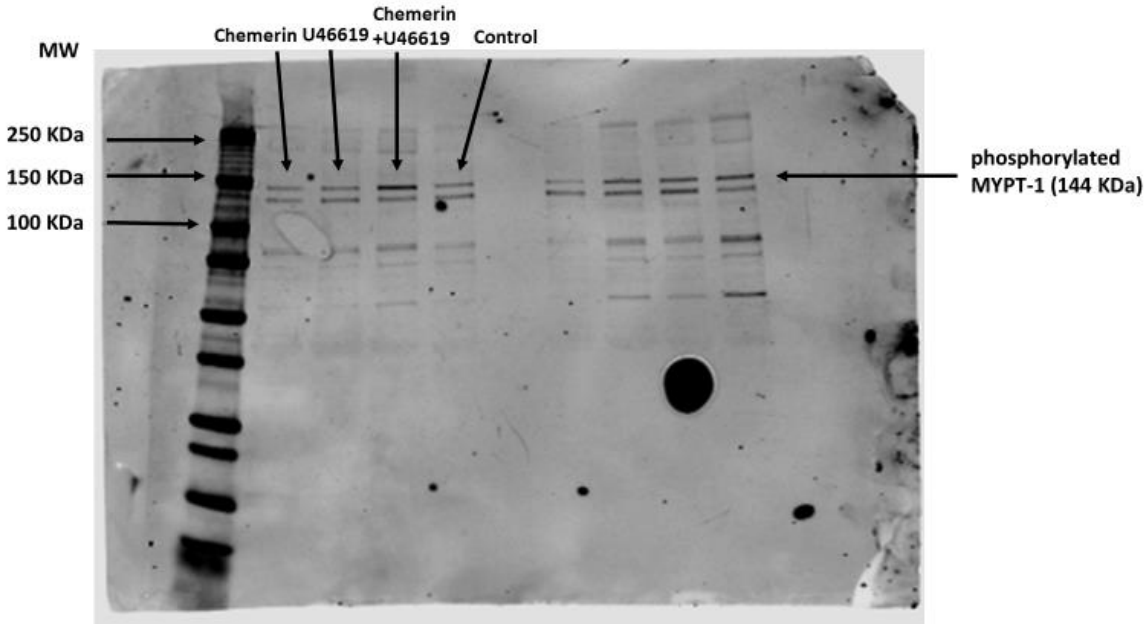


Figure 4. Full immunoblot showing expression of phosphorylated MYPT-1 in 5 µg of PCA following treatment with chemerin-9 only, U46619 only, chemerin-9 in the presence of U46619 (chemerin + U46619) or control (basal condition). (see Figure 4.8).

References

1. WHO. *Cardiovascular Diseases (CVDs) Fact Sheet*. 2017; Available from: https://www.who.int/news-room/fact-sheets/detail/cardiovascular-diseases-(cvds).
2. Foundation, B.H., *UK Factsheet.* 2021.
3. Nangia, R., H. Singh, and K. Kaur, *Prevalence of cardiovascular disease (CVD) risk factors.* medical journal armed forces india, 2016. **72**(4): p. 315-319.
4. Lu, Y., et al., *Metabolic mediators of the effects of body-mass index, overweight, and obesity on coronary heart disease and stroke: a pooled analysis of 97 prospective cohorts with 1· 8 million participants.* Lancet (London, England), 2013. **383**(9921): p. 970-983.
5. Eckel, R.H., S.M. Grundy, and P.Z. Zimmet, *The metabolic syndrome.* The lancet, 2005. **365**(9468): p. 1415-1428.
6. Hubert, H.B., et al., *Obesity as an independent risk factor for cardiovascular disease: a 26-year follow-up of participants in the Framingham Heart Study.* Circulation, 1983. **67**(5): p. 968-977.
7. Eckel, R.H., *Obesity and heart disease: a statement for healthcare professionals from the Nutrition Committee, American Heart Association.* Circulation, 1997. **96**(9): p. 3248-3250.
8. Rey‐Lopez, J., et al., *The prevalence of metabolically healthy obesity: a systematic review and critical evaluation of the definitions used.* Obesity reviews, 2014. **15**(10): p. 781-790.
9. Organisation, W.H. *Obesity and overweight*. 2020 [cited 2021 20 January]; Available from: https://www.who.int/news-room/fact-sheets/detail/obesity-and-overweight.
10. Poirier, P., et al., *Obesity and cardiovascular disease: pathophysiology, evaluation, and effect of weight loss: an update of the 1997 American Heart Association Scientific Statement on Obesity and Heart Disease from the Obesity Committee of the Council on Nutrition, Physical Activity, and Metabolism.* Circulation, 2006. **113**(6): p. 898-918.
11. Koliaki, C., S. Liatis, and A. Kokkinos, *Obesity and cardiovascular disease: revisiting an old relationship.* Metabolism, 2019. **92**: p. 98-107.
12. Ho, K.K., et al., *The epidemiology of heart failure: the Framingham Study.* Journal of the American College of Cardiology, 1993. **22**(4 Supplement 1): p. A6-A13.
13. Kenchaiah, S., et al., *Obesity and the risk of heart failure.* New England Journal of Medicine, 2002. **347**(5): p. 305-313.
14. Krittanawong, C., et al., *Meta-analysis comparing frequency of overweight versus normal weight in patients*

with new-onset heart failure. The American Journal of Cardiology, 2018. **121**(7): p. 836-843.
15. Hall, J.E., et al., *Mechanisms of obesity-associated cardiovascular and renal disease.* The American journal of the medical sciences, 2002. **324**(3): p. 127-137.
16. Frohlich, E.D., *Clinical management of the obese hypertensive patient.* Cardiology in review, 2002. **10**(3): p. 127-138.
17. DeMarco, V.G., A.R. Aroor, and J.R. Sowers, *The pathophysiology of hypertension in patients with obesity.* Nature Reviews Endocrinology, 2014. **10**(6): p. 364.
18. Redón, J., et al., *Independent impact of obesity and fat distribution in hypertension prevalence and control in the elderly.* Journal of hypertension, 2008. **26**(9): p. 1757-1764.
19. Luque-Ramírez, M., et al., *Obesity is the major determinant of the abnormalities in blood pressure found in young women with the polycystic ovary syndrome.* The Journal of Clinical Endocrinology & Metabolism, 2007. **92**(6): p. 2141-2148.
20. Kotsis, V., et al., *Impact of obesity on 24-hour ambulatory blood pressure and hypertension.* Hypertension, 2005. **45**(4): p. 602-607.
21. Cho, E., et al., *A prospective study of obesity and risk of coronary heart disease among diabetic women.* Diabetes care, 2002. **25**(7): p. 1142-1148.
22. Sjöström, L., et al., *Bariatric surgery and long-term cardiovascular events.* Jama, 2012. **307**(1): p. 56-65.
23. Avram, A.S., M.M. Avram, and W.D. James, *Subcutaneous fat in normal and diseased states: 2. Anatomy and physiology of white and brown adipose tissue.* Journal of the American Academy of Dermatology, 2005. **53**(4): p. 671-83.
24. Wozniak, S.E., et al., *Adipose tissue: the new endocrine organ? A review article.* Digestive diseases and sciences, 2009. **54**(9): p. 1847-1856.
25. Zhang, Y., et al., *Positional cloning of the mouse obese gene and its human homologue.* Nature, 1994. **372**(6505): p. 425-432.
26. Kershaw, E.E. and J.S. Flier, *Adipose tissue as an endocrine organ.* The Journal of Clinical Endocrinology and Metabolism, 2004. **89**(6): p. 2548-56.
27. Sacks, H.S. and J.N. Fain, *Human epicardial adipose tissue: a review.* American heart journal, 2007. **153**(6): p. 907-917.

28. Saely, C.H., K. Geiger, and H. Drexel, *Brown versus white adipose tissue: a mini-review.* Gerontology, 2012. **58**(1): p. 15-23.
29. Brown, N.K., et al., *Perivascular adipose tissue in vascular function and disease: a review of current research and animal models.* Arteriosclerosis, Thrombosis, and Vascular Biology, 2014. **34**(8): p. 1621-30.
30. Wankhade, U.D., et al., *Novel browning agents, mechanisms, and therapeutic potentials of brown adipose tissue.* BioMed research international, 2016. **2016**.
31. Heaton, J.M., *The distribution of brown adipose tissue in the human.* Journal of anatomy, 1972. **112**(Pt 1): p. 35.
32. Nedergaard, J., T. Bengtsson, and B. Cannon, *Unexpected evidence for active brown adipose tissue in adult humans.* American Journal of Physiology-Endocrinology and Metabolism, 2007.
33. Cypess, A.M., et al., *Identification and importance of brown adipose tissue in adult humans.* New England Journal of Medicine, 2009. **360**(15): p. 1509-1517.
34. Bonet, M.L., P. Oliver, and A. Palou, *Pharmacological and nutritional agents promoting browning of white adipose tissue.* Biochimica et Biophysica Acta (BBA)-Molecular and Cell Biology of Lipids, 2013. **1831**(5): p. 969-985.
35. Harms, M. and P. Seale, *Brown and beige fat: development, function and therapeutic potential.* Nature medicine, 2013. **19**(10): p. 1252-1263.
36. Vitali, A., et al., *The adipose organ of obesity-prone C57BL/6J mice is composed of mixed white and brown adipocytes.* Journal of lipid research, 2012. **53**(4): p. 619-629.
37. Ibrahim, M.M., *Subcutaneous and visceral adipose tissue: structural and functional differences.* obesity reviews, 2010. **11**(1): p. 11-8.
38. Wajchenberg, B.L., *Subcutaneous and visceral adipose tissue: their relation to the metabolic syndrome.* Endocrine Reviews, 2000. **21**(6): p. 697-738.
39. Tchernof, A. and J.-P. Després, *Pathophysiology of human visceral obesity: an update.* Physiological reviews, 2013.
40. Chaldakov, G.N., et al., *Adipoparacrinology–vascular periadventitial adipose tissue (tunica adiposa) as an example.* Cell Biology International, 2012. **36**(3): p. 327-330.
41. Gil-Ortega, M., et al., *Regional differences in perivascular adipose tissue impacting vascular homeostasis.* Trends in Endocrinology & Metabolism, 2015. **26**(7): p. 367-375.

42. Daly, C.J., *Examining vascular structure and function using confocal microscopy and 3d imaging techniques*, in *Biomedical Visualisation*. 2019, Springer. p. 97-106.
43. Szasz, T., G.F. Bomfim, and R.C. Webb, *The influence of perivascular adipose tissue on vascular homeostasis.* Vascular Health and Risk Management, 2013. **9**: p. 105-16.
44. Cheng, C.K., et al., *Perivascular adipose tissue: the sixth man of the cardiovascular system.* Cardiovascular drugs and therapy, 2018. **32**(5): p. 481-502.
45. Frontini, A. and S. Cinti, *Distribution and development of brown adipocytes in the murine and human adipose organ.* Cell metabolism, 2010. **11**(4): p. 253-256.
46. Chatterjee, T.K., et al., *Human coronary artery perivascular adipocytes overexpress genes responsible for regulating vascular morphology, inflammation, and hemostasis.* Physiological Genomics, 2013. **45**(16): p. 697-709.
47. Chatterjee, T.K., et al., *Proinflammatory phenotype of perivascular adipocytes: influence of high-fat feeding.* Circulation research, 2009. **104**(4): p. 541-549.
48. Sacks, H.S., et al., *Uncoupling protein-1 and related messenger ribonucleic acids in human epicardial and other adipose tissues: epicardial fat functioning as brown fat.* The Journal of Clinical Endocrinology and Metabolism, 2009. **94**(9): p. 3611-5.
49. Galvez-Prieto, B., et al., *Comparative expression analysis of the renin-angiotensin system components between white and brown perivascular adipose tissue.* Journal of Endocrinology, 2008. **197**(1): p. 55-64.
50. Soltis, E.E. and L.A. Cassis, *Influence of perivascular adipose tissue on rat aortic smooth muscle responsiveness.* Clinical and Experimental Hypertension. Part A: Theory and Practice, 1991. **13**(2): p. 277-96.
51. Mattu, H.S. and H.S. Randeva, *Role of adipokines in cardiovascular disease.* The Journal of endocrinology, 2013. **216**(1): p. T17.
52. Szasz, T. and R.C. Webb, *Perivascular adipose tissue: more than just structural support.* Clinical Science, 2012. **122**(1): p. 1-12.
53. Akoumianakis, I. and C. Antoniades, *The interplay between adipose tissue and the cardiovascular system: is fat always bad?* Cardiovascular research, 2017. **113**(9): p. 999-1008.
54. Rajsheker, S., et al., *Crosstalk between perivascular adipose tissue and blood vessels.* Current opinion in pharmacology, 2010. **10**(2): p. 191-196.

55. Almabrouk, T., et al., *Perivascular fat, AMP‐activated protein kinase and vascular diseases.* British Journal of Pharmacology, 2014. **171**(3): p. 595-617.
56. Barandier, C., J.-P. Montani, and Z. Yang, *Mature adipocytes and perivascular adipose tissue stimulate vascular smooth muscle cell proliferation: effects of aging and obesity.* American Journal of Physiology-Heart and Circulatory Physiology, 2005. **289**(5): p. H1807-H1813.
57. Huang, F., et al., *Leptin-induced vascular smooth muscle cell proliferation via regulating cell cycle, activating ERK1/2 and NF-κB.* Acta Biochimica et Biophysica Sinica, 2010. **42**(5): p. 325-331.
58. Wang, P., et al., *Perivascular adipose tissue-derived visfatin is a vascular smooth muscle cell growth factor: role of nicotinamide mononucleotide.* Cardiovascular research, 2009. **81**(2): p. 370-380.
59. Shyu, K.-G., et al., *Resistin contributes to neointimal formation via oxidative stress after vascular injury.* Clinical Science, 2011. **120**(3): p. 121-129.
60. Akoumianakis, I., A. Tarun, and C. Antoniades, *Perivascular adipose tissue as a regulator of vascular disease pathogenesis: identifying novel therapeutic targets.* British journal of pharmacology, 2017. **174**(20): p. 3411-3424.
61. Chang, L., et al., *Loss of perivascular adipose tissue on peroxisome proliferator–activated receptor-γ deletion in smooth muscle cells impairs intravascular thermoregulation and enhances atherosclerosis.* Circulation, 2012. **126**(9): p. 1067-1078.
62. Löhn, M., et al., *Periadventitial fat releases a vascular relaxing factor.* The FASEB Journal, 2002. **16**(9): p. 1057-1063.
63. Gao, Y.-J., et al., *Perivascular adipose tissue modulates vascular function in the human internal thoracic artery.* The Journal of thoracic and cardiovascular surgery, 2005. **130**(4): p. 1130-1136.
64. Malinowski, M., et al., *Perivascular tissue of internal thoracic artery releases potent nitric oxide and prostacyclin-independent anticontractile factor.* European journal of cardio-thoracic surgery, 2008. **33**(2): p. 225-231.
65. Abu Bakar, H., et al., *Sensory innervation of perivascular adipose tissue: a crucial role in artery vasodilatation and leptin release.* Cardiovascular research, 2017. **113**(8): p. 962-972.
66. Lynch, F.M., et al., *Perivascular adipose tissue-derived adiponectin activates BKCa channels to induce*

anticontractile responses. American Journal of Physiology-Heart and Circulatory Physiology, 2013. **304**(6): p. H786-H795.
67. Virtanen, K.A., et al., *Functional brown adipose tissue in healthy adults.* New England Journal of Medicine, 2009. **360**(15): p. 1518-1525.
68. Lee, R.M., et al., *Endothelium-dependent relaxation factor released by perivascular adipose tissue.* Journal of hypertension, 2009. **27**(4): p. 782-790.
69. Dashwood, M.R., et al., *Does periadventitial fat-derived nitric oxide play a role in improved saphenous vein graft patency in patients undergoing coronary artery bypass surgery?* Journal of vascular research, 2007. **44**(3): p. 175-181.
70. Donovan, J., et al., *Coronary artery hypoxic vasorelaxation is augmented by perivascular adipose tissue through a mechanism involving hydrogen sulphide and cystathionine - β - synthase.* Acta Physiologica, 2018. **224**(4): p. e13126.
71. Costa, R.M., et al., *H2O2 generated from mitochondrial electron transport chain in thoracic perivascular adipose tissue is crucial for modulation of vascular smooth muscle contraction.* Vascular pharmacology, 2016. **84**: p. 28-37.
72. Gao, Y.-J., et al., *Perivascular adipose tissue promotes vasoconstriction: the role of superoxide anion.* Cardiovascular research, 2006. **71**(2): p. 363-373.
73. Gao, Y.-J., *Dual modulation of vascular function by perivascular adipose tissue and its potential correlation with adiposity/lipoatrophy-related vascular dysfunction.* Current pharmaceutical design, 2007. **13**(21): p. 2185-2192.
74. Ramirez, J., E. O'Malley, and W. Ho, *Pro - contractile effects of perivascular fat in health and disease.* British Journal of Pharmacology, 2017. **174**(20): p. 3482-3495.
75. Gálvez-Prieto, B., et al., *Comparative expression analysis of the renin-angiotensin system components between white and brown perivascular adipose tissue.* Journal of Endocrinology, 2008. **197**(1): p. 55-64.
76. Lu, C., et al., *Mechanisms for perivascular adipose tissue-mediated potentiation of vascular contraction to perivascular neuronal stimulation: the role of adipocyte-derived angiotensin II.* European journal of pharmacology, 2010. **634**(1-3): p. 107-112.
77. Meyer, M.R., et al., *Regulation of vascular smooth muscle tone by adipose-derived contracting factor.* PloS one, 2013. **8**(11): p. e79245.

78. Ayala‐Lopez, N. and S.W. Watts, *New actions of an old friend: perivascular adipose tissue's adrenergic mechanisms.* British Journal of Pharmacology, 2017. **174**(20): p. 3454-3465.
79. Ayala‐Lopez, N., et al., *Perivascular adipose tissue contains functional catecholamines.* Pharmacology research & perspectives, 2014. **2**(3): p. e00041.
80. Lehman, S.J., et al., *Peri-aortic fat, cardiovascular disease risk factors, and aortic calcification: the Framingham Heart Study.* Atherosclerosis, 2010. **210**(2): p. 656-661.
81. Greenstein, A.S., et al., *Local inflammation and hypoxia abolish the protective anticontractile properties of perivascular fat in obese patients.* Circulation, 2009. **119**(12): p. 1661.
82. Aghamohammadzadeh, R., et al., *Effects of bariatric surgery on human small artery function: evidence for reduction in perivascular adipocyte inflammation, and the restoration of normal anticontractile activity despite persistent obesity.* Journal of the American College of Cardiology, 2013. **62**(2): p. 128-135.
83. Bussey, C.E., et al., *Obesity-related perivascular adipose tissue damage is reversed by sustained weight loss in the rat.* Arteriosclerosis, Thrombosis, and Vascular Biology, 2016. **36**(7): p. 1377-1385.
84. Sarin, S., et al., *Clinical significance of epicardial fat measured using cardiac multislice computed tomography.* The American Journal of Cardiology, 2008. **102**(6): p. 767-71.
85. Greif, M., et al., *Pericardial adipose tissue determined by dual source CT is a risk factor for coronary atherosclerosis.* Arteriosclerosis, Thrombosis, and Vascular Biology, 2009. **29**(5): p. 781-6.
86. Eiras, S., et al., *Extension of coronary artery disease is associated with increased IL-6 and decreased adiponectin gene expression in epicardial adipose tissue.* Cytokine, 2008. **43**(2): p. 174-80.
87. Ahmad, A.A., M.D. Randall, and R.E. Roberts, *Sex differences in the regulation of porcine coronary artery tone by perivascular adipose tissue: a role of adiponectin?* British journal of pharmacology, 2017. **174**(16): p. 2773-2783.
88. Mohammed, M., et al., *Vasodilator effects of leptin on canine isolated mesenteric arteries and veins.* Clinical and experimental pharmacology and physiology, 2007. **34**(8): p. 771-774.

89. Nakagawa, K., et al., *Leptin causes vasodilation in humans.* Hypertension Research, 2002. **25**(2): p. 161-165.
90. Noblet, J.N., et al., *Leptin augments coronary vasoconstriction and smooth muscle proliferation via a Rho-kinase-dependent pathway.* Basic research in cardiology, 2016. **111**(3): p. 25.
91. Ozen, G., et al., *Control of human vascular tone by prostanoids derived from perivascular adipose tissue.* Prostaglandins & other lipid mediators, 2013. **107**: p. 13-17.
92. Ahmad, A.A., M.D. Randall, and R.E. Roberts, *Sex differences in the role of phospholipase A2 -dependent arachidonic acid pathway in the perivascular adipose tissue function in pigs.* The Journal of Physiology, 2017.
93. Kennedy, A.J., et al., *Chemerin Elicits Potent Constrictor Actions via Chemokine‐Like Receptor 1 (CMKLR 1), not G‐Protein‐Coupled Receptor 1 (GPR 1), in Human and Rat Vasculature.* Journal of the American Heart Association, 2016. **5**(10): p. e004421.
94. Watts, S.W., et al., *Chemerin connects fat to arterial contraction.* Arteriosclerosis, thrombosis, and vascular biology, 2013. **33**(6): p. 1320-1328.
95. Brian, J.E. and F.M. Faraci, *Tumor Necrosis Factor- - Induced Dilatation of Cerebral Arterioles.* Stroke-a Journal of Cerebral Circulation, 1998. **29**(2): p. 509-514.
96. Johns, D.G. and R.C. Webb, *TNF-α-induced endothelium-independent vasodilation: a role for phospholipase A2-dependent ceramide signaling.* American Journal of Physiology-Heart and Circulatory Physiology, 1998. **275**(5): p. H1592-H1598.
97. Wagner, E.M., *TNF-α induced bronchial vasoconstriction.* American Journal of Physiology-Heart and Circulatory Physiology, 2000. **279**(3): p. H946-H951.
98. Ohkawa, F., et al., *Inhibitory effect of interleukin-6 on vascular smooth muscle contraction.* American Journal of Physiology-Heart and Circulatory Physiology, 1994. **266**(3): p. H898-H902.
99. Schleifenbaum, J., et al., *Systemic peripheral artery relaxation by KCNQ channel openers and hydrogen sulfide.* Journal of hypertension, 2010. **28**(9): p. 1875-1882.
100. Nagpal, S., et al., *Tazarotene-induced gene 2 (TIG2), a novel retinoid-responsive gene in skin.* Journal of Investigative Dermatology, 1997. **109**(1): p. 91-5.

101. Helfer, G. and Q.F. Wu, *Chemerin: a multifaceted adipokine involved in metabolic disorders.* Journal of Endocrinology, 2018. **238**(2): p. R79-R94.
102. Kennedy, A.J. and A.P. Davenport, *International union of basic and clinical pharmacology CIII: chemerin receptors CMKLR1 (Chemerin1) and GPR1 (Chemerin2) nomenclature, pharmacology, and function.* Pharmacological Reviews, 2018. **70**(1): p. 174-196.
103. Marchese, A., et al., *Cloning of human genes encoding novel G protein-coupled receptors.* Genomics, 1994. **23**(3): p. 609-618.
104. Barnea, G., et al., *The genetic design of signaling cascades to record receptor activation.* Proceedings of the National Academy of Sciences of the United States of America, 2008. **105**(1): p. 64-9.
105. Inci, S., G. Aksan, and P. Dogan, *Chemerin as an independent predictor of cardiovascular event risk.* Therapeutic Advances in Endocrinology and Metabolism, 2016. **7**(2): p. 57-68.
106. Fan, P., et al., *Cloning and characterization of a novel human chemokine receptor.* Biochemical and biophysical research communications, 1998. **243**(1): p. 264-268.
107. Zabel, B.A., et al., *Mast cell-expressed orphan receptor CCRL2 binds chemerin and is required for optimal induction of IgE-mediated passive cutaneous anaphylaxis.* Journal of Experimental Medicine, 2008. **205**(10): p. 2207-20.
108. Ferland, D.J. and S.W. Watts, *Chemerin: A comprehensive review elucidating the need for cardiovascular research.* Pharmacological Research, 2015. **99**: p. 351-61.
109. De Henau, O., et al., *Signaling properties of chemerin receptors CMKLR1, GPR1 and CCRL2.* PLoS One, 2016. **11**(10): p. e0164179.
110. Gantz, I., et al., *Molecular cloning of a novel receptor (CMKLR1) with homology to the chemotactic factor receptors.* Cytogenetic and Genome Research, 1996. **74**(4): p. 286-90.
111. Wittamer, V., et al., *Specific recruitment of antigen-presenting cells by chemerin, a novel processed ligand from human inflammatory fluids.* Journal of Experimental Medicine, 2003. **198**(7): p. 977-985.
112. Kaur, J., et al., *Identification of chemerin receptor (ChemR23) in human endothelial cells: chemerin-induced endothelial angiogenesis.* Biochemical and Biophysical Research Communications, 2010. **391**(4): p. 1762-8.

113. Roh, S.-g., et al., *Chemerin—a new adipokine that modulates adipogenesis via its own receptor.* Biochemical and biophysical research communications, 2007. **362**(4): p. 1013-1018.
114. Parlee, S.D., et al., *Serum chemerin levels vary with time of day and are modified by obesity and tumor necrosis factor-{alpha}.* Endocrinology, 2010. **151**(6): p. 2590-602.
115. Arita, M., et al., *Stereochemical assignment, antiinflammatory properties, and receptor for the omega-3 lipid mediator resolvin E1.* The Journal of experimental medicine, 2005. **201**(5): p. 713-722.
116. Goralski, K.B., et al., *Chemerin, a novel adipokine that regulates adipogenesis and adipocyte metabolism.* Journal of Biological Chemistry, 2007. **282**(38): p. 28175-88.
117. Sell, H., et al., *Chemerin is a novel adipocyte-derived factor inducing insulin resistance in primary human skeletal muscle cells.* Diabetes, 2009. **58**(12): p. 2731-2740.
118. Zhou, J.-x., et al., *Chemerin C9 peptide induces receptor internalization through a clathrin-independent pathway.* Acta Pharmacologica Sinica, 2014. **35**(5): p. 653.
119. Ferland, D.J., et al., *Chemerin-induced arterial contraction is Gi-and calcium-dependent.* Vascular pharmacology, 2017. **88**: p. 30-41.
120. Ferland, D.J., A.E. Mullick, and S.W. Watts, *Chemerin as a driver of hypertension: A consideration.* American Journal of Hypertension, 2020. **33**(11): p. 975-986.
121. Wittamer, V., et al., *The C-terminal nonapeptide of mature chemerin activates the chemerin receptor with low nanomolar potency.* Journal of Biological Chemistry, 2004. **279**(11): p. 9956-9962.
122. Arita, M., et al., *Resolvin E1 selectively interacts with leukotriene B4 receptor BLT1 and ChemR23 to regulate inflammation.* The Journal of Immunology, 2007. **178**(6): p. 3912-3917.
123. Bozaoglu, K., et al., *Chemerin is a novel adipokine associated with obesity and metabolic syndrome.* Endocrinology, 2007. **148**(10): p. 4687-4694.
124. Krautbauer, S., et al., *Chemerin is highly expressed in hepatocytes and is induced in non-alcoholic steatohepatitis liver.* Experimental and molecular pathology, 2013. **95**(2): p. 199-205.
125. Zabel, B.A., et al., *Chemoattractants, extracellular proteases, and the integrated host defense response.* Experimental hematology, 2006. **34**(8): p. 1021-1032.

126. Zabel, B.A., et al., *Chemerin activation by serine proteases of the coagulation, fibrinolytic, and inflammatory cascades.* Journal of Biological Chemistry, 2005. **280**(41): p. 34661-34666.
127. Kaur, J., et al., *Chemerin in human cardiovascular disease.* Vascular Pharmacology, 2018. **110**: p. 1-6.
128. Guillabert, A., et al., *Role of neutrophil proteinase 3 and mast cell chymase in chemerin proteolytic regulation.* Journal of leukocyte biology, 2008. **84**(6): p. 1530-1538.
129. De Palma, G., et al., *The possible role of ChemR23/Chemerin axis in the recruitment of dendritic cells in lupus nephritis.* Kidney international, 2011. **79**(11): p. 1228-1235.
130. Zabel, B.A., A.M. Silverio, and E.C. Butcher, *Chemokine-like receptor 1 expression and chemerin-directed chemotaxis distinguish plasmacytoid from myeloid dendritic cells in human blood.* The Journal of Immunology, 2005. **174**(1): p. 244-251.
131. Albanesi, C., et al., *Chemerin expression marks early psoriatic skin lesions and correlates with plasmacytoid dendritic cell recruitment.* Journal of Experimental Medicine, 2009. **206**(1): p. 249-258.
132. Parolini, S., et al., *The role of chemerin in the colocalization of NK and dendritic cell subsets into inflamed tissues.* Blood, 2007. **109**(9): p. 3625-3632.
133. Hart, R. and D.R. Greaves, *Chemerin contributes to inflammation by promoting macrophage adhesion to VCAM-1 and fibronectin through clustering of VLA-4 and VLA-5.* The Journal of Immunology, 2010. **185**(6): p. 3728-3739.
134. Buechler, C., *Chemerin, a novel player in inflammatory bowel disease.* Cellular and Molecular Immunology, 2014. **11**(4): p. 315.
135. Fatima, S.S., et al., *New roles of the multidimensional adipokine: chemerin.* Peptides, 2014. **62**: p. 15-20.
136. Mariani, F. and L. Roncucci, *Chemerin/chemR23 axis in inflammation onset and resolution.* Inflammation Research, 2015. **64**(2): p. 85-95.
137. Cash, J.L., A.R. Christian, and D.R. Greaves, *Chemerin peptides promote phagocytosis in a ChemR23-and Syk-dependent manner.* The Journal of Immunology, 2010. **184**(9): p. 5315-5324.
138. Chakaroun, R., et al., *Effects of weight loss and exercise on chemerin serum concentrations and adipose tissue expression in human obesity.* Metabolism, 2012. **61**(5): p. 706-714.

139. Landgraf, K., et al., *Chemerin as a mediator between obesity and vascular inflammation in children.* The Journal of Clinical Endocrinology & Metabolism, 2012. **97**(4): p. E556-E564.
140. Shin, H.Y., et al., *Chemerin levels are positively correlated with abdominal visceral fat accumulation.* Clinical endocrinology, 2012. **77**(1): p. 47-50.
141. Sell, H., et al., *Chemerin correlates with markers for fatty liver in morbidly obese patients and strongly decreases after weight loss induced by bariatric surgery.* The Journal of Clinical Endocrinology & Metabolism, 2010. **95**(6): p. 2892-2896.
142. Ress, C., et al., *Effect of bariatric surgery on circulating chemerin levels.* European journal of clinical investigation, 2010. **40**(3): p. 277-280.
143. Ernst, M.C., et al., *Disruption of the chemokine-like receptor-1 (CMKLR1) gene is associated with reduced adiposity and glucose intolerance.* Endocrinology, 2012. **153**(2): p. 672-682.
144. Kostopoulos, C.G., et al., *Chemerin and CMKLR1 expression in human arteries and periadventitial fat: a possible role for local chemerin in atherosclerosis?* BMC cardiovascular disorders, 2014. **14**(1): p. 56.
145. Spiroglou, S.G., et al., *Adipokines in periaortic and epicardial adipose tissue: differential expression and relation to atherosclerosis.* Journal of atherosclerosis and thrombosis, 2010. **17**(2): p. 115-130.
146. Yang, M., et al., *Elevated plasma levels of chemerin in newly diagnosed type 2 diabetes mellitus with hypertension.* Journal of Investigative Medicine, 2010. **58**(7): p. 883-886.
147. Gu, P., et al., *Chemerin is associated with inflammatory markers and metabolic syndrome phenotypes in hypertension patients.* Clinical and experimental hypertension, 2014. **36**(5): p. 326-332.
148. Watts, S.W., et al., *The chemerin knockout rat reveals chemerin dependence in female, but not male, experimental hypertension.* The FASEB Journal, 2018. **32**(12): p. 6596-6614.
149. Ferland, D.J., et al., *Whole-body but not hepatic knockdown of chemerin by antisense oligonucleotide decreases blood pressure in rats.* Journal of Pharmacology and Experimental Therapeutics, 2018. **365**(2): p. 212-218.
150. Ferland, D.J., et al., *Different blood pressure responses in hypertensive rats following chemerin mRNA inhibition in*

dietary high fat compared to dietary high salt conditions. Physiological Genomics, 2019.
151. Darios, E.S., et al., *The adipokine chemerin amplifies electrical field-stimulated contraction in the isolated rat superior mesenteric artery.* American Journal of Physiology-Heart and Circulatory Physiology, 2016. **311**(2): p. H498-H507.
152. Lobato, N., et al., *The adipokine chemerin augments vascular reactivity to contractile stimuli via activation of the MEK-ERK1/2 pathway.* Life sciences, 2012. **91**(13-14): p. 600-606.
153. Hanthazi, A., et al., *Chemerin influences endothelin-and serotonin-induced pulmonary artery vasoconstriction in rats.* Life sciences, 2019. **231**: p. 116580.
154. Silva, M.A., et al., *Statin-related adverse events: a meta-analysis.* Clinical therapeutics, 2006. **28**(1): p. 26-35.
155. NHS. *Statins*. 2021 [cited 2021; Available from: https://www.nhs.uk/conditions/statins/.
156. Pedersen, T.R., et al., *Safety and tolerability of cholesterol lowering with simvastatin during 5 years in the Scandinavian Simvastatin Survival Study.* Archives of internal medicine, 1996. **156**(18): p. 2085-2092.
157. Members:, W.C., et al., *ACC/AHA/NHLBI clinical advisory on the use and safety of statins.* Circulation, 2002. **106**(8): p. 1024-1028.
158. Siegel-Axel, D., *Cerivastatin: a cellular and molecular drug for the future?* Cellular and Molecular Life Sciences CMLS, 2003. **60**(1): p. 144-164.
159. du Souich, P., G. Roederer, and R. Dufour, *Myotoxicity of statins: mechanism of action.* Pharmacology & therapeutics, 2017. **175**: p. 1-16.
160. Kaufmann, P., et al., *Toxicity of statins on rat skeletal muscle mitochondria.* Cellular and Molecular Life Sciences CMLS, 2006. **63**(19-20): p. 2415-2425.
161. Apostolopoulou, M., A. Corsini, and M. Roden, *The role of mitochondria in statin‐induced myopathy.* European journal of clinical investigation, 2015. **45**(7): p. 745-754.
162. Shitara, Y. and Y. Sugiyama, *Pharmacokinetic and pharmacodynamic alterations of 3-hydroxy-3-methylglutaryl coenzyme A (HMG-CoA) reductase inhibitors: drug-drug interactions and interindividual differences in transporter and metabolic enzyme functions.* Pharmacology & Therapeutics, 2006. **112**(1): p. 71-105.
163. Manzoni, M. and M. Rollini, *Biosynthesis and biotechnological production of statins by filamentous fungi and application of these cholesterol-lowering drugs.*

Applied Microbiology and Biotechnology, 2002. **58**(5): p. 555-64.
164. Pedersen, T.R., *Pleiotropic effects of statins: evidence against benefits beyond LDL-cholesterol lowering.* American Journal of Cardiovascular Drugs, 2010. **10 Suppl 1**: p. 10-7.
165. Germershausen, J.I., et al., *Tissue selectivity of the cholesterol-lowering agents lovastatin, simvastatin and pravastatin in rats in vivo.* Biochemical and Biophysical Research Communications, 1989. **158**(3): p. 667-75.
166. Prueksaritanont, T., et al., *Mechanistic studies on metabolic interactions between gemfibrozil and statins.* Journal of Pharmacology and Experimental Therapeutics, 2002. **301**(3): p. 1042-1051.
167. Garcia, M., et al., *Clinical pharmacokinetics of statins.* Methods and Findings in Experimental and Clinical Pharmacology 2003. **25**(6): p. 457-481.
168. Stancu, C. and A. Sima, *Statins: mechanism of action and effects.* Journal of cellular and molecular medicine, 2001. **5**(4): p. 378-387.
169. Schachter, M., *Chemical, pharmacokinetic and pharmacodynamic properties of statins: an update.* Fundamental & clinical pharmacology, 2005. **19**(1): p. 117-125.
170. Asztalos, B.F., et al., *Comparing the effects of five different statins on the HDL subpopulation profiles of coronary heart disease patients.* Atherosclerosis, 2002. **164**(2): p. 361-9.
171. Branchi, A., et al., *Lowering effects of four different statins on serum triglyceride level.* European journal of clinical pharmacology, 1999. **55**(7): p. 499-502.
172. Tamargo, J., et al., *Lipid-lowering therapy with statins, a new approach to antiarrhythmic therapy.* Pharmacology & therapeutics, 2007. **114**(1): p. 107-126.
173. Takemoto, M. and J.K. Liao, *Pleiotropic effects of 3-hydroxy-3-methylglutaryl coenzyme a reductase inhibitors.* Arteriosclerosis, thrombosis, and vascular biology, 2001. **21**(11): p. 1712-1719.
174. Packard, C., et al., *Influence of pravastatin and plasma lipids on clinical events in the West of Scotland Coronary Prevention Study (WOSCOPS).* Circulation, 1998. **97**(15): p. 1440-1445.
175. Sacks, F.M., et al., *The effect of pravastatin on coronary events after myocardial infarction in patients with average cholesterol levels.* New England Journal of Medicine, 1996. **335**(14): p. 1001-1009.

176. O'Driscoll, G., D. Green, and R.R. Taylor, *Simvastatin, an HMG-coenzyme A reductase inhibitor, improves endothelial function within 1 month.* Circulation, 1997. **95**(5): p. 1126-31.
177. Laufs, U., et al., *Upregulation of endothelial nitric oxide synthase by HMG CoA reductase inhibitors.* Circulation, 1998. **97**(12): p. 1129-1135.
178. Omori, H., et al., *Direct in vivo evidence of a vascular statin: a single dose of cerivastatin rapidly increases vascular endothelial responsiveness in healthy normocholesterolaemic subjects.* British Journal of Clinical Pharmacology, 2002. **54**(4): p. 395-9.
179. Wolfrum, S., K.S. Jensen, and J.K. Liao, *Endothelium-dependent effects of statins.* Arteriosclerosis, Thrombosis, and Vascular Biology, 2003. **23**(5): p. 729-36.
180. Correa, V., Jr., et al., *Blood pressure-lowering effect of simvastatin: a placebo-controlled randomized clinical trial with 24-h ambulatory blood pressure monitoring.* Journal of Human Hypertension, 2014. **28**(1): p. 62-7.
181. Zhou, Q. and J.K. Liao, *Pleiotropic effects of statins. - Basic research and clinical perspectives.* Circulation journal, 2010. **74**(5): p. 818-26.
182. Oesterle, A., U. Laufs, and J.K. Liao, *Pleiotropic Effects of Statins on the Cardiovascular System.* Circulation Research, 2017. **120**(1): p. 229-243.
183. Noguchi, Y., et al., *Newly synthesized Rho A, not Ras, is isoprenylated and translocated to membranes coincident with progression of the G1 to S phase of growth-stimulated rat FRTL-5 cells.* Journal of Biological Chemistry, 1998. **273**(6): p. 3649-3653.
184. Brown, J.H., D.P. Del Re, and M.A. Sussman, *The Rac and Rho hall of fame: a decade of hypertrophic signaling hits.* Circulation research, 2006. **98**(6): p. 730-742.
185. Bergdahl, A., et al., *Lovastatin induces relaxation and inhibits L‐type Ca2+ current in the rat basilar artery.* Pharmacology & toxicology, 2003. **93**(3): p. 128-134.
186. López, J., et al., *Participation of K+ channels in the endothelium-dependent and endothelium-independent components of the relaxant effect of rosuvastatin in rat aortic rings.* Journal of cardiovascular pharmacology and therapeutics, 2008. **13**(3): p. 207-213.
187. Almukhtar, H., et al., *Effect of simvastatin on vascular tone in porcine coronary artery: Potential role of the mitochondria.* Toxicology and applied pharmacology, 2016. **305**: p. 176-185.

188. Lorkowska, B. and S. Chlopicki, *Statins as coronary vasodilators in isolated bovine coronary arteries--involvement of PGI2 and NO.* Prostaglandins, Leukotrienes & Essential Fatty Acids, 2005. **72**(2): p. 133-8.
189. Alvarez De Sotomayor, M., et al., *Characterization of endothelial factors involved in the vasodilatory effect of simvastatin in aorta and small mesenteric artery of the rat.* British Journal of Pharmacology, 2000. **131**(6): p. 1179-87.
190. Rattan, S., *3-Hydroxymethyl coenzyme A reductase inhibition attenuates spontaneous smooth muscle tone via RhoA/ROCK pathway regulated by RhoA prenylation.* American Journal of Physiology-Gastrointestinal and Liver Physiology, 2010. **298**(6): p. G962-9.
191. Ali, N., et al., *Current statins show calcium channel blocking activity through voltage gated channels.* BMC Pharmacology and Toxicology, 2016. **17**(1): p. 43.
192. Yin, Q.-f. and Y. Xiong, *Pravastatin restores DDAH activity and endothelium-dependent relaxation of rat aorta after exposure to glycated protein.* Journal of cardiovascular pharmacology, 2005. **45**(6): p. 525-532.
193. Muramatsu, J., et al., *Hemodynamic changes associated with reduction in total cholesterol by treatment with the HMG-CoA reductase inhibitor pravastatin.* Atherosclerosis, 1997. **130**(1-2): p. 179-182.
194. Hasegawa, M., et al., *Functional involvement of rat organic anion transporter 3 (rOat3; Slc22a8) in the renal uptake of organic anions.* Journal of Pharmacology and Experimental Therapeutics, 2002. **300**(3): p. 746-753.
195. Juncos, L.I., L.A. Juncos, and N.H. García, *The antihypertensive actions of statins: modulation by salt intake.* American journal of hypertension, 2012. **25**(11): p. 1140-1148.
196. Koh, K.K., et al., *Vascular and metabolic effects of combined therapy with ramipril and simvastatin in patients with type 2 diabetes.* Hypertension, 2005. **45**(6): p. 1088-1093.
197. Zhao, Y., P.M. Vanhoutte, and S.W. Leung, *Vascular nitric oxide: Beyond eNOS.* Journal of Pharmacological Sciences, 2015. **129**(2): p. 83-94.
198. Ming, X.-F., et al., *Rho GTPase/Rho kinase negatively regulates endothelial nitric oxide synthase phosphorylation through the inhibition of protein kinase B/Akt in human endothelial cells.* Molecular and cellular biology, 2002. **22**(24): p. 8467-8477.

199. Shiga, N., et al., *Long-term inhibition of RhoA attenuates vascular contractility by enhancing endothelial NO production in an intact rabbit mesenteric artery.* Circulation research, 2005. **96**(9): p. 1014-1021.
200. Feron, O., et al., *Hydroxy-methylglutaryl-coenzyme A reductase inhibition promotes endothelial nitric oxide synthase activation through a decrease in caveolin abundance.* Circulation, 2001. **103**(1): p. 113-8.
201. Rezaie-Majd, A., et al., *Simvastatin reduces expression of cytokines interleukin-6, interleukin-8, and monocyte chemoattractant protein-1 in circulating monocytes from hypercholesterolemic patients.* Arteriosclerosis, thrombosis, and vascular biology, 2002. **22**(7): p. 1194-1199.
202. Niwa, S., T. Totsuka, and S. Hayashi, *Inhibitory effect of fluvastatin, an HMG-CoA reductase inhibitor, on the expression of adhesion molecules on human monocyte cell line.* International journal of immunopharmacology, 1996. **18**(11): p. 669-675.
203. Ridker, P.M., et al., *Measurement of C-reactive protein for the targeting of statin therapy in the primary prevention of acute coronary events.* New England Journal of Medicine, 2001. **344**(26): p. 1959-1965.
204. Ridker, P.M., et al., *Inflammation, pravastatin, and the risk of coronary events after myocardial infarction in patients with average cholesterol levels.* Circulation, 1998. **98**(9): p. 839-844.
205. Nakata, M., et al., *Effects of statins on the adipocyte maturation and expression of glucose transporter 4 (SLC2A4): implications in glycaemic control.* Diabetologia, 2006. **49**(8): p. 1881-1892.
206. Ishihara, N., et al., *Atorvastatin increases Fads1, Fads2 and Elovl5 gene expression via the geranylgeranyl pyrophosphate-dependent Rho kinase pathway in 3T3-L1 cells.* Molecular Medicine Reports, 2017. **16**(4): p. 4756-4762.
207. Li, X., et al., *Lovastatin inhibits adipogenic and stimulates osteogenic differentiation by suppressing PPARγ2 and increasing Cbfa1/Runx2 expression in bone marrow mesenchymal cell cultures.* Bone, 2003. **33**(4): p. 652-659.
208. Zeng, Z.-H., et al., *The functional changes of the perivascular adipose tissue in spontaneously hypertensive rats and the effects of atorvastatin therapy.* Clinical and experimental hypertension, 2009. **31**(4): p. 355-363.

209. Wójcicka, G., et al., *Differential effects of statins on endogenous H2S formation in perivascular adipose tissue.* Pharmacological research, 2011. **63**(1): p. 68-76.
210. Parisi, V., et al., *Statin therapy modulates thickness and inflammatory profile of human epicardial adipose tissue.* International journal of cardiology, 2019. **274**: p. 326-330.
211. Maresca, F., et al., *Adipokines, vascular wall, and cardiovascular disease: a focused overview of the role of adipokines in the pathophysiology of cardiovascular disease.* Angiology, 2015. **66**(1): p. 8-24.
212. Takagi, T., et al., *Effect of pravastatin on the development of diabetes and adiponectin production.* Atherosclerosis, 2008. **196**(1): p. 114-121.
213. Ando, H., et al., *Effects of atorvastatin and pravastatin on glucose tolerance, adipokine levels and inflammatory markers in hypercholesterolaemic patients.* Clinical and Experimental Pharmacology and Physiology, 2008. **35**(9): p. 1012-1017.
214. Nomura, S., et al., *Effects of pitavastatin on monocyte chemoattractant protein-1 in hyperlipidemic patients.* Blood coagulation & fibrinolysis, 2009. **20**(6): p. 440-447.
215. Blanco-Colio, L.M., et al., *Adiponectin plasma levels are increased by atorvastatin treatment in subjects at high cardiovascular risk.* European journal of pharmacology, 2008. **586**(1-3): p. 259-265.
216. Sakamoto, K., T. Sakamoto, and H. Ogawa, *The effect of 6 months of treatment with pravastatin on serum adiponection concentrations in Japanese patients with coronary artery disease and hypercholesterolemia: a pilot study.* Clinical therapeutics, 2006. **28**(7): p. 1012-1021.
217. Gannagé-Yared, M.-H., et al., *Pravastatin does not affect insulin sensitivity and adipocytokines levels in healthy nondiabetic patients.* Metabolism, 2005. **54**(7): p. 947-951.
218. Sonmez, A., et al., *The effect of fluvastatin on plasma adiponectin levels in dyslipidaemia.* Clinical endocrinology, 2006. **64**(5): p. 567-572.
219. Otto, C., et al., *Short-term therapy with atorvastatin or fenofibrate does not affect plasma ghrelin, resistin or adiponectin levels in type 2 diabetic patients with mixed hyperlipoproteinaemia.* Acta diabetologica, 2007. **44**(2): p. 65-68.
220. Forst, T., et al., *Effect of simvastatin and/or pioglitazone on insulin resistance, insulin secretion, adiponectin, and proinsulin levels in nondiabetic patients at cardiovascular*

risk—the PIOSTAT Study. Metabolism, 2007. **56**(4): p. 491-496.
221. Naderali, E.K., et al., *The effects of physiological and pharmacological weight loss on adiponectin and leptin mRNA levels in the rat epididymal adipose tissue.* European journal of pharmacology, 2008. **579**(1-3): p. 433-438.
222. Nakamura, T., et al., *Increase in circulating levels of adiponectin after treatment with statin and fibrate in patients with coronary artery disease and hyperlipidemia.* Atherosclerosis, 2007. **193**(2): p. 449-451.
223. Koh, K.K., et al., *Beneficial effects of fenofibrate to improve endothelial dysfunction and raise adiponectin levels in patients with primary hypertriglyceridemia.* Diabetes care, 2005. **28**(6): p. 1419-1424.
224. Westphal, S. and C. Luley, *Preferential increase in high-molecular weight adiponectin after niacin.* Atherosclerosis, 2008. **198**(1): p. 179-183.
225. Westphal, S., et al., *Adipokines and treatment with niacin.* Metabolism, 2006. **55**(10): p. 1283-1285.
226. Wanders, D., E.P. Plaisance, and R.L. Judd, *Pharmacological effects of lipid-lowering drugs on circulating adipokines.* World journal of diabetes, 2010. **1**(4): p. 116.
227. Perelas, A., A. Tsoulkani, and D. Perrea, *Effects of lipid-lowering drugs on adiponectin.* Current Vascular Pharmacology, 2010. **8**(6): p. 836-848.
228. Von Eynatten, M., et al., *Adipocytokines as a novel target for the anti-inflammatory effect of atorvastatin in patients with type 2 diabetes.* Diabetes Care, 2005. **28**(3): p. 754-755.
229. Zhao, S.-p. and Z.-h. Wu, *Atorvastatin reduces serum leptin concentration in hypercholesterolemic rabbits.* Clinica chimica acta, 2005. **360**(1-2): p. 133-140.
230. Damci, T., et al., *Fenofibrate treatment is associated with better glycemic control and lower serum leptin and insulin levels in type 2 diabetic patients with hypertriglyceridemia.* European Journal of Internal Medicine, 2003. **14**(6): p. 357-360.
231. Belfort, R., et al., *Fenofibrate reduces systemic inflammation markers independent of its effects on lipid and glucose metabolism in patients with the metabolic syndrome.* The Journal of Clinical Endocrinology & Metabolism, 2010. **95**(2): p. 829-836.
232. Yang, J., et al., *Effect of niacin on adipocyte leptin in hypercholesterolemic rabbits.* Cardiovascular Pathology, 2008. **17**(4): p. 219-225.

233. Westphal, S., et al., *Extended-release niacin raises adiponectin and leptin.* Atherosclerosis, 2007. **193**(2): p. 361-365.
234. Tunçez, A., et al., *Comparative effects of atorvastatin 80 mg and rosuvastatin 40 mg on the levels of serum endocan, chemerin, and galectin-3 in patients with acute myocardial infarction.* Anatolian Journal of Cardiology, 2019. **22**(5): p. 240.
235. Guo, Y., et al., *Simvastatin inhibits the adipogenesis of bone marrow-derived mesenchymal stem cells through the downregulation of chemerin/CMKLR1 signaling.* International Journal of Molecular Medicine, 2020.
236. Kopp, C., et al., *Nicotinic acid increases adiponectin secretion from differentiated bovine preadipocytes through G-protein coupled receptor signaling.* International journal of molecular sciences, 2014. **15**(11): p. 21401-21418.
237. Sever, P.S., et al., *Prevention of coronary and stroke events with atorvastatin in hypertensive patients who have average or lower-than-average cholesterol concentrations, in the Anglo-Scandinavian Cardiac Outcomes Trial--Lipid Lowering Arm (ASCOT-LLA): a multicentre randomised controlled trial.* Drugs, 2004. **64 Suppl 2**: p. 43-60.
238. Lelovas, P.P., N.G. Kostomitsopoulos, and T.T. Xanthos, *A comparative anatomic and physiologic overview of the porcine heart.* Journal of the American Association for Laboratory Animal Science, 2014. **53**(5): p. 432-438.
239. Suzuki, Y., A.C. Yeung, and F. Ikeno, *The representative porcine model for human cardiovascular disease.* Journal of Biomedicine and Biotechnology, 2010. **2011**.
240. Owen, M.K., et al., *Perivascular adipose tissue potentiates contraction of coronary vascular smooth muscle: influence of obesity.* Circulation, 2013. **128**(1): p. 9-18.
241. Ohyama, K., et al., *Association of coronary perivascular adipose tissue inflammation and drug-eluting stent–induced coronary hyperconstricting responses in pigs: 18F-fluorodeoxyglucose positron emission tomography imaging study.* Arteriosclerosis, thrombosis, and vascular biology, 2017. **37**(9): p. 1757-1764.
242. Sirtori, C.R., *The pharmacology of statins.* Pharmacological research, 2014. **88**: p. 3-11.
243. Álvarez De Sotomayor, M., et al., *Characterization of endothelial factors involved in the vasodilatory effect of simvastatin in aorta and small mesenteric artery of the rat.* British journal of pharmacology, 2000. **131**(6): p. 1179-1187.

244. Uydeş-Doğan, B.S., et al., *Relaxant effects of pravastatin, atorvastatin and cerivastatin on isolated rat aortic rings.* Life sciences, 2005. **76**(15): p. 1771-1786.
245. Ghaffari, N., et al., *Acute modulation of vasoconstrictor responses by pravastatin in small vessels.* Circulation Journal, 2011. **75**(6): p. 1506-1514.
246. Wong, P., R. Roberts, and M. Randall, *Sex differences in endothelial function in porcine coronary arteries: a role for H2O2 and gap junctions?* British journal of pharmacology, 2014. **171**(11): p. 2751-2766.
247. Almukhtar, H., et al., *Effect of simvastatin on vascular tone in porcine coronary artery: Potential role of the mitochondria.* Toxicology and Applied Pharmacology, 2016. **305**: p. 176-185.
248. Fong, C.W., *Statins in therapy: understanding their hydrophilicity, lipophilicity, binding to 3-hydroxy-3-methylglutaryl-CoA reductase, ability to cross the blood brain barrier and metabolic stability based on electrostatic molecular orbital studies.* European journal of medicinal chemistry, 2014. **85**: p. 661-674.
249. Kaesemeyer, W.H., et al., *Pravastatin sodium activates endothelial nitric oxide synthase independent of its cholesterol-lowering actions.* Journal of the American College of Cardiology, 1999. **33**(1): p. 234-241.
250. LÖHN, M., et al., *Periadventitial fat releases a vascular relaxing factor.* The FASEB Journal, 2002. **16**(9): p. 1057-1063.
251. Antonopoulos, A.S., et al., *Adiponectin as a link between type 2 diabetes and vascular NADPH oxidase activity in the human arterial wall: the regulatory role of perivascular adipose tissue.* Diabetes, 2015. **64**(6): p. 2207-2219.
252. Buechler, C., et al., *Chemerin isoforms and activity in obesity.* International journal of molecular sciences, 2019. **20**(5): p. 1128.
253. Ernst, M.C. and C.J. Sinal, *Chemerin: at the crossroads of inflammation and obesity.* Trends in Endocrinology & Metabolism, 2010. **21**(11): p. 660-7.
254. Lee, S.-E., et al., *Effects of statins on coronary atherosclerotic plaques: the PARADIGM study.* JACC: Cardiovascular Imaging, 2018. **11**(10): p. 1475-1484.
255. Iwata, A., et al., *Inhibitory effect of statins on inflammatory cytokine production from human bronchial epithelial cells.* Clinical & Experimental Immunology, 2012. **168**(2): p. 234-240.

256. Chamberlain, L.H., *Inhibition of isoprenoid biosynthesis causes insulin resistance in 3T3-L1 adipocytes.* FEBS letters, 2001. **507**(3): p. 357-361.
257. Randall, M.D. and T.M. Griffith, *Modulation of vasodilatation to levcromakalim by hypoxia and EDRF in the rabbit isolated ear: a comparison with pinacidil, sodium nitroprusside and verapamil.* British journal of pharmacology, 1993. **109**(2): p. 386-393.
258. Zebisch, K., et al., *Protocol for effective differentiation of 3T3-L1 cells to adipocytes.* Analytical biochemistry, 2012. **425**(1): p. 88-90.
259. Ramirez-Zacarias, J., F. Castro-Munozledo, and W. Kuri-Harcuch, *Quantitation of adipose conversion and triglycerides by staining intracytoplasmic lipids with Oil red O.* Histochemistry, 1992. **97**(6): p. 493-497.
260. Sun, X. and M.B. Zemel, *Calcium and 1, 25 - dihydroxyvitamin D3 regulation of adipokine expression.* Obesity, 2007. **15**(2): p. 340-348.
261. Park, W.S., et al., *Functional expression of smooth muscle-specific ion channels in TGF-β1-treated human adipose-derived mesenchymal stem cells.* American Journal of Physiology-Cell Physiology, 2013. **305**(4): p. C377-C391.
262. Parlee, S.D., et al., *Serum chemerin levels vary with time of day and are modified by obesity and tumor necrosis factor-α.* Endocrinology, 2010. **151**(6): p. 2590-2602.
263. Tomita, M., et al., *Astrocyte production of the chemokine macrophage inflammatory protein-2 is inhibited by the spice principle curcumin at the level of gene transcription.* Journal of Neuroinflammation, 2005. **2**(1): p. 1-7.
264. Quayle, J.M., M. Nelson, and N. Standen, *ATP-sensitive and inwardly rectifying potassium channels in smooth muscle.* Physiological reviews, 1997. **77**(4): p. 1165-1232.
265. Zhao, R.-j. and H. Wang, *Chemerin/ChemR23 signaling axis is involved in the endothelial protection by K ATP channel opener iptakalim.* Acta Pharmacologica Sinica, 2011. **32**(5): p. 573-580.
266. Hwang, H.-H., et al., *Identification of the target proteins of rosiglitazone in 3T3-L1 adipocytes through proteomic analysis of cytosolic and secreted proteins.* Molecules and cells, 2011. **31**(3): p. 239-246.
267. Riss, T.L., et al., *Cell viability assays.* Assay Guidance Manual [Internet], 2016.
268. Curry, L., et al., *Simvastatin inhibits L-type Ca2+-channel activity through impairment of mitochondrial function.* Toxicological Sciences, 2019. **169**(2): p. 543-552.

269. Singh, P., et al., *Statins decrease leptin expression in human white adipocytes.* Physiological reports, 2018. **6**(2): p. e13566.
270. Ganesan, S. and M.K. Ito, *Coenzyme Q10 ameliorates the reduction in GLUT4 transporter expression induced by simvastatin in 3T3-L1 adipocytes.* Metabolic syndrome and related disorders, 2013. **11**(4): p. 251-255.
271. Saiki, A., et al., *Pitavastatin enhanced lipoprotein lipase expression in 3T3-L1 preadipocytes.* Journal of atherosclerosis and thrombosis, 2005. **12**(3): p. 163-168.
272. Keskitalo, J.E., et al., *Different effects of the ABCG2 c. 421C> A SNP on the pharmacokinetics of fluvastatin, pravastatin and simvastatin.* Pharmacogenomics, 2009. **10**(10): p. 1617-1624.
273. Ross, M.F., et al., *Accumulation of lipophilic dications by mitochondria and cells.* Biochemical journal, 2006. **400**(1): p. 199-208.
274. Thelen, K.M., et al., *Brain cholesterol synthesis in mice is affected by high dose of simvastatin but not of pravastatin.* Journal of Pharmacology and Experimental Therapeutics, 2006. **316**(3): p. 1146-1152.
275. Schramm, M., et al., *Novel dihydropyridines with positive inotropic action through activation of Ca 2+ channels.* Nature, 1983. **303**(5917): p. 535-537.
276. Oguri, A., et al., *Involvement of CaV3. 1 T-type calcium channels in cell proliferation in mouse preadipocytes.* American Journal of Physiology-Cell Physiology, 2010. **298**(6): p. C1414-C1423.
277. Kopp, A., et al., *Toll-like receptor ligands cause proinflammatory and prodiabetic activation of adipocytes via phosphorylation of extracellular signal-regulated kinase and c-Jun N-terminal kinase but not interferon regulatory factor-3.* Endocrinology, 2010. **151**(3): p. 1097-1108.
278. Lira, F.S., et al., *Both adiponectin and interleukin-10 inhibit LPS-induced activation of the NF-κB pathway in 3T3-L1 adipocytes.* Cytokine, 2012. **57**(1): p. 98-106.
279. Monnier, J., et al., *Expression, regulation, and function of atypical chemerin receptor CCRL2 on endothelial cells.* The Journal of Immunology, 2012. **189**(2): p. 956-967.
280. Bauer, S., et al., *Sterol regulatory element-binding protein 2 (SREBP2) activation after excess triglyceride storage induces chemerin in hypertrophic adipocytes.* Endocrinology, 2011. **152**(1): p. 26-35.
281. Zhang, X.-Y., et al., *Anaphylatoxin C5a induces inflammation and reduces insulin sensitivity by activating*

TLR4/NF-kB/PI3K signaling pathway in 3T3-L1 adipocytes. Biomedicine & Pharmacotherapy, 2018. **103**: p. 955-964.
282. Pahan, K., et al., *Lovastatin and phenylacetate inhibit the induction of nitric oxide synthase and cytokines in rat primary astrocytes, microglia, and macrophages.* The Journal of clinical investigation, 1997. **100**(11): p. 2671-2679.
283. Paumelle, R., et al., *Acute antiinflammatory properties of statins involve peroxisome proliferator–activated receptor-α via inhibition of the protein kinase C signaling pathway.* Circulation research, 2006. **98**(3): p. 361-369.
284. Song, S.-H., et al., *Cloning, expression analysis, and regulatory mechanisms of bovine chemerin and chemerin receptor.* Domestic animal endocrinology, 2010. **39**(2): p. 97-105.
285. Bai, X.-J., et al., *Nicotine may affect the secretion of adipokines leptin, resistin, and visfatin through activation of KATP channel.* Nutrition, 2016. **32**(6): p. 645-648.
286. Uhiara, C.O., S.P. Alexander, and R.E. Roberts, *Simvastatin evokes an unpredicted inhibition of β-adrenoceptor-mediated vasodilatation in porcine coronary artery.* European journal of pharmacology, 2012. **690**(1-3): p. 158-163.
287. Seto, S.W., et al., *Acute simvastatin inhibits K ATP channels of porcine coronary artery myocytes.* PloS one, 2013. **8**(6): p. e66404.
288. Lehrke, M. and M.A. Lazar, *The many faces of PPARγ.* Cell, 2005. **123**(6): p. 993-999.
289. Bouskila, M., U. Pajvani, and P. Scherer, *Adiponectin: a relevant player in PPAR γ-agonist-mediated improvements in hepatic insulin sensitivity?* International journal of obesity, 2005. **29**(1): p. S17-S23.
290. Muruganandan, S., et al., *Chemerin, a novel peroxisome proliferator-activated receptor γ (PPARγ) target gene that promotes mesenchymal stem cell adipogenesis.* Journal of Biological Chemistry, 2011. **286**(27): p. 23982-23995.
291. Bajaj, M.S., et al., *Irradiation-induced secretion of BMP4 by marrow cells causes marrow adipogenesis post-myelosuppression.* Stem cell research, 2016. **17**(3): p. 646-653.
292. Grip, O., S. Janciauskiene, and S. Lindgren, *Atorvastatin activates PPAR-γ and attenuates the inflammatory response in human monocytes.* Inflammation Research, 2002. **51**(2): p. 58-62.
293. Balakumar, P. and N. Mahadevan, *Interplay between statins and PPARs in improving cardiovascular outcomes:*

a double‐edged sword? British journal of pharmacology, 2012. **165**(2): p. 373-379.
294. Nissen, S.E. and K. Wolski, *Effect of rosiglitazone on the risk of myocardial infarction and death from cardiovascular causes.* New England Journal of Medicine, 2007. **356**(24): p. 2457-2471.
295. Carmona, M., et al., *Fenofibrate prevents Rosiglitazone-induced body weight gain in ob/ob mice.* International journal of obesity, 2005. **29**(7): p. 864-871.
296. Weng, C., et al., *Effects of chemerin/CMKLR1 in obesity-induced hypertension and potential mechanism.* American journal of translational research, 2017. **9**(6): p. 3096.
297. Jialal, I., et al., *Increased chemerin and decreased omentin-1 in both adipose tissue and plasma in nascent metabolic syndrome.* The Journal of Clinical Endocrinology & Metabolism, 2013. **98**(3): p. E514-E517.
298. Bhattacharya, B. and R. Roberts, *Enhancement of α2‐adrenoceptor‐mediated vasoconstriction by the thromboxane‐mimetic U46619 in the porcine isolated ear artery: role of the ERK–MAP kinase signal transduction cascade.* British journal of pharmacology, 2003. **139**(1): p. 156-162.
299. Roberts, R., D. Kendall, and V. Wilson, *α2‐Adrenoceptor and NPY receptor‐mediated contractions of porcine isolated blood vessels: evidence for involvement of the vascular endothelium.* British journal of pharmacology, 1999. **128**(8): p. 1705-1712.
300. Khalil, R.A. *Regulation of vascular smooth muscle function*. in *Colloquium Series on Integrated Systems Physiology: From Molecule to Function*. 2010. Morgan & Claypool Life Sciences.
301. Brozovich, F., et al., *Mechanisms of vascular smooth muscle contraction and the basis for pharmacologic treatment of smooth muscle disorders.* Pharmacological reviews, 2016. **68**(2): p. 476-532.
302. Roberts, R.E., *The extracellular signal-regulated kinase (ERK) pathway: a potential therapeutic target in hypertension.* Journal of experimental pharmacology, 2012. **4**: p. 77.
303. Somlyo, A.P. and A.V. Somlyo, *Ca2+ sensitivity of smooth muscle and nonmuscle myosin II: modulated by G proteins, kinases, and myosin phosphatase.* Physiological reviews, 2003. **83**(4): p. 1325-1358.
304. Roberts, R.E., *The role of Rho kinase and extracellular regulated kinase-mitogen-activated protein kinase in α2-adrenoceptor-mediated vasoconstriction in the porcine*

palmar lateral vein. Journal of Pharmacology and Experimental Therapeutics, 2004. **311**(2): p. 742-747.
305. Dudley, D.T., et al., *A synthetic inhibitor of the mitogen-activated protein kinase cascade.* Proceedings of the National Academy of Sciences, 1995. **92**(17): p. 7686-7689.
306. Davies, S.P., et al., *Specificity and mechanism of action of some commonly used protein kinase inhibitors.* Biochemical Journal, 2000. **351**(1): p. 95-105.
307. Gianni, D., et al., *A novel and specific NADPH oxidase-1 (Nox1) small-molecule inhibitor blocks the formation of functional invadopodia in human colon cancer cells.* ACS chemical biology, 2010. **5**(10): p. 981-993.
308. Graziani, F., et al., *Thromboxane production in morbidly obese subjects.* The American journal of cardiology, 2011. **107**(11): p. 1656-1661.
309. Traupe, T., et al., *Obesity increases prostanoid-mediated vasoconstriction and vascular thromboxane receptor gene expression.* Journal of hypertension, 2002. **20**(11): p. 2239-2245.
310. Wang, L., et al., *Relationship of serum chemerin to obesity and type 2 diabetes mellitus.* Zhonghua yi xue za zhi, 2009. **89**(4): p. 235-238.
311. Du, X.-Y., et al., *Regulation of chemerin bioactivity by plasma carboxypeptidase N, carboxypeptidase B (activated thrombin-activable fibrinolysis inhibitor), and platelets.* Journal of Biological Chemistry, 2009. **284**(2): p. 751-758.
312. Wadsworth, R., *Vasoconstrictor and vasodilator effects of hypoxia.* Trends in pharmacological sciences, 1994. **15**(2): p. 47-53.
313. Bozaoglu, K., et al., *Chemerin, a novel adipokine in the regulation of angiogenesis.* The Journal of Clinical Endocrinology & Metabolism, 2010. **95**(5): p. 2476-2485.
314. Qiao, Y.-N., et al., *Myosin phosphatase target subunit 1 (MYPT1) regulates the contraction and relaxation of vascular smooth muscle and maintains blood pressure.* Journal of Biological Chemistry, 2014. **289**(32): p. 22512-22523.
315. Nakamura, N., et al., *Chemerin promotes angiogenesis in vivo.* Physiological reports, 2018. **6**(24): p. e13962.
316. Cohen, P., *The development and therapeutic potential of protein kinase inhibitors.* Current opinion in chemical biology, 1999. **3**(4): p. 459-465.
317. Liu, Q., et al., *Developing irreversible inhibitors of the protein kinase cysteinome.* Chemistry & biology, 2013. **20**(2): p. 146-159.

318. Börsch-Haubold, A.G., S. Pasquet, and S.P. Watson, *Direct inhibition of cyclooxygenase-1 and-2 by the kinase inhibitors SB 203580 and PD 98059: SB 203580 also inhibits thromboxane synthase.* Journal of Biological Chemistry, 1998. **273**(44): p. 28766-28772.
319. Kumar, J.D., et al., *Mesenchymal stem cells exhibit regulated exocytosis in response to chemerin and IGF.* PloS one, 2015. **10**(10): p. e0141331.
320. Zabel, B.A., et al., *Chemokine-like receptor 1 expression by macrophages in vivo: regulation by TGF-β and TLR ligands.* Experimental hematology, 2006. **34**(8): p. 1106-1114.
321. Armitage, J., *The safety of statins in clinical practice.* The Lancet, 2007. **370**(9601): p. 1781-1790.
322. Pedersen, T.R. and J.A. Tobert, *Simvastatin: a review.* Expert opinion on pharmacotherapy, 2004. **5**(12): p. 2583-2596.
323. Su, X., et al., *Chemerin in inflammatory diseases.* Clinica Chimica Acta, 2021.
324. Xia, N. and H. Li, *The role of perivascular adipose tissue in obesity‐induced vascular dysfunction.* British journal of pharmacology, 2017. **174**(20): p. 3425-3442.
325. Costa, R.M., et al., *Perivascular adipose tissue as a relevant fat depot for cardiovascular risk in obesity.* Frontiers in physiology, 2018. **9**: p. 253.
326. Fernández-Alfonso, M.S., et al., *Mechanisms of perivascular adipose tissue dysfunction in obesity.* International journal of endocrinology, 2013. **2013**.
327. Kachur, S., et al., *Obesity and cardiovascular diseases.* Minerva medica, 2017. **108**(3): p. 212-228.
328. Sinnott, S.-J., et al., *Trends for prevalence and incidence of resistant hypertension: population based cohort study in the UK 1995-2015.* bmj, 2017. **358**.